JOURNAL OF APPLIED PHYSICS

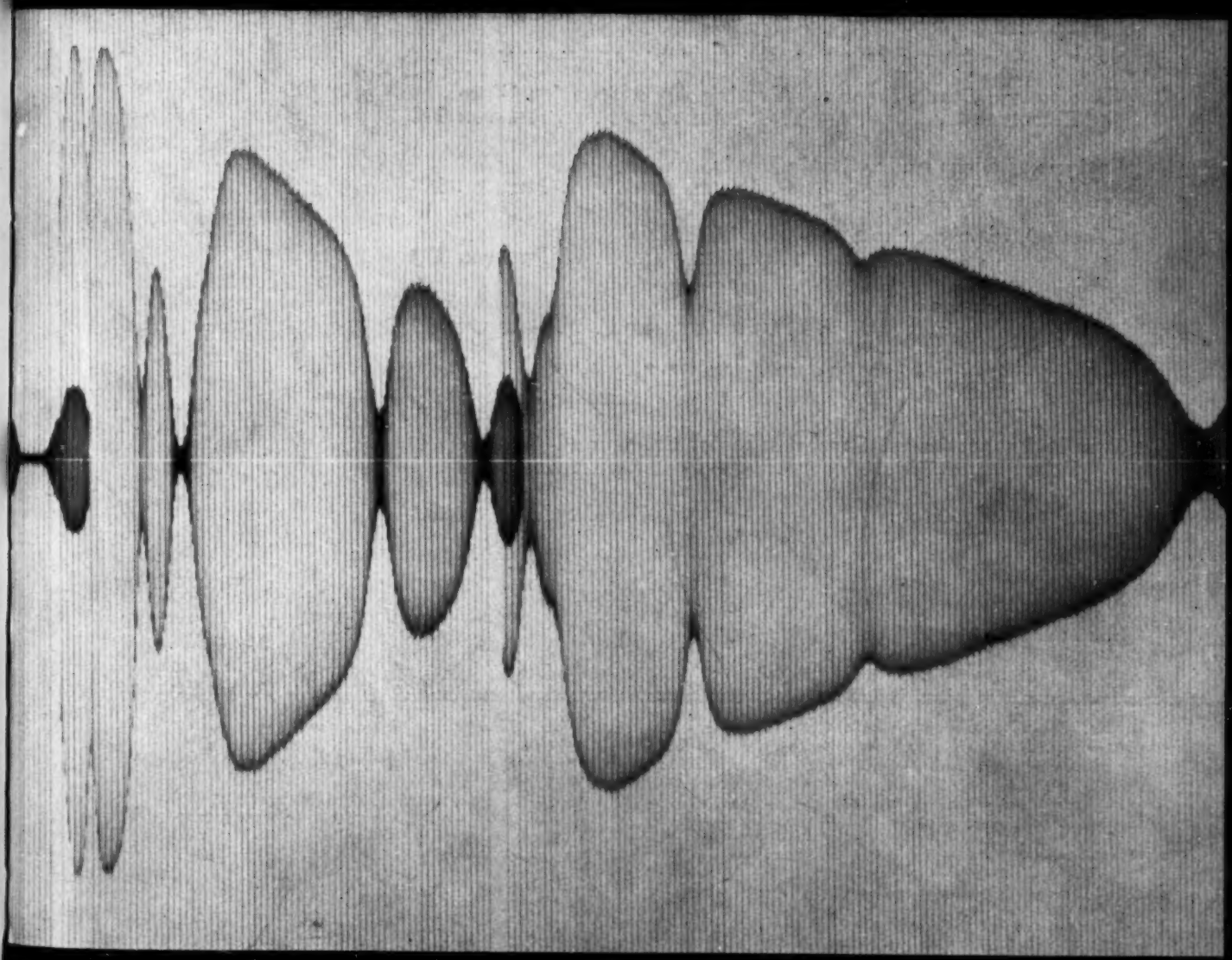

JOURNAL OF APPLIED PHYSICS

Vol. 17, No. 3 MARCH, 1946

In This Issue

Page

Contributed Original Research

Film-Lubrication between Spherical Surfaces: with an Application to the Theory of the Four-Ball Lubricant Testing Instrument J. HOWLETT 137

Analysis of Multicomponent Mixtures of Hydrocarbons in the Liquid Phase by Means of Infra-Red Absorption Spectroscopy D. L. FRY, R. E. NUSBAUM, AND H. M. RANDALL 150

Wide Range Static Strength Testing Apparatus for Glass Rods T. C. BAKER AND F. W. PRESTON 162

Fatigue of Glass under Static Loads T. C. BAKER AND F. W. PRESTON 170

Effect of Water on the Strength of Glass T. C. BAKER AND F. W. PRESTON 179

Fatigue Modulus of Glass J. L. GLATHART AND F. W. PRESTON 189

Induction Heating of Hollow Metallic Cylinders ANDREW GEMANT 195

Tensile Properties of Several Special Steels and Certain Other Materials under Pressure P. W. BRIDGMAN 201

Letter to the Editor: GEORGE G. BRUCK 213

In Every Issue

Here and There 213

New Booklets 214

Index to Advertisers xxvi

BOARD OF EDITORS

ELMER HUTCHISSON, *Editor*

Associate Editors

R. BOWLING BARNES
OTTO BEECK
W. F. BUSSE
S. H. CALDWELL
CLARK GOODMAN
SELIG HECHT
W. JAMES LYONS
PAUL E. SABINE
FREDERICK SEITZ
J. R. TOWNSEND

Publication of the American Institute of Physics

ADMINISTRATIVE STAFF

HENRY A. BARTON, *Director*

MARGARET S. GRIFFIN *Publications Manager*

THEODORE VORBURGER, *Business Manager*

JOHN T. TATE, *Adviser on Publications*

GOVERNING BOARD

PAUL E. KLOPSTEG, *Chairman*

WALLACE WATERFALL, *Secretary*

GEORGE B. PEGRAM, *Treasurer*

T. D. COPE
R. B. DOW
L. A. DUBRIDGE
FLOYD A. FIRESTONE
HARVEY FLETCHER
R. C. GIBBS
K. S. GIBSON
HERMANN MARK
A. G. WORTHING
JOHN T. TATE
L. W. TAYLOR
N. W. TAYLOR

The JOURNAL OF APPLIED PHYSICS, published monthly at Prince and Lemon Sts., Lancaster, Pa., is devoted to physics in its role as the science basic to other natural sciences and to the arts and industries. Previous to 1937 this publication was known as PHYSICS. The JOURNAL OF APPLIED PHYSICS publishes editorials, news of physicists, and reviews, as well as technical papers of applied physics.

Manuscripts should be submitted to Elmer Hutchisson, Editor, Case School of Applied Science, Cleveland 6, Ohio.

Subscriptions and orders for back numbers should be addressed to Prince and Lemon Streets, Lancaster, Pa. or to the American Institute of Physics, 57 East 55 Street, New York 22, N. Y.

Subscription Price	U. S. AND CANADA	ELSEWHERE
To members of scientific societies	$5.00	$5.70
To all others	7.00	7.70

Back Number Prices

Complete set: Vol. 1, July, 1931–Vol. 16, 1945—$101.50
Yearly back number rate: $7.70
Single copies: $0.70 each.

Changes of address and proofs should be addressed to the Publications Manager.

Advertising rates supplied on request. Orders, advertising copy, and cuts should be sent to the American Institute of Physics.

Entered as second class matter January 22, 1937, at the Post Office at Lancaster, Pennsylvania, under the Act of March 3, 1879
Accepted for mailing at the special rate of postage provided for in the Act of February 28, 1925, authorized May 2, 1932.

Copyright 1946, by the American Institute of Physics.

Journal
of
Applied Physics

Volume 17, Number 3 March, 1946

Film-Lubrication between Spherical Surfaces: with an Application to the Theory of the Four-Ball Lubricant Testing Instrument

J. Howlett
Physics Department, University of Manchester, Manchester, England, and Research Department, London, Midland and Scottish Railway Company, Ltd., Derby, England

(Received July 19, 1945)

The paper is concerned mainly with the flow of viscous liquid between the outer surfaces of two equal spheres placed in an infinite body of the liquid so that the "minimum separation" of the surfaces (the distance apart at the points of closest approach) is small compared with the radius; one sphere is held at rest, the other rotates at constant speed about an axis which does not pass through the center of the fixed sphere. The assumption is made that the surfaces are separated by a continuous film of liquid to which the classical theory of hydrodynamical lubrication can be applied—that is, "boundary lubrication" and actual contact between the surfaces are excluded; the partial differential equation (the Reynolds equation) for the pressure distribution in this film is set up, and it is shown that with a suitable choice of boundary conditions a solution can be found in very simple form. From this solution are deduced the total force exerted by the liquid on the moving sphere and the torque, about the axis of rotation, of the forces acting on the fixed sphere. The results are applied to the particular case of the four-ball lubricant testing instrument, in which a sphere is made to rotate about a vertical axis, under axial load, in the central space formed by a set of three equal spheres held stationary so as to touch one another with their centers in a horizontal plane; the whole set of spheres is immersed in the lubricant to be tested. The relations finally obtained express the load on the moving sphere and the torque on the set of fixed spheres in terms of the radius of the spheres, the velocity of rotation, and the viscosity of the liquid; they involve as a parameter the minimum separation of the moving sphere from the fixed spheres, and elimination of this gives the relation between the measurable quantities, load, and torque, which could provide a basis for the use of the instrument as a viscometer. It is found that the torque is a very slowly varying function of the load, being approximately proportional to the logarithm of the load. Further, if it is assumed that the hydrodynamical theory of lubrication is valid only for films whose thickness is greater than some agreed minimum, then the expression for the load on the moving sphere, into which the minimum separation enters, provides a criterion for the range of conditions (of which the load is much the most important) within which the theory does in fact apply to the instrument. Numerical examples are considered, and it is shown that, with allowance for wide departures from the standard size and speed of operation of the instrument, the maximum load which can be supported by the moving sphere in the hydrodynamical regime cannot be expected to exceed a few hundred grams weight; for loads of greater order the standard continuous-film theory cannot hold, and the forces on the spheres are no longer determined by the viscosity of the liquid.

INTRODUCTION

IN the last few years a great deal of attention has been given to the properties of lubricants under conditions of "extreme pressure," that is, under pressures so great (of the order of 10^4 kg wt./cm^2) that it is not to be expected that the lubricated surfaces are separated by the continuous film which characterizes hydrodynamical

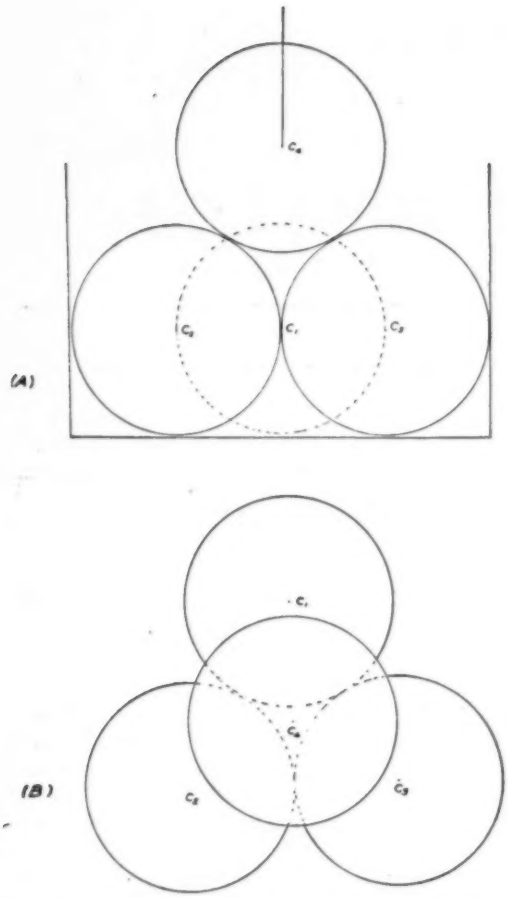

FIG. 1. (A) Elevation and (B) plan of the 4-ball instrument. C_1, C_2, C_3 are the centers of the stationary spheres and C_4 that of the rotating sphere.

or "thick film" lubrication. The literature of the subject has many references to the Boerlage four-ball testing instrument.[1]

The instrument seems to have become a standard piece of apparatus in this field, but at the same time it seems that the interpretation of the measurements made with it is not always certain. There is an obvious question which must present itself in any general discussion of the theory of the apparatus, and which should be amenable to theoretical investigation; this is, can the instrument behave in any circumstances according to the laws of hydrodynamical lubrication, and if it can, what is the range of operating conditions over which this is possible? There seems to be no published investigation of this point; the present paper attempts a treatment based only on classical hydrodynamical theory.

We may recall here that the four-ball instrument consists essentially (see Fig. 1) of a set of three equal spheres held rigidly in a fixed cup so as to touch one another with their centers in a horizontal plane, with a fourth sphere rotated under load about a vertical axis in the central space of the fixed spheres; the whole is immersed in the lubricant to be tested. Details of some methods of use with great loads (which are not really relevant to our present purpose) are given in other papers.[1] We base this investigation on two fundamental assumptions; first that the spheres are not deformed by the load, and second, that the flow of liquid around and between the spheres obeys the classical equations of viscous flow, in particular that a continuous film in the hydrodynamical sense (as distinct from the "boundary lubrication" sense) is formed between the moving sphere and each fixed sphere.

We attack the problem indirectly by first developing the relation between the thickness of this film at its thinnest part (the "minimum film thickness," say) and the load applied to the axis. Suppose we find a relation $W=W(h_0)$ between the load W and this minimum thickness h_0—involving of course all the parameters of the problem—the radius of the spheres, the angular velocity of the rotating sphere, and the viscosity of the liquid. Suppose also that we have reason to believe that a film of thickness less than some value d does not behave as a lubricating film in the hydrodynamical sense; then we may deduce that the assumption of hydrodynamical lubrication ceases to hold for loads exceeding the value $W(d)$ corresponding to the thickness $h_0=d$. Conversely we may deduce that for loads less than this value there will be in fact lubrication of the hydrodynamical type. We have thus a criterion for the range of application of the classical theory.

A complete and rigorous investigation of the problem would involve the solving of the full equations for the flow around the spheres, and with a geometry so complicated no success could be expected from such an undertaking: indeed it was shown by Lamb[2] that even the apparently

[1] G. D. Boerlage, Engineering **136**, 46 (1933). O. Beeck, J. App. Phys. **12**, 512 (1941). D. Clayton, Inst. Mech. Eng., Discussion on Lubrication **2**, 282 (1937). R. Schnurmann, Engineering **149**, 567 (1940).

[2] H. Lamb, Hydrodynamics (Cambridge University Press, London, 1932), p. 589.

simple problem of a sphere rotating in an infinite body of liquid is intractable if the velocity exceeds a very small value. To bring the problem within the scope of reasonably simple analysis we make the following further assumptions:

A. The flow in the immediate vicinity of the moving sphere and any one of the fixed spheres is unaffected by the presence of the other spheres.

B. The film formed between the moving sphere and any fixed sphere is sufficiently thin for the standard assumptions of classical film-theory to hold; that is,

(*a*) the inertia terms in the equations of motion can be neglected,
(*b*) the pressure can be regarded as constant across the film, and
(*c*) rates of change of velocity measured across the film are much greater than those measured in any other direction.

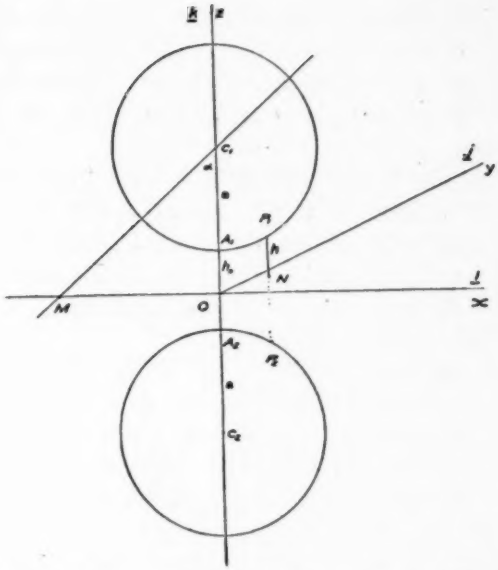

FIG. 2. Geometry of the 2-sphere system considered.

There is also the over-riding assumption, implied in the use of the hydrodynamical equations, that the only relevant physical property of the lubricant is its viscosity; and we shall take this as constant throughout the film.

With these assumptions the problem is reduced to the solving of the Reynolds equation for the flow between one pair of spherical surfaces, that is, the partial differential equation for the pressure distribution in the film. The general outline of the investigation is then as follows: First (§§1, 2) the Reynolds equation is set up and the boundary conditions are obtained. It is then shown that with a suitable choice of boundary conditions there is a very simple solution which is computed as a numerical function. From this we deduce (§4) the total load supported by the film; and a further analysis (§5) leads to the expression for the viscous-frictional torque exerted on the stationary sphere. Finally we apply these results to the particular case of the four-ball instrument and derive the criterion for the range of working within which we may suppose hydrodynamical lubrication to occur.

The final conclusion is that the usual conditions of heavy loads are far outside this range, as is to be expected, so that in these circumstances the relevant property of the lubricant is not its viscosity. The results have other points of interest, however; for example, the instrument could be used as a viscometer, for which purpose it would have the advantage of permitting wide variations in the working conditions, including the rate of shear; the relations obtained here provide a basis for the calibration of the instrument for that purpose.[3] It was partly to this end that the determination of the torque was made. Also there is the point of mathematical interest that the investigation leads to an exact solution of the Reynolds equation, which is very seldom possible; it has in fact been stated[4] that the equation cannot be solved in finite terms if the boundaries of the flow have curvature in two directions.

1. THE PRESSURE EQUATION (REYNOLDS EQUATION)

In Fig. 2, C_1, C_2 are the centers of two spheres of radius a; the first sphere rotates with angular velocity ω about the line MC_1 (which in the four-ball machine is vertical) and the second sphere is at rest; the inclination of MC_1 to C_1C_2 is taken as an arbitrary angle α whose value in the final application will be deduced from the geometry of the instrument.

[3] It would be necessary to make a series of calibrations with liquids of widely differing viscosities to allow for possible changes in the dynamical pattern of the flow.

[4] See, for example, R. O. Boswell, *Film Lubrication* (Longmans Green and Company, New York, 1928).

The coordinate system $Oxyz$ is chosen so that (a) O is the mid-point of C_1C_2, (b) Oz coincides with the line of centers C_1C_2, and (c) the axis MC_1 lies in the plane zx (in the figure, M lies on Ox).

Let p be the pressure and $\mathbf{v}$ the fluid velocity at any point; let the thickness of the film at any section be $2h$, and let the minimum thickness be $2h_0$. Thus in the figure $NP_1=NP_2=h$, $OA_1=OA_2=h_0$ and P_1P_2 have coordinates (x, y, h) and $(x, y, -h)$, respectively.

By assumption A, p is a function of x and y only, and the whole treatment of the problem depends on the partial differential equation in x and y satisfied by p. The derivation of this equation is a standard piece of analysis, but as we shall need in a later section some of the intermediate equations we may conveniently indicate here the main steps in the process.

If the fluid velocity $\mathbf{v}$ has components u, v, w, then the assumption B permits us to reduce the general equations of motion to

$$\frac{\partial p}{\partial x}=\mu\frac{\partial^2 u}{\partial z^2},\quad \frac{\partial p}{\partial y}=\mu\frac{\partial^2 v}{\partial z^2},\quad \frac{\partial p}{\partial z}=0. \tag{1}$$

Let the velocity of the general point P_1 on the surface of the moving sphere have components U, V, W. Every point on the second sphere has zero velocity, so we can write the boundary conditions for these equations

$$\begin{array}{llll} \text{at} & z=h & u=U & v=V \quad w=W; \\ \text{at} & z=-h & u=0 & v=0 \quad w=0. \end{array}$$

Hence by integration with respect to z

$$\begin{aligned} u&=\frac{z+h}{2h}U+\frac{z^2-h^2}{2\mu}\frac{\partial p}{\partial x}, \\ v&=\frac{z+h}{2h}V+\frac{z^2-h^2}{2\mu}\frac{\partial p}{\partial y}. \end{aligned} \tag{2}$$

Now the flow must satisfy the continuity equation $\operatorname{div}\mathbf{v}=0$

$$\text{i.e.,}\qquad \frac{\partial u}{\partial x}+\frac{\partial v}{\partial y}+\frac{\partial w}{\partial z}=0. \tag{3}$$

If we substitute for u and v the values given by (2) and then integrate the resulting equation for w between the limits $-h$ and h so that

$$\int_{-h}^{h}\left(\frac{\partial u}{\partial x}+\frac{\partial v}{\partial y}\right)dz=-\int_{-h}^{h}\frac{\partial w}{\partial z}dz=-W,$$

we shall have eliminated the velocities u, v, w and derived an equation for p alone. We obtain

$$\begin{aligned} &\frac{\partial}{\partial x}\left(h^3\frac{\partial p}{\partial x}\right)+\frac{\partial}{\partial y}\left(h^3\frac{\partial p}{\partial y}\right) \\ &\qquad=\tfrac{3}{2}\mu W+\tfrac{3}{2}\mu h\left(\frac{\partial U}{\partial x}+\frac{\partial V}{\partial y}\right), \end{aligned} \tag{4}$$

which is the Reynolds equation, in rather more general form than is usually quoted.

So far the argument has been quite general and Eq. (4) holds for any system of the type we are considering; we must now obtain the analytical expressions for h, U, V, W which relate to our particular problem.

The expression for the film-thickness h is easily obtained, for if (x, y, h) is any point on the upper (moving) sphere, the distance from the center of the sphere is a, and so

$$x^2+y^2+(a+h_0-h)^2=a^2, \tag{5}$$

which defines h.

It is convenient to use the variable

$$a+h_0-h=Z. \tag{5a}$$

Then

$$x^2+y^2+Z^2=a^2, \tag{5b}$$

and the derivatives of h, which we shall need, are

$$\frac{\partial h}{\partial x}=-\frac{\partial Z}{\partial x}=\frac{x}{Z}, \tag{5c}$$

$$\frac{\partial h}{\partial y}=-\frac{\partial Z}{\partial y}=\frac{y}{Z}. \tag{5d}$$

The velocities U, V, W are most readily derived by a vector method. Let $\mathbf{i}$, $\mathbf{j}$, $\mathbf{k}$ be the usual unit vectors along the coordinate axes; then (Fig. 2) the vector angular velocity of the sphere is

$$\boldsymbol{\omega}=\omega(\sin\alpha\mathbf{i}+\cos\alpha\mathbf{k}),$$

and if $\mathbf{r}$ is the vector C_1P_1 the velocity of P_1 is $\boldsymbol{\omega}\wedge\mathbf{r}$. Now

$$\mathbf{r}=x\mathbf{i}+y\mathbf{j}-Z\mathbf{k},$$

so

$$U\mathbf{i}+V\mathbf{j}+W\mathbf{k}=\omega(\sin\alpha\mathbf{i}+\cos\alpha\mathbf{k})\wedge(x\mathbf{i}+y\mathbf{j}-Z\mathbf{k}),$$

and equating the coefficients of **i**, **j**, **k** on the two sides of this equation gives the required expressions:

$$\begin{aligned} U&=-\omega y\cos\alpha,\\ V&=\omega(x\cos\alpha+Z\sin\alpha),\\ W&=\omega y\sin\alpha, \end{aligned} \tag{6}$$

from which we have

$$\frac{\partial U}{\partial x}=0,\quad \frac{\partial V}{\partial y}=-\frac{\omega y}{Z}\sin\alpha.$$

Substitution of these values in (4) gives as the fundamental equation for the problem

$$\frac{\partial^2 p}{\partial x^2}+\frac{\partial^2 p}{\partial y^2}+\frac{3}{2h}\left(x\frac{\partial p}{\partial x}+y\frac{\partial p}{\partial y}\right)=\frac{3\mu\omega\sin\alpha}{2h^3}\left(1-\frac{h}{Z}\right)y. \tag{7}$$

We can at once simplify the form of this equation by changing from Cartesian coordinates x, y to polars r, θ defined by

$$x=r\cos\theta,\quad y=r\sin\theta.$$

The transformed equation is

$$\frac{\partial^2 p}{\partial r^2}+\left(\frac{1}{r}+\frac{3r}{Zh}\right)\frac{\partial p}{\partial r}+\frac{1}{r^2}\frac{\partial^2 p}{\partial\theta^2}=\frac{3\mu\omega\sin\alpha}{2h^3}\left(1-\frac{h}{Z}\right)r\sin\theta, \tag{8}$$

where

$$h=a+h_0-Z,\quad Z^2=a^2-r^2,$$

and a most important point is that h and Z are functions of r only.

In this as in most problems it is of great advantage to work in terms of dimensionless variables; a little algebraic manipulation shows that if we define the dimensionless quantities ρ, Π, s_0 by the relations

$$\rho=r/(2ah_0)^{\frac{1}{2}},\quad \Pi=p/\tfrac{3}{2}\mu\omega\sin\alpha(2a/h_0)^{\frac{1}{2}},\quad s_0=h_0/a,$$

the equation can be written

$$\frac{\partial^2\Pi}{\partial\rho^2}+L\frac{\partial\Pi}{\partial\rho}+\frac{1}{\rho^2}\frac{\partial^2\Pi}{\partial\theta^2}=M\sin\theta,$$

where L, M are functions of ρ only, given by

$$L=\frac{1}{\rho}+\frac{3\rho}{(1-2s_0\rho^2)^{\frac{1}{2}}}(1+s_0-2s_0\rho^2), \tag{9a}$$

$$M=\rho\left[\frac{1}{2}\cdot\frac{1+s_0+(1-2s_0\rho^2)^{\frac{1}{2}}}{1+s_0+\rho^2}\right]^3\times[2-(1+s_0)(1-2s_0\rho^2)^{\frac{1}{2}}]. \tag{9b}$$

If finally we regard $s_0=h_0/a$ as a small quantity, and in (9a, b) neglect s_0 in comparison with unity, we obtain the simpler forms

$$L=\frac{1}{\rho}+\frac{6\rho}{1+\rho^2}, \tag{9c}$$

$$M=\frac{\rho}{(1+\rho^2)^3}. \tag{9d}$$

In this last case we can write the equation in the form

$$\frac{\partial^2\Pi}{\partial\rho^2}+\left(\frac{1}{\rho}+\frac{6\rho}{1+\rho^2}\right)\frac{\partial\Pi}{\partial\rho}+\frac{1}{\rho^2}\frac{\partial^2\Pi}{\partial\theta^2}=\frac{\rho}{(1+\rho^2)^3}\sin\theta, \tag{10}$$

which is remarkable in that it is completely free from all the parameters of the problem: all these have been absorbed into the dimensionless variables Π, ρ. This single equation therefore covers all possible values of a, μ, α, ω; but in dealing with this form we must remember that the original Eq. (9) has a singularity at $r=a$ (where $Z=0$) so the range of ρ must be restricted to correspond to a range of r stopping well short of this point. This is, of course, quite in accordance with physical ideas; for at all points on the circle $r=a$ the tangent planes to the two spheres are parallel to the z axis (to put it less formally, the surfaces are diverging infinitely rapidly) and well before this the film will have become thicker than the basic assumptions will permit.

2. BOUNDARY CONDITIONS

Before we can make any use of the pressure equation we must ascribe to p a set of boundary conditions, and it is here that the real difficulty of the problem is met. We are dealing with an elliptic equation for p in the two independent

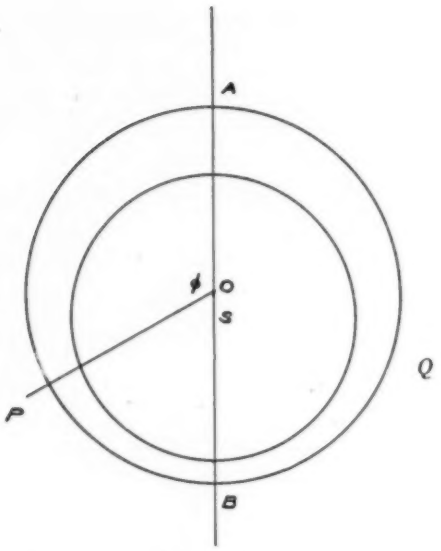

FIG. 3. Geometry of the complete journal bearing. *S*, *O* are the centers of the journal and the bearing, respectively.

variables x, y (or the equivalent variables r, θ) and general theory tells us that to obtain a unique solution we need to know the values of p at all points of a closed curve in the xy plane. The possibility of finding a solution in reasonably simple form is intimately bound up with the choice of this curve and of the set of values of p along the curve.

The difficulty arises because the film has no definite boundaries defined *a priori* by the geometry of the apparatus, but merges gradually into the main body of the fluid where the assumptions **A** and **B** are not valid. This is not to say that the problem is not defined physically: strictly the boundaries are the free surface of the liquid, the inner surface of the cup, and the four spherical surfaces; and the problem is defined by the obvious conditions of pressure and velocity at these surfaces. But in view of the small chance of finding a strict solution we must look for an alternative set of conditions for our simplified system, relying on general physical principles in making our choice.

An obvious condition is that in the main body of the liquid, and in fact everywhere except in the immediate vicinity of the point of closest approach of the two spheres, the pressure must be practically atmospheric; if, therefore, we choose the atmospheric value as the zero of pressure the solution for p must reduce to very small (numerical) values everywhere except in this region, that is, for all except small values of r. This can be idealized to the statement

$$p=0 \quad \text{for} \quad r \geq r_0,$$

where r_0 is some value considerably less than a, and suggests that for the boundary condition we might take

$$p=0 \quad \text{for} \quad r=r_0, \quad 0 \leq \theta \leq 2\pi,$$

i.e., the vanishing of p on a circle of radius r_0. This however is not a suitable condition; for the equation for p has what we may call "skew symmetry" about the origin: if in (7) we replace x, y by $-x$, $-y$ we merely change the sign of the right side. We get the same effect by replacing θ by $\theta+\pi$ in (8) or (9). If therefore the set of boundary values has the same property, the whole solution will itself have this property; that is, in polars, if in the region $0<\theta<\pi$ the solution is $p=p(r, \theta)$ then in the region $\pi<\theta<2\pi$ the solution will be $p=p(r, \theta+\pi)=-p(r, \theta)$. Since the suggested set of values has in fact this property, the use of this condition will lead to a solution in which positive and negative values of equal magnitude appear in pairs; the immediate conclusion, that the resultant load supported by the film is zero, is unacceptable, and not less so is the implication that in half the film the liquid is in a state of negative pressure.

At this stage we can profit from a glance at the theory of the complete journal bearing, the geometry of which is shown in Fig. 3. The classical treatment of Sommerfeld[5] deals with a bearing of infinite length (so that no flow in the axial direction need be considered) and effectively solves the Reynolds' equation corresponding to the flow in the annular space between the two cylindrical surfaces, with the condition that the pressure and its derivatives are continuous and periodic functions of the angular coordinate ϕ; the striking feature of the solution is that it gives positive pressures in the region $APB(0<\phi<\pi)$ and equal negative pressures in the region $AQB(\pi<\phi<2\pi)$. This prediction of negative pressures has led to much criticism of Sommerfeld's work; and it seems to be generally agreed that his premises depart seriously from the truth in that

[5] A. Sommerfeld, Zeits. f. math. Physik **50**, 97–155 (1904).

they make no provision for the replacement of the lubricant which is forced out of the ends of any real bearing, however long; in practice a bearing is connected to a source of the lubricant so that the leakage is continuously replaced. A rigorous treatment incorporating this feature would require a strict solution of the Reynolds' equation taking into account both radial and axial flow, and this seems to present insuperable mathematical difficulties; but an approximate solution developed by Morgan and Muskat[6] suggests that the introduction of a source does in fact suppress the negative pressures. A less sound but much simpler treatment has been given by Gümbel;[7] this writer, having assumed the connection to a source at atmospheric pressure, say at the point of maximum film-thickness $\phi=0$, then neglects the axial flow and suggests three possible empirical conditions to determine p:

I. The pressure falls to zero at the section of minimum thickness and remains zero until the position of the source is reached (traveling round the bearing in the direction of rotation of the axle), i.e., $p=0$ when $\phi=\pi$, and for $\pi\leq\phi\leq 2\pi$.

II. The pressure has its maximum value at the section of minimum thickness and is zero between that point and the position of the source, i.e., $dp/d\phi=0$ when $\phi=\pi$, and $p=0$ for $\pi<\phi\leq 2\pi$.

III. p and $dp/d\phi$ vanish simultaneously (the position at which this occurs being determined by the two conditions) and $p=0$ between this point and the position of the source.

What Gümbel assumes is in effect that the lubricating film breaks from the moving surface either at or just beyond the narrowest section; the first two suggested conditions imply a discontinuity in either p or $dp/d\phi$; the third is a little less drastic but no less arbitrary in essence. Nevertheless Gümbel, using these as working hypotheses, finds that the numerical solutions corresponding to the different possibilities do not differ seriously amongst themselves and are in reasonable agreement with experimental observations. He therefore concludes that his treatment, if not well founded logically, does at least give useful numerical results. A further application of what is effectively Gümbel's third condition has been made by Peppler[8] in a study of the lubrication between the outer surfaces of a pair of cylinders—e.g., a pair of rollers—and he too finds good agreement between theory and observation.

If we compare the two problems—the flow between the spheres and that in the cylindrical bearing—we see that they have one feature in common, namely that they both deal with the flow in a channel of which a large part is divergent in the direction of flow; and as it is a general result of the classical theory of viscous flow that negative pressures are associated with divergent flow, we have here the fundamental reason for our difficulty. The essential feature of Morgan and Muskat's solution is the introduction of the source, and clearly the conditions of the present problem do not permit this; hence we are led to try the application of Gümbel's empirical treatment. Here the main flow is along the y axis and we may suppose that the film breaks from the moving surface along the x axis (since this is the position of narrowest section); in polars, along the lines $\theta=\pi$, $\theta=2\pi$. Further, relying upon Gümbel's results, we may choose from the conditions I, II, III the one which gives the simplest solution, and we find that this is condition I. We therefore take the boundary conditions as—

$$\begin{aligned} &p=0 \quad \text{for} \quad \theta=\pi, \quad \theta=2\pi; \quad 0\leq r\leq r_0, \\ &p=0 \quad \text{for} \quad r=r_0, \quad \pi\leq\theta\leq 2\pi, \end{aligned} \tag{11a}$$

where r_0 is yet to be determined. Thus we investigate the solution of the pressure equation over a semi-circular region of the xy plane, and effectively neglect any contribution to the pressure from the flow in the diverging region.

3. SOLUTION OF THE PRESSURE EQUATION

The actual solution of the Reynolds equation (9) with the boundary conditions (11a) is easily seen to be

$$\Pi=g\sin\theta, \tag{12}$$

where g is a function of ρ only defined by the differential equation

$$\frac{d^2g}{d\rho^2}+L\frac{dg}{d\rho}-\frac{1}{\rho^2}g=M, \tag{13}$$

with the boundary conditions

$$g=0 \quad \text{when} \quad \rho=0, \quad \rho=\rho_0.$$

[6] F. Morgan and M. Muskat, J. App. Phys. **9**, 393 (1938).
[7] L. Gümbel, Zeits. f. tech. Physik **3**, 94 (March, 1922).
[8] K. O. Peppler, V.D.I. Forschungs. 391 (1938).

TABLE I. Solutions for g.[a]

ρ	$G_1\times10^3$	$G_2\times10^3$	$g\times10^3$	$G_1\times10^3$	$G_2\times10^3$	$g\times10^3$
0	0	0	0	0	0	0
0.1	0	10	−10	0	10	−10
2	1	19	−18	1	19	−18
3	3	28	−24	3	28	−25
4	6	36	−29	6	36	−30
5	11	43	−31	11	43	−32
6	16	48	−31	16	48	−32
7	22	53	−30	22	53	−31
8	27	57	−29	27	57	−30
9	32	61	−28	33	61	−28
1.0	38	63	−24	38	63	−25
1.1	43	66	−23	43	66	−23
1.2	47	68	−20	48	68	−20
1.3	51	70	−18	52	70	−18
1.4	55	71	−15	56	71	−15
1.5	58	73	−14	59	73	−14
1.6	60	74	−13	62	74	−12
1.7	63	75	−10	64	75	−11
1.8	65	77	−9	67	76	−9
1.9	67	77	−8	69	77	−8
2.0	69	78	−7	71	77	−7
2.0	69	78	−7	71	77	−7
2.2	72	80	−6	74	80	−6
2.4	75	82	−5	76	82	−6
2.6	77	83	−4	79	83	−4
2.8	79	84	−3	81	84	−3
3.0	80	85	−3	82	85	−3
3.2	82	87	−2	85	87	−2
3.6	84	88	−2	86	88	−2
3.8	85	89	−2	88	89	−1
4.0	86	90	−2	89	90	−1
4.2	87	91	−1	90	91	−1
4.4	88	91	−1	90	91	−1
4.6	89	92	−1	91	92	−1
4.8	90	92	0	92	92	0
5.0	91	93	0	93	93	0

[a] g is defined by $g=G_1+\lambda G_2$ with λ chosen so that $g=0$ when $\rho=5.0$. The three-decimal values given above have been obtained by rounding off the original four-decimal values.

For this function satisfies both the partial differential equation and the boundary conditions, and is therefore a possible solution. The general uniqueness theorem then tells us that this is the only solution.

All that remains now is to find the solution of Eq. (13), and although there seems to be no simple closed analytical form for the function $g(\rho)$ a numerical solution is very easily constructed.

This function can be expressed in the form

$$g=G_1+\lambda G_2,$$

where G_1 is any solution of the equation

$$G_1''+LG_1'-\frac{1}{\rho^2}G_1=M \qquad (13a)$$

(dashes denoting differentiation with respect to ρ), and G_2 is a suitably chosen complementary function, that is a solution of

$$G_2''+LG_2'-\frac{1}{\rho^2}G_2=0, \qquad (13b)$$

and λ is a numerical constant to be chosen later. With the forms of L, M given by (9a) and (9b) it is readily seen that:

(a) The only solutions for G_1 and G_2 which are finite at $\rho=0$ must vanish at this point; near $\rho=0$ they have the forms

$$G_1=\tfrac{1}{8}\rho^2[1-\tfrac{7}{4}\rho^2+\cdots],$$
$$G_2=\rho[1-\tfrac{3}{4}\rho^2+\cdots].$$

(b) Neither G_1 nor G_2 can vanish for any other value of ρ. Therefore if $g=G_1+\lambda G_2$ we have at once $g=0$ for $\rho=0$, and we can find λ so that $g=0$ for $\rho=\rho_0$ [in fact, $\lambda=-G_1(\rho_0)/G_2(\rho_0)$]. The problem is now reduced to the integration of Eqs. (13a), (13b) with the conditions

$$G_1=0,\quad G_1'=0\quad\text{at}\quad\rho=0,$$
$$G_2=0,\quad G_2'=1\quad\text{at}\quad\rho=0,$$

which can be carried out by standard technique.

Since there is a choice of two forms for the functions L, M two distinct integrations were made, one with the approximate forms of (9c), (9d) and one with the "exact" forms of (9a), (9b) taking $h_0/a=1/200$—this should rank as rather a large value, as we shall see later. These numerical results are given in Table I, and it is at once clear that the error of the approximation is negligible. But the most important property of the functions G_1 and G_2 revealed by the numerical solutions is that they quickly attain virtually constant values; more particularly, their values remain sensibly constant for $\rho\geq5$. It follows that for any given value of λ the function $g=G_1+\lambda G_2$ is itself sensibly constant for $\rho\geq5$. Therefore if we take for ρ_0 any value not less than 5, we shall have, with $\lambda=-G_1(\rho_0)/G_2(\rho_0)$, $g=0$ for $\rho=\rho_0$. In other words, although the quantity ρ_0 is not formally defined its choice need cause no difficulty. The value chosen for the solution of Table I was $\rho_0=5.0$.

A little reflection shows that this lack of sensitivity to the exact position of the boundary is to be expected on physical grounds. For in the immediate vicinity of the region of closest ap-

proach of the two spheres—which is the only region we consider—the pressure must fall off very rapidly with increasing distance from the actual point of closest approach, and therefore so long as we ensure that the boundary is in the region where the pressure has fallen to a small value, the exact position cannot have any great effect on the solution.

4. TOTAL LOAD SUPPORTED BY THE FILM

Since the pressure p does not vary through the thickness of the film the total load supported is simply the integral of p over the xy plane.

Thus,

$$\text{load } P=\int\int p\,dx\,dy=\int_{\pi}^{2\pi}\int_{0}^{r_0} p\,r\,dr\,d\theta$$

$$=\tfrac{3}{2}\mu\omega\sin\alpha\left(\frac{2a}{h_0}\right)^{\frac{1}{2}}\cdot 2ah_0\int_{\pi}^{2\pi}\int_{0}^{\rho_0}\Pi\rho\,d\rho\,d\theta$$

$$=12Ka^2\mu\omega\sin\alpha(2a/h_0)^{\frac{1}{2}} \text{ since } \Pi=g\sin\theta,$$

where

$$K=-\int_{0}^{\rho_0}\rho g(\rho)\,d\rho.$$

From the solutions given in Table I we find

for $s_0=1/200$, $K=0.057$,
$s_0=0$, $K=0.053$ (the approximate case).

Clearly there is no point in keeping many decimals in a quantity such as K, so we may take as a round value $K=1/20$ and write the final result as

$$P=\tfrac{3}{5}a^2\mu\omega\sin\alpha(2a/h_0)^{\frac{1}{2}}. \qquad (14)$$

It is from this equation alone that we derive our criterion for the range of validity of the classical theory; but it is convenient to postpone this until we have obtained the corresponding relation for the torque exerted by the viscous-frictional forces, and have applied both results to the particular orientation of spheres found in the four-ball instrument. These topics are dealt with in the next two sections.

5. TORQUE ON THE STATIONARY SPHERE

As was explained in the Introduction it was considered desirable to obtain the expression for the torque exerted on the stationary sphere in the four-ball apparatus, and this section gives a derivation of the corresponding relation for the pair of spheres considered in the preceding sections. It cannot be claimed that the result obtained here gives anything more than an indication of the leading term of the required relation. For on the one hand we can take into account only the conditions in the region where the flow is converging, since we know nothing of the conditions in the diverging region; and on the other, the unknown dimension r_0 (of which the expression for the load was found to be effectively independent) appears explicitly in the final expression. Nevertheless the result should show the essential features of the relation.

The problem is to find the viscous-frictional torque on a curved surface immersed in a body of liquid whose motion is essentially three-dimensional; this is necessarily rather complicated, and after various attempts to construct an approximate solution it was decided that the only satisfactory method was to use the fundamental tensor-relations for the shear-stress in the liquid. Only the final expression for the torque is needed here, and it would serve no useful purpose to give at this stage the rather heavy algebra of the derivation; but as no explicit treatment of the general case was found in the standard textbooks the analysis is given in an Appendix.

If Γ is the torque about the axis of rotation exerted by the fluid on the stationary sphere, we find the approximate relation

$$\Gamma/\tfrac{1}{2}\pi a^3\mu\omega=\tfrac{1}{5}+\left[\log_e\left(\frac{a}{h_0}\right)-1\right]\sin^2\alpha,$$

and if we put $\log_e(a/h_0)=2.3\log_{10}(a/h_0)$,

$$\Gamma/\tfrac{1}{2}\pi a^3\mu\omega=(\tfrac{1}{5}-\sin^2\alpha)+2.3\sin^2\alpha\log_{10}\left(\frac{a}{h_0}\right). \qquad (15)$$

6. APPLICATION TO THE FOUR-BALL INSTRUMENT

To derive from the foregoing results the expressions for the load and torque for the four-ball instrument we have only to determine the angle α between the axis of the rotating sphere and the line joining the center of this sphere to the center of any one of the fixed spheres.

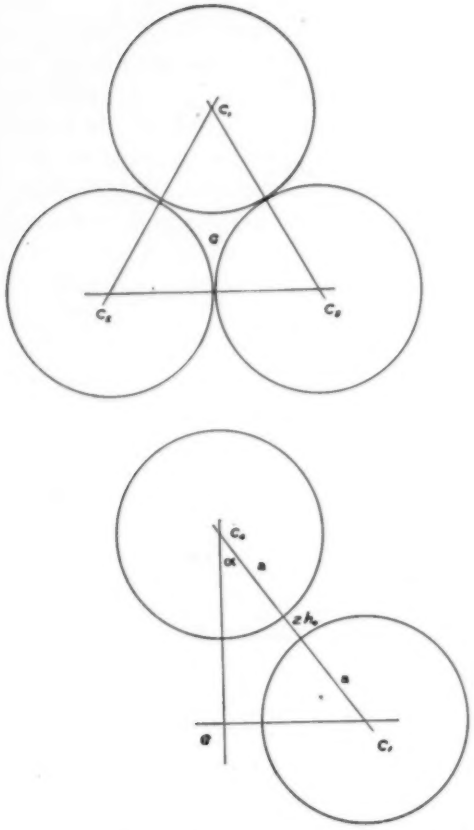

FIG. 4. Geometry of the 4-ball instrument.

The geometry of the system is shown in Fig. 4. It is clear that the vertical axis of rotation must pass through the centroid G of the triangle formed by the centers C_1, C_2, C_3 of the fixed spheres.

Then

$$C_1G=\frac{2\sqrt{3}}{3}a,$$

and so, from the triangle C_4GC_1,

$$\sin\alpha=GC_1/C_1C_4=\frac{2\sqrt{3}}{3}a\Big/2(a+h_0)=(\tfrac{1}{3})^{\frac{1}{2}}\cdot\frac{a}{a+h_0}.$$

Since $h_0\ll a$, we may take

$$\sin\alpha=(\tfrac{1}{3})^{\frac{1}{2}},\quad \cos\alpha=(\tfrac{2}{3})^{\frac{1}{2}}\quad(\alpha\doteq 35°\ 16').\qquad(16)$$

The load P determined in §4 acts along the line of centers C_1C_4; by symmetry therefore the total load supported by the three spheres has zero horizontal component and the vertical component is $3P\cos\alpha$. Thus the total load on the axis is, by (14) and (16),

$$W=3P\cos\alpha=\frac{6}{5}a^2\mu\omega\left(\frac{2a}{h_0}\right)^{\frac{1}{2}}.\qquad(17)$$

The total torque on the axis is, by (15) and (16),

$$T=3\Gamma=\tfrac{3}{2}\pi a^3\mu\omega\left[-\frac{2}{15}+0.77\log_{10}\left(\frac{a}{h_0}\right)\right].\qquad(18)$$

If now we eliminate a/h_0 from these relations, we get the relation between T and W

$$T/\tfrac{3}{2}\pi a^3\mu\omega--=-\frac{2}{15}+1.54\log_{10}\left[W\Big/\frac{6\sqrt{2}}{5}a^2\mu\omega\right],\qquad(19)$$

showing that if experimental values of T and W are found and $T/a^3\mu\omega$ is plotted against $\log(W/a^2\mu\omega)$, then the points should lie on a straight line.

The sizes of the quantities involved are best shown by a numerical example. In applying the relations we must remember that all quantities are presumed to be given in absolute units, so that if a is measured in centimeters, ω in radians per sec., and μ in c.g.s. units (poises) then W will be given in dynes and T in dyne-centimeters.

The usual size of instrument corresponds to spheres of 1-cm diameter, so $a=\frac{1}{2}$; for a rather viscous lubricant we may take $\mu=10$ c.g.s. units at moderate temperatures. Let us take $\omega=N$ r.p.m. $=2\pi N/60$ radians per sec. and $h_0/a=10^{-n}$ (so that $h_0=\frac{1}{2}\cdot 10^{-n}$ cm).

A normal speed of rotation is 1500 r.p.m. and with this value we find (rounding off the numerical coefficients)

$$W=500\times 10^{n/2}\text{ dynes}=0.51\times 10^{n/2}\text{ g wt.},$$
$$T=720n-125\text{ dyne cm}=0.74n-0.13\text{ g cm}.$$

By taking different values for n we obtain a series of related values of load and torque corresponding to a series of film-thicknesses h_0; the results for the range $2\leq n\leq 6$ (i.e., for film-thicknesses ranging from 5×10^{-3} to 5×10^{-7} cm) are given in Fig. 5.

It is now clear that no great loads can be supported by the apparatus if the conditions of film-lubrication are to be fulfilled. There is a lower limit to the thickness of the film, fixed by the size of the irregularities of the surfaces, for

which a value of the order of 10^{-4} cm has been suggested. With this value and even the rather viscous oil considered above, the load W cannot greatly exceed 50 g wt.; even if the speed were raised to 3000 r.p.m., the permissible load would rise only to about 100 g wt. Evidently a load of the order of a kilogram represents a virtual impossibility for an instrument of this size under conditions of film-lubrication, unless it can be established that this regime can be maintained with film-thicknesses of the order of 10^{-6} cm. It is quite certain that under the usual conditions of operation—with loads of 20 to 1000 kg—there can be no hydrodynamical lubrication; this is of course only what was expected, but the investigation has provided the criterion from which we can deduce the range of conditions in which the behavior of the apparatus obeys the laws of hydrodynamical lubrication.

APPENDIX. TORQUE ON THE STATIONARY SPHERE

The stress at any point in a viscous liquid has six independent components which form a symmetrical tensor of the second rank. This tensor is

$$\Psi = -pI + \mu T,$$

where I is the unit tensor and T is the shear-stress tensor, and these can be conveniently written in "dyadic" form

$$I = \mathbf{ii} + \mathbf{jj} + \mathbf{kk},$$

$$T = 2\sum \frac{\partial u}{\partial x}\mathbf{ii} + \sum\left(\frac{\partial w}{\partial y} + \frac{\partial v}{\partial z}\right)(\mathbf{jk} + \mathbf{kj}),$$

where **ijk** are as before the unit vectors along the coordinate axes.[9]

The force on a surface of unit area whose normal has the direction of the unit vector **n** is itself a vector and is given by the scalar product of **n** with the stress tensor in the form

$$\mathbf{F}_n = \Psi \cdot \mathbf{n} = -p\mathbf{n} + \mu T \cdot \mathbf{n}.$$

Now if a force **F** is applied at a point P whose position vector with respect to a fixed point M is **r**, the moment of **F** about M is $\mathbf{r} \wedge \mathbf{F}$; and if through M there passes a fixed axis whose direction is the unit vector **t** then the torque about this axis is $\mathbf{t} \cdot \mathbf{r} \wedge \mathbf{F}$. Thus if for **F** we take the hydrodynamical force $\mathbf{F}_n$, we have the general result that the torque γ about the axis **t** of the force exerted by the liquid on the unit area at the point **r** is

$$\gamma = \mathbf{t} \cdot \mathbf{r} \wedge \mathbf{F}_n = \mathbf{t} \cdot \mathbf{r} \wedge (-p\mathbf{n} + \mu T \cdot \mathbf{n}),$$

where it is understood that the pressure p and the stress-tensor T are evaluated at the point **r**.

The resultant torque Γ of the force exerted on the surface S in the liquid is then simply the integral of γ

i.e., $$\Gamma = \int \gamma dS$$

taken over the surface S.

This result is perfectly general; in any particular case we have only to substitute the appropriate values for **t** (given by the position and direction of the axis), **r**, **n** (given by the form and position of the surface), and p, T (given by the velocity distribution of the flow).

We are interested in the torque, about the axis of rotation of the moving sphere, of the force exerted by the liquid on the fixed sphere; we therefore choose for **t**, **r**, **n** the following values (Fig. 2).

MC_1 is the axis of rotation of the moving sphere and P_2 the general point $(x, y, -h)$ on the fixed sphere.

Then

$$\mathbf{t} = \sin\alpha\mathbf{i} + \cos\alpha\mathbf{k},$$
$$\mathbf{r} = \mathbf{MP}_2 = [x + (a + h_0)\tan\alpha]\mathbf{i} + y\mathbf{j} - h\mathbf{k}.$$

The surface being spherical, the normal at any point has the same direction as the radius drawn

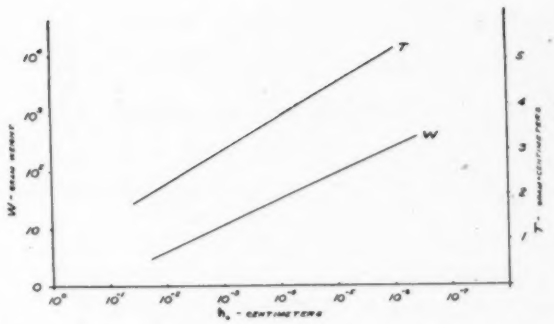

FIG. 5. Numerical values for load (W) and torque (T) for varying minimum film-thickness (h_0).

[9] C. E. Weatherburn, *Advanced Vector Analysis* (G. Bell and Sons, London, 1928), p. 149.

to that point; therefore,

$$a\mathbf{n}=\mathbf{C}_2\mathbf{P}_2=x\mathbf{i}+y\mathbf{j}+Z\mathbf{k}.$$

Evaluating the triple product we find

$$\gamma=(yF_z+ZF_y)\sin\alpha + (xF_y-yF_x)\cos\alpha+2hF_y\sin\alpha,$$

where F_x, F_y, F_z are the components of $\mathbf{F}_n$.

In order to evaluate the tensor components, we need explicit forms for the pressure p and the velocity derivatives $\partial u/\partial x$, etc. The Eqs. (2) and the continuity Eq. (3) together determine these latter; all except $(\partial w/\partial x)$, $(\partial w/\partial y)$ are given immediately, and for these we have first to determine w by integration of $\partial w/\partial z$ with the condition $w=0$ when $z=-h$, and then to differentiate these with respect to x and y in turn. Putting $z=-h$ in these expressions then gives the values required. Since

$$a\mathbf{F}_n=a\mathbf{n}\cdot\Psi=-(x\mathbf{i}+y\mathbf{j}+Z\mathbf{k})p + \mu(x\mathbf{i}+y\mathbf{j}+Z\mathbf{k})\cdot T, = F_x\mathbf{i}+F_y\mathbf{j}+F_z\mathbf{k},$$

we can now express the force components as functions of x and y and hence also the torque γ; the algebra is straightforward but rather heavy, and the final result is

$$\frac{2Zh}{\mu\omega a}\gamma=(x^2+y^2)\cos^2\alpha+2(a+h_0)x\cos\alpha\sin\alpha$$

$$+\left[(a^2+x^2)+\frac{3}{2}\left(1-\frac{h}{Z}\right)y^2+2hZ\right]\sin^2\alpha \qquad \text{(a)}$$

$$-\frac{2h^2}{\mu\omega}\left(x\frac{\partial p}{\partial y}-y\frac{\partial p}{\partial x}\right)\cos\alpha \qquad \text{(b)}$$

$$-\frac{h^2}{\mu\omega Z}\left[y\left(x\frac{\partial p}{\partial x}+y\frac{\partial p}{\partial y}\right)+2Z^2\frac{\partial p}{\partial y}\right]\sin\alpha \qquad \text{(b)}$$

$$-\frac{4h^3}{\mu\omega}\frac{\partial p}{\partial y}\sin\alpha+\frac{4h^4Zy}{a^2\mu\omega}(\nabla^2 p)\sin\alpha \qquad \text{(A)}$$

(the indications "a" and "b" will be explained later).

We have now to integrate this expression over a suitable area of the spherical surface; if we introduce the plane polar coordinates r, θ as in §2 we have for the element of area the expression

$$dS=rdrd\theta/(1-r^2/a^2)^{\frac{1}{2}},$$

and the limits for the integration are $\pi\leq\theta\leq 2\pi$, $0\leq r\leq r_0$. Alternatively we can use a pair of angular coordinates θ, ϕ, where θ is defined as before and ϕ by the relation $r=a\sin\phi$. The limits are now $\pi\leq\theta\leq 2\pi$, $0\leq\phi\leq\phi_0$, where $r_0=a\sin\phi_0$, and the element of area is

$$dS=a^2\sin\phi d\theta d\phi.$$

The first set of coordinates is more convenient for dealing with the terms in γ which involve p explicitly, and the second for the other terms. We have also the relations

$$Z=a+h_0-h=(a^2-r^2)^{\frac{1}{2}}=a\cos\phi,$$

$$r=\rho(2ah_0)^{\frac{1}{2}}$$

$$p=\tfrac{3}{2}\mu\omega\sin\alpha\left(\frac{2a}{h_0}\right)^{\frac{1}{2}}g(\rho)\sin\theta,$$

the function g being given numerically (Table I).

Examination of the terms of (A) shows that those marked (a) vanish identically on integration and that those marked (b) lead to expressions which are of higher order in h/a than the remainder, and which may therefore be neglected since this is a small quantity and we want only the leading term in the expression. Thus we have to integrate only the terms

$$\frac{x^2+y^2}{hZ},\quad\left(\frac{a^2+\frac{1}{2}y^2}{hZ}+2\right)\sin^2\alpha,\quad\frac{2h}{\mu\omega}\frac{\partial p}{\partial y}\sin\alpha.$$

The integration is straightforward and the result is

$$\Gamma/\tfrac{1}{2}\pi a^3\mu\omega=1-\cos\phi_0-\log\cos\phi_0 + \sin^2\alpha[2(1-\cos\phi_0) + \tfrac{1}{2}(1-\cos\phi_0-\log\cos\phi_0) + \log(1+s_0-\cos\phi_0)/s_0\cos\phi_0] + O(s_0\log s_0)-12\sin^2\alpha\int_0^{\rho_0}\rho^2 g\,d\rho,$$

where all logarithms are to the base e.

The leading terms of this expression can be written

$$\Gamma/\tfrac{1}{2}\pi a^3\mu\omega = A + (\log a/h_0 + B)\sin^2\alpha,$$

where

$$A = 1 - \cos\phi_0 - \log\cos\phi_0$$

$$B = 2(1-\cos\phi_0) + \tfrac{1}{4}(1-\cos\phi_0-\log\cos\phi_0) + \log[(1-\cos\phi_0)/\cos\phi_0] - 12\int_0^{\rho_0}\rho^2 g\,d\rho.$$

From the values of $g(\rho)$ in Table I we find

$$-12\int_0^{\rho_0}\rho^2 g\,d\rho = -12\times(-0.098) = 1.2 \text{ approx.},$$

but we cannot hope to determine the values of the terms involving $\cos\phi_0$ with any precision, since we have no precise knowledge of the value of ϕ_0. However we can obtain a rough estimate by the following argument. ϕ_0 is defined by $a\sin\phi_0 = r_0$, where r_0 measures the extent of the region to which the film-theory may be applied. This dimension is determined by the thickness h of the film, and there is the relation

$$h = a + h_0 - (a^2 - r^2)^{\frac{1}{2}} = a + h_0 - a\cos\phi.$$

If we can say that the theory can be applied for thicknesses up to a value h_m, then we can take for ϕ_0 the value given by

$$\cos\phi_0 = 1 - (h_m - h_0)/a.$$

We cannot say that this maximum permissible thickness has a definite value, since the value must depend upon the particular conditions prevailing; but we may not unreasonably suppose it to be considerably greater than the greatest value (10^{-2} cm) of h_0 considered here, so that ϕ_0 is effectively independent of h_0, and $\cos\phi_0 = 1 - h_m/a$. If as a working hypothesis we assume that h_m is not less than about a millimeter, we have the figure 0.1 as an indication of the order of lower limit of h_m/a (since the radius a is of the order of unity) and 0.9 for the upper limit of $\cos\phi_0$.

There is also the relation $\sin\phi_0 = r_0/a$, and the analysis given in the preceding pages makes considerable use of the assumption that r_0 is considerably less than a (since the exact equation for the pressure has a singularity at $r = a$). We may suppose $r_0/a < \frac{1}{2}$, and hence it is suggested that $\cos\phi_0 > \frac{1}{2}(3)^{\frac{1}{2}} = 0.866$.

These arguments are very specious, but they suggest that the order of the constants A, B will be given by taking a value in the region of 0.9 for $\cos\phi_0$; if we tabulate the values for a few values of $\cos\phi_0$ we get

$\cos\phi_0$	A	B
0.95	0.1	−1.7
.90	0.2	−0.9
.85	0.3	−0.3
.80	0.4	+0.1

so we shall not be seriously in error if we choose the round values

$$A = \tfrac{1}{5},\quad B = -1.$$

Thus we have the result that the torque is a linear function of $\log a/h_0$ having approximately the form

$$\Gamma/\tfrac{1}{2}\pi a^3\mu\omega = \tfrac{1}{5} + \left[\log_e\left(\frac{a}{h_0}\right) - 1\right]\sin^2\alpha.$$

This indicates a very slow variation with a/h_0 and it is for this reason that the expression for γ was evaluated in full; it is difficult to ensure that a "leading term" type of argument applied early in the calculation does not neglect terms which are in fact significant.

ACKNOWLEDGMENTS

This investigation was made at the request of Dr. R. Schnurmann of the Manchester Oil Refinery Ltd. (England). The author wishes to express his appreciation of Dr. Schnurmann's personal interest in the work and of his valuable discussion and criticism, and of his company's permission to publish the work. Also the author acknowledges with gratitude the advice he has had from Professor D. R. Hartree, F.R.S.

The Analysis of Multicomponent Mixtures of Hydrocarbons in the Liquid Phase by Means of Infra-Red Absorption Spectroscopy

D. L. FRY, R. E. NUSBAUM
Research Laboratories Division, General Motors Corporation, Detroit, Michigan

AND

H. M. RANDALL
Randall Laboratory of Physics, University of Michigan, Ann Arbor, Michigan

(Received October 17, 1945)

This is a general method of applying infra-red absorption spectroscopy to the analysis of multicomponent hydrocarbon mixtures in the liquid phase. The procedure is calibrated by measuring optical densities of synthetic standard samples. A constant thickness cell is used for both standard and unknown samples. Two procedures for converting optical densities to concentrations are described. Examples are given for four- and five-component mixtures. Data are presented to show the reproducibility of repeated measurements of optical density on the same sample, and results are given to show the agreement between the infra-red analyses and the known composition of synthetic mixtures.

INTRODUCTION

A GENERAL method of applying infra-red absorption spectroscopy to the analysis of multicomponent hydrocarbon mixtures in the liquid phase has been developed and has been applied to two particular mixtures, one containing four components and the other five components. It is an empirical method based upon analytical curves prepared from absorption measurements of pure samples of the components to be found in the unknowns and of binary mixtures of these components.

A number of papers on the application of infra-red absorption spectroscopy to analytical problems have been published. Most of these have been concerned with the analysis of binary mixtures. However, two papers have described methods for the analysis of more complicated mixtures. Brattain, Rasmussen, and Cravath[1] have described a method for analyzing multicomponent mixtures in the vapor phase. This method is most useful when the components are in the vapor phase under normal conditions of temperature and pressure, but can also be used with considerably more difficulty when the compounds are liquids under normal conditions. A method for analyzing a multicomponent mixture in the liquid phase has been described by Nielsen and Smith[2] and the analysis of a three-component mixture has been discussed as an example. This method can be used only over concentration ranges for which deviations from Beer's law are negligible.

The procedures described in the present paper are used for multicomponent mixtures in the liquid phase and are applicable even though the concentrations of any of the components of the mixture vary from 0 to 100 percent.

The absorption of monochromatic radiation as it traverses an absorbing liquid is expressed by Beer's law.

$$acx = \log_{10}(I_0/I), \tag{1}$$

where I is the intensity of the radiation transmitted by x centimeters of liquid containing a concentration c of the absorbing materials; I_0 is the intensity of the radiation impinging on the liquid; and a is a constant of proportionality, known as the absorption coefficient. a is constant for any monochromatic radiation regardless of the values of c, x, or I_0.

For a mixture of two or more non-associating components, all of which selectively absorb somewhat over the whole infra-red region, Beer's law takes the following form for monochromatic radiation:

$$(a_1c_1+a_2c_2+a_3c_3+\cdots+a_nc_n)x = \log_{10}\frac{I_0}{I}, \tag{2}$$

[1] R. Robert Brattain, R. S. Rasmussen, and A. M. Cravath, J. App. Phys. **14**, 418 (1943).

[2] J. Rud Nielsen and Don C. Smith, Ind. Eng. Chem. Anal. Ed. **15**, 609 (1943).

where a_1 is the absorption coefficient of material (1) and c_1 its concentration in the cell of thickness x; a_2, $a_3 \cdots a_n$ and c_2, $c_3 \cdots c_n$ are the corresponding values for materials 2, $3 \cdots n$.

In actual practice, however, Eq. (1) and, therefore, Eq. (2) does not hold exactly. This is shown experimentally by the fact that a curve of log I_0/I as a function of concentration with a constant thickness cell is not a straight line. This results from the fact that no spectrometer produces a monochromatic image at the receiver. Instead, there is produced an image containing a wave-length band $\Delta\lambda$.

Equation (3) is obtained by combining Eqs. (1) and (2).

$$\text{Log}\frac{I_0}{I}=\log\frac{I_0}{I_1}+\log\frac{I_0}{I_2}+\cdots+\log\frac{I_0}{I_n}. \quad (3)$$

The terms

$$\log\frac{I_0}{I_1}, \quad \log\frac{I_0}{I_2}, \quad \cdots\log\frac{I_0}{I_n}$$

are the values obtained for materials 1, $2 \cdots n$ at the chosen spectral position. In other words, the equation states that the optical density of a mixture is equal to the sum of the optical densities of the individual components of the mixture. Equation (3) does not contain the absorption coefficient and, therefore, is not subject to the same limitations as are (1) and (2).

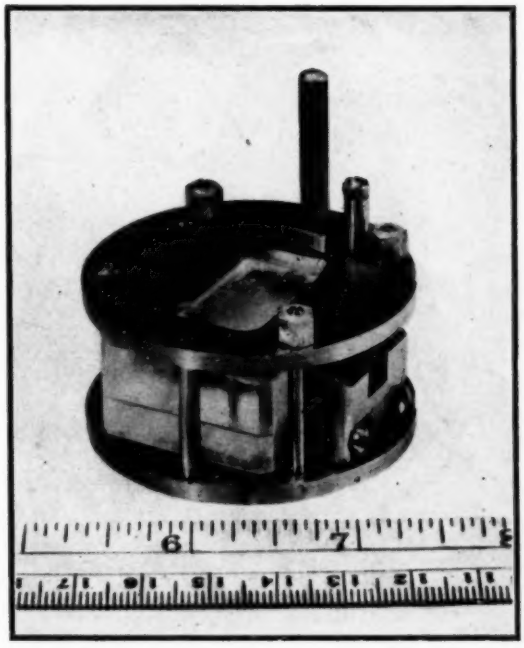

FIG. 1. An assembled cell used to obtain the infra-red absorption of liquids.

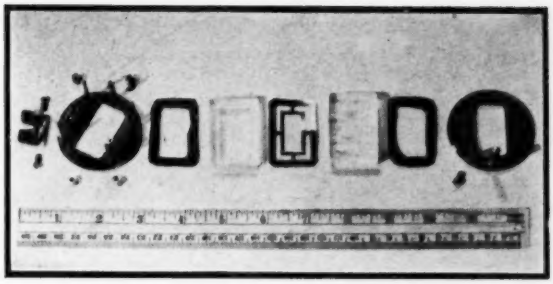

FIG. 2. Unassembled parts of a cell used in measuring the infra-red absorption of liquids.

DEVELOPMENT OF ANALYTICAL PROCEDURE

The problem in the work described here, as well as in the work of others, has been to develop a method of applying absorption spectroscopy taking into account these limitations of Beer's law. The fundamental problem of quantitative analysis in absorption spectroscopy is the determination of the log I_0/I values with sufficiently high accuracy, and the conversion of these values to percent concentration of the components in the mixture.

Absorption Cells

In the present work, optical densities are measured with a University of Michigan infrared spectrophotometer[3,4] equipped with a sodium chloride prism. Two cells are used. The background cell, consisting of a single salt plate $\frac{1}{2}''$ thick, is used to determine I_0 values. The absorption cell, shown in Fig. 1 and Fig. 2, is a modification of a cell described by Randall.[5] The frame which holds the salt plates is designed particularly for use with the University of Michigan instrument.

Starting from the left, each piece in Fig. 2 goes on top of the previous one. The salt plates of the absorption cell are $\frac{1}{4}''$ thick. They are separated by a platinum shim, the thickness of

[3] H. M. Randall and John Strong, Rev. Sci. Inst. **2**, 585 (1931).
[4] Robert A. Oetjen and H. M. Randall, unpublished thesis, University of Michigan, 1941.
[5] H. M. Randall, Rev. Sci. Inst. **10**, 195 (1939).

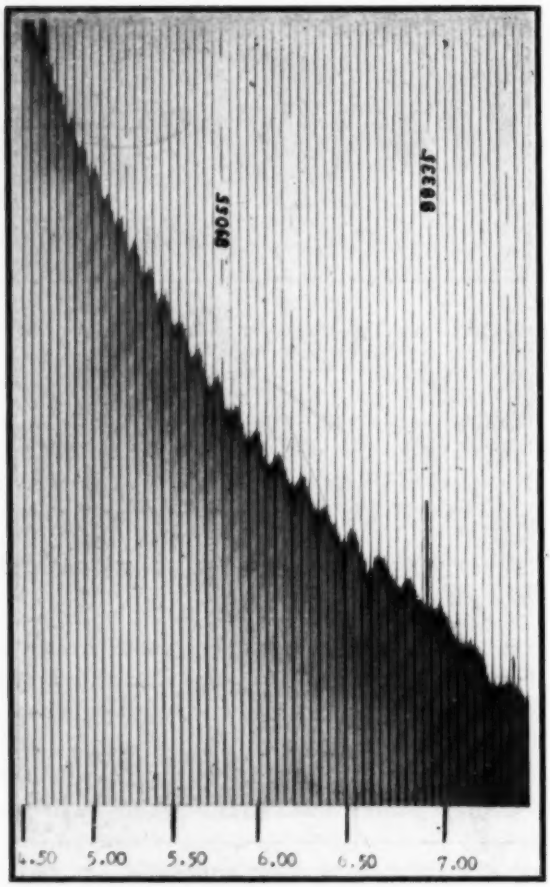

FIG. 3. A record of the interference fringe pattern obtained with a cell 0.152 mm thick.

which determines the thickness of the absorbing layer of sample. For the work described here the shim is 0.152 mm thick. The positions of the salt plates and the shim are determined by the dowl pins in the cell supports. Two rubber washers separate the salt from the stainless steel housing. After the cell is assembled, a mercury seal is established by introducing mercury into the trough in the lower plate through a hole which extends through the upper salt plate, rubber washer, and support. The liquid to be examined is introduced through one of the two holes on the side of the upper plate. Rubber pads are pressed over the holes to seal them without putting pressure on the contents of the cell. This method of sealing makes it possible to use the cell in an evacuated source box. The cell can be taken apart, cleaned, and reassembled in less than 10 minutes. However, it can be refilled in less than two minutes by expelling the liquid with an air syringe and filling with an eye dropper.

In order to use the present method successfully, it is important that the thickness of the absorption cell remain constant. The two salt plates are ground flat with corundum in ethyl alcohol, and polished on a piece of white felt stretched over a piece of plate glass. Titanium oxide is used as the abrasive for polishing, and ethyl alcohol is used to wet the titanium oxide. The finished plates are examined with an optical flat and sodium light, and if they are not flat within four diffraction fringes (i.e., 0.0012 mm) the process is repeated. The plates are examined frequently to determine whether cleaning has caused deviation from flatness.

The cells are supported in a tube directly in front of the salt window at the entrance slit of the spectrometer. The notch in the frame of the cell locates it in a given fixed position in front of the slit. The cells are handled by means of a knurled rod screwed into the upper plate.

The thickness of the cell is determined by the interference fringe method as described by Smith and Miller.[6] (See Fig. 3.) Repeat measurements made several months apart show the thickness to be 0.152 ± 0.0005 mm.

Spectral Positions

The approximate spectral positions at which optical densities are determined are selected from the records of the spectra of the pure components in the region from 3 to 13.5μ. (See Fig. 4.)

In order to obtain high resolution for these records the spectrograph is operated with narrow slits and slow rotation of the prism. The source of light is a Nernst glower. The light beam is interrupted by means of a shutter having a period of 3.8 seconds, and the output of the thermopile is amplified by a Firestone amplifier.[7] The recording galvanometer is five meters from the camera drum. The spectra are recorded in small sections with constant slits, and an overlapping of these sections of spectrum occurs whenever the slit widths are changed. Table I gives the maximum theoretical resolution ob-

[6] Don C. Smith and Elmer C. Miller, J. Opt. Soc. Am. **34**, 130 (1944).
[7] F. A. Firestone, Rev. Sci. Inst. **3**, 163 (1932).

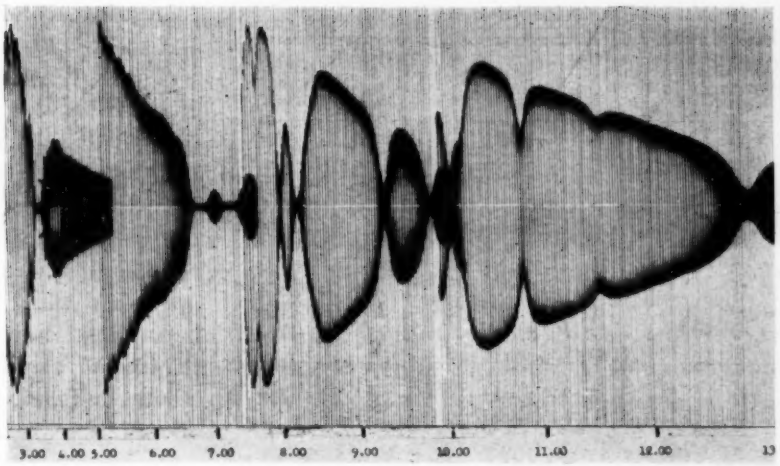

FIG. 4. The absorption spectrum of 2,2 dimethylbutane in the region 2.5 to 13.5μ.

tainable with the slit widths necessary to get half scale deflections with this amplifier.[4] Actually the resolution realized with the instrument is somewhat less than the theoretical value.

In the analysis of an n component mixture it is necessary and sufficient to determine log I_0/I values of the mixtures at n different spectral positions. When a procedure is being developed for a given mixture, the spectra of the pure components are examined and n positions are selected in such a way that a different component contributes a maximum amount of absorption at each position. It is desirable but not necessary that at each wave-length position the absorption of one component be greater than that due to any other component; and further, that the component showing major absorption be different at each of the n wave-length positions. The spectral positions which yield most accurate analyses are those at which the absorption of one component is large compared to the sum of the absorptions of all other components (assuming all components are present in concentrations similar to those in an unknown mixture). In general, this condition is found at the position of maximum absorption of a band for one component.

There are some other factors to be considered in the selection of these wave-length positions. For example, in order to reduce the time necessary to make an analysis, it may be desirable to select bands near each other. It may be desirable to select positions which are outside of the water vapor region. If one thickness of the absorption cell is to be used, the selection of the wave-length positions may depend upon the intensities of the bands; however, as far as possible, thinner absorption cells should be used when the bands are strong, and thicker ones should be used when the bands are weak. The selection of these positions is often complicated by the fact that several bands interfere with one another. This difficulty can be minimized by using the narrowest slits permitted by the sensitivity of the receiver and the available amplification of its output.

Determination of log I_0/I Values

For the measurement of log I_0/I values, the thermopile in the spectrometer is connected directly to a galvanometer with a sensitivity of one-tenth microvolt per millimeter at one meter.

TABLE I. Theoretical resolution of the spectrograph.

λ	Actual slit widths*	Effective slit widths	$\frac{\lambda}{d\lambda}$	$B\frac{dn}{d\lambda}$
2μ	0.04 mm	0.0097μ	208	640
3	0.04	0.0117	257	440
4	0.05	0.0128	314	560
5	0.06	0.0118	424	640
6	0.07	0.0117	514	800
7	0.08	0.0117	600	960
8	0.09	0.0117	686	1080
9	0.11	0.0127	711	1160
10	0.13	0.0130	768	1240
11	0.16	0.0140	787	1560
12	0.20	0.0163	738	1720
13	0.24	0.0183	711	1800
14	0.35	0.0238	589	2080
15	0.55	0.0339	443	2240

* These slit widths produce half scale deflection.

TABLE II. Resolution for operating conditions.

Spectral position $\lambda(\mu)$	Actual slit widths (mm)	Effective slit width (μ) ($d\lambda$)	Actual resolution $\lambda/d\lambda$	Prism resolution $Bdn/d\lambda$
8.23	0.55	0.071	116	1100
8.55	0.60	0.075	114	1120
8.88	0.70	0.092	96	1152
10.50	0.90	0.085	123	1400
11.28	1.10	0.096	117	1600
9.13	0.7	0.080	114	1168
10.31	0.9	0.088	117	1336
11.89	1.2	0.100	119	1704
12.30	1.3	0.116	107	1752

The scale-to-galvanometer distance for the present work is five meters. With this system it is necessary to use wider slits and therefore to accept lower resolution than that realized with the amplifier, but the accuracy of measurements is much better. The actual resolutions for the slit widths used are shown in Table II.

When the procedure for a given mixture is developed, the slit widths for each spectral position are set to give approximately 400-mm deflection when a non-absorbing material (background cell) is in the light path. Of course, after the necessary calibrations have been made for the analysis of a particular mixture, the same slit widths must always be used for this analysis.

After the proper slit widths have been selected, the spectral positions are re-examined under the conditions which would be used in making the analyses, that is with wide slits and very slow rotation of the prism. These records for the hexanes are shown in Fig. 5. The upper line on each of the records shows the deflection of the galvanometer for the background cell. The bottom lines in the figures show the zero positions, and displacements along these lines in the vertical direction represent zero shift. The absorption curves lying between the background curve and the zero lines are as designated. Correct log I_0/I values can be obtained only if (1) the deflection of the galvanometer is a known function of the energy striking the thermopile and (2) all energy reaching the thermopile lies in the selected wave-length interval. In the present case, all tests have shown the galvanometer system to be linear. However, the energy reaching the thermopile actually includes some energy in addition to that from the wave-length interval, $\Delta\lambda$. This wave-length interval is determined by the slit width and the region of the spectrum for which the spectrometer is set. The radiation in this wave-length interval which passes through the absorption cell and strikes the thermopile is the radiation which should be measured. Any other energy which causes a change in the galvanometer deflection (or other measuring instrument) when the shutter is opened is called false energy and its effect must be taken into account.

Most of this false energy is probably due to scattering from various parts of the spectrometer of radiation in the region 1 to 4μ which is the region of maximum intensity incident on the

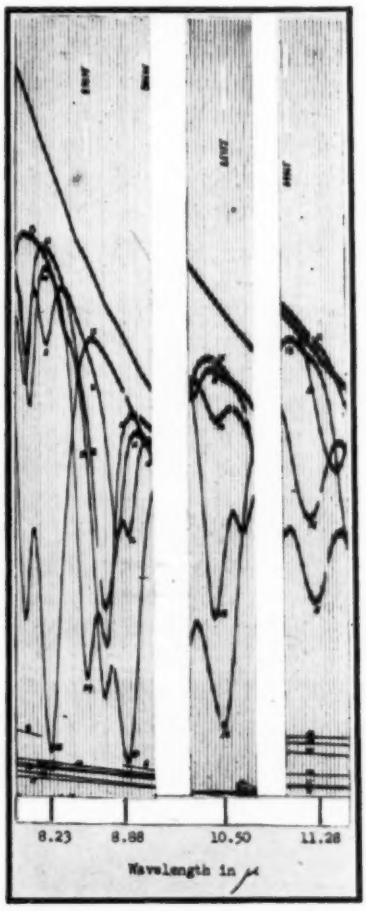

FIG. 5. Portions of the spectra of the five hexanes.

Curve no.	Component	Position of band
11	n hexane	11.28μ
12	3 methylpentane	10.50
13	2,3 dimethylbutane	8.88
14	2 methylpentane	8.55
15	2,2 dimethylbutane	8.23

entrance slit. This energy interferes mostly at long wave-lengths (6 to 15μ) where the true energy is small and the slits are wide. When working above 7μ most of the false energy can be cancelled out by using a mica shutter which transmits most of the radiation up to 5μ but none above 7μ. In this case the radiation below 5μ always passes into the spectrometer and is therefore included in the "zero" reading. Only the radiation of wave-lengths greater than 7μ is interrupted by the mica shutter. However, this method does not cancel out all the false energy; therefore, more refinement is necessary. A method of making partial correction for the remaining false energy has been established by using a piece of Cellophane which has two regions of 100 percent absorption, one at 9.15μ and one at 11.90μ, and obtaining the difference in the galvanometer deflections when the cells are in the light path with, first the Cellophane, and second the mica shutter. The amount of false energy when the background cell is in the light path is different from the amount when the liquid cell is in, but is practically the same for all liquids used in the liquid cell. It is proportional to I_0 at any given wave-length and therefore can be expressed as a percent of I_0. The false energy values at the two bands in the spectrum of the Cellophane film have been plotted on a graph showing wave-length *versus* false energy and a straight line has been drawn between the points. (See Fig. 6.) Curve (1) is for the background cell and curve (2) is for the liquid cell with any of the nine pure components in it. At every spectral position and given slit width, I_0 is made the same for all observations. Therefore, the false energy corrections can be converted to mm deflection and subtracted from the I and I_0 values obtained, as shown in Table III.

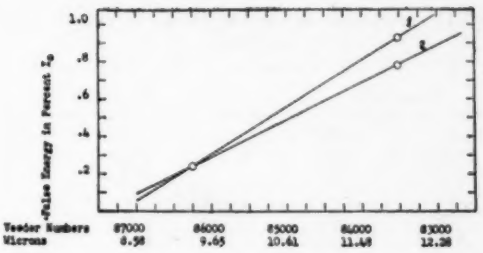

FIG. 6. False energy as a function of wave-length.

With the equipment used in this work there is some zero drift and the intensity of the light source is not perfectly controlled. For this reason the procedure in making a measurement at a given spectral position consists of making three readings as follows: (*a*) with the absorption cell alone in the light path, (*b*) with the cell plus a mica shutter in the light path, and (*c*) with the absorption cell again alone in the light path.

The averaging of (*a*) and (*c*) in general cancels out the zero drift and the subtraction of this average from (*b*) gives (*k*). This number is proportional to the difference in the energy which falls on the thermopile with the two shutter positions. In other words, (*k*) is proportional to the energy which is interrupted by a mica shutter. A similar value (*L*) is obtained with the background cell. Then because the source may have changed its intensity during this interval of time, a value similar to (*k*), called (*m*), is again obtained. (*k*) and (*m*) are then averaged to give (*n*). This should, in general, cancel out any errors due to slow changes in the source. (*n*), therefore, is I plus the false energy F and

TABLE III. False energy corrections for each spectral position and slit width.

Principal absorber	$\lambda(\mu)$	cm^{-1}	Slit widths (mm.)	I_0 (mm)	False energy correction I_0 (mm)	I (mm)
2,3 dimethylbutene−1	9.13	1096	0.70	320.0	0.5	0.5
2,3 dimethylbutene−2	10.31	970	0.90	345.0	2.0	1.5
2,2,3 trimethylbutene	11.89	841	1.30	390.0	3.5	3.0
Methylpentenes	12.30	813	1.40	375.0	4.0	3.5
2,2 dimethylbutane	8.23	1215	0.55	450.0	0.5	0.5
2 methylpentane	8.55	1170	0.60	420.0	0.5	0.5
2,3 dimethylbutane	8.88	1126	0.70	495.0	0.5	0.5
2 methylpentane	10.50	952	0.90	430.0	2.0	2.0
n hexane	11.28	886	1.10	430.0	3.0	2.5

TABLE IV. Standard deviations of log I_0/I values for two samples.

Sample 223		Sample 756	
0.549	0.549	0.153	0.154
.550	.554	.153	.154
.548	.545	.153	.150
.548	.547	.152	.151
.548	.548	.150	.150
.549	.548	.152	.149
.547	.544	.149	.153
.551	.548	.155	.148
.550	.546	.153	.147
.552	.548	.145	.150
.551	.552	.149	.151
.547	.550	.150	.150
.549	.550	.151	.152
.546	.551	.151	.149
.548	.548	.149	.151
Average	.548		.151
Max. dev. from the mean	.004		.006
Std. dev.	.0022		.0023

(L) is I_0 plus the false energy F_0. These observations are written in a data sheet as follows:

Absorption cell			Background cell		
Shutter open (a) (g)	Shutter closed (b) (h)	Shutter open (c) (j)	Shutter open (d)	Shutter closed (e)	Shutter open (f)

The values of I_0+F_0 and $I+F$ are obtained from the above readings in the following manner:

$$(b)-\left[\frac{(a)+(c)}{2}\right]=(k), \quad (e)-\left[\frac{(d)+(f)}{2}\right]=(L),$$

$$(h)-\left[\frac{(g)+(j)}{2}\right]=(m), \qquad \frac{(k)+(m)}{2}=(n),$$

$$(L)=I_0+F_0, \quad (n)=I+F.$$

F and F_0 are the false energy values which are subtracted to determine I_0 and I (see Table III).

It is essential in this method that changes in optical densities due to unavoidable changes in the two cells be known. It is, therefore, desirable to have a standard absorbing material which can be checked daily. This check is made with a "pure" sample of 2,2,3 trimethylbutene at 11.89μ at the beginning and end of each day. When the log I_0/I deviates from the standard value (0.600) by more than 0.003, all values of log I_0/I determined on that day are corrected by adding or subtracting the indicated amount.

Reproducibility in Determining log I_0/I Values

Thirty determinations of log I_0/I values at one spectral position for two samples have been made over a period of three months. These values are listed in Table IV.

The standard deviations for the two sets of data are essentially the same even though the amount of absorption differs. For this particular case a change of 0.002 in log I_0/I represents a change of 0.3 percent in the concentration of the component sought. For a cell twice as thick it would represent 0.15 percent, for one-half as thick, 0.6 percent. Likewise the deviation in terms of percent concentration would be more or less, depending on whether the principal absorber absorbs more or less at this wave-length.

Analytical Curves

In making infra-red analyses it is necessary to convert values of log I_0/I to concentrations. The conversion may be made by means of analytical curves each of which shows log I_0/I as a function of concentration of a particular compound. In the present work with liquids, the data for such a curve are obtained by measuring log I_0/I with binary mixtures in the absorption cell.

The amount of absorbing material in the path is varied by using a cell of constant thickness and diluting the absorber with one of the compounds which has a high transmission at the wave-length in question. Three series of binary mixtures were made for the four-component mixture and four series were made for the hexane mixture. These solutions have concentrations as shown in Table V. It will be seen that for the four-component problem, one of the components of all the mixtures is 2,3 dimethylbutene−2. This was selected because it absorbs strongly at only one of the spectral positions. At all the other positions it absorbs very little. In the case of the hexane series 2,2 dimethylbutane was selected as the common component.

The preliminary analytical curves are obtained by plotting, for each spectral position, a curve showing percent concentration of the material diluted, which is 100 percent in the "a" solution (Table V), *versus* the log I_0/I for each of the binary mixtures (a through h) in the series. For the four-component problem, this means three

TABLE V. Compositions of binary mixtures used for analytical curves.

Mixture series no.	Components	Amounts by percent volume							
		a	*b*	*c*	*d*	*e*	*f*	*g*	*h*
		Four component mixtures							
1	Methylpentenes	100	64	32	16	8	4	2	0
	2,3 dimethylbutene−2	0	36	68	84	92	96	98	100
2	2,3 dimethylbutene−1	100	64	32	16	8	4	2	0
	2,3 dimethylbutene−2	0	36	68	84	92	96	98	100
3	2,2,3 trimethylbutene	100	64	32	16	8	4	2	0
	2,3 dimethylbutene−2	0	36	68	84	92	96	98	100
		Hexane mixtures							
11	Normal hexane	100	80	60	30	15	7	4	0
	2,2 dimethylbutane	0	20	40	70	85	93	96	100
12	3 methylpentane	100	80	60	40	20	10	5	0
	2,2 dimethylbutane	0	20	40	60	80	90	95	100
13	2,3 dimethylbutane	100	80	60	40	20	10	5	0
	2,2 dimethylbutane	0	20	40	60	80	90	95	100
14	2 methylpentane	100	80	60	40	20	10	5	0
	2,2 dimethylbutane	0	20	40	60	80	90	95	100

curves at each of the four spectral positions, and for the hexanes, four curves at each of the five spectral positions.

The final analytical curves are obtained from these preliminary curves by a procedure which will now be described. First, the final analytical curve of the component which has the least absorption at the spectral position being considered is drawn as a straight line from the (0.0) point to the point at 100 percent concentration. This is illustrated by Fig. 7 which is a graph of the preliminary and final analytical curves at 9.31μ for the four-component mixture. At this spectral position 2,2,3 trimethylbutene (*C*, Fig. 7) is the least absorbing pure compound. The contribution of this component to the log I_0/I value of the binary mixtures of this compound with 2,3 dimethylbutene−2 is determined from this final curve for 2,2,3 trimethylbutene. This contribution (lower *C* curve, Fig. 7) is subtracted from the preliminary curve of the binary mixture of these two components (upper *C* curve, Fig. 7) at a convenient number of points. These differences are the contribution to the log I_0/I values of 2,3 dimethylbutene−2 in each binary mixture and, when plotted against the concentration of 2,3 dimethylbutene−2, represent the final analytical curve of this component. As 2,3 dimethylbutene−2 is the common component in binary mixtures of each of the other compounds, the final analytical curves for the remaining two compounds can be obtained by a series of subtractions similar to that described above. (Subtract difference between upper and lower *C* curves from upper *A* and *D* curves to obtain lower *A* and *D* curves). In this way an analytical curve for each of the components in the four-component mixture has been obtained

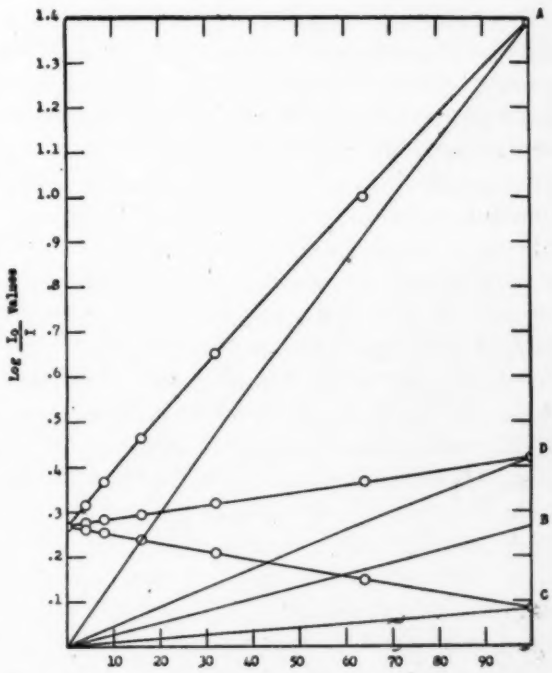

FIG. 7. Analytical curves at 9.31μ. Curves with circles are preliminary curves.

A. 2,3 dimethylbutene−1
B. 2,3 dimethylbutene−2
C. 2,2,3 trimethylbutene
D. methylpentene

at each of the four spectral positions (16 curves). For the hexane mixtures there are five curves at each of five spectral positions or a total of 25 curves.

After the analytical curves are obtained, it is possible to analyze mixtures which contain any or all of the components in any possible concentration. To do this, it is necessary only to obtain the log I_0/I values at all the spectral positions (n, if an n component mixture) and to convert them to concentrations by use of one of the two methods described below.

Two Methods of Converting Optical Densities to Concentrations

One method of converting optical densities to concentrations is a method of graphical approximation. In this case the analyses are arrived at by successive approximations based upon the final analytical curves. (See Fig. 7.) This method presupposes that the optical density of the mixture is equal to the sum of the optical densities of the component parts of that mixture as expressed in Eq. (3).

In converting optical densities to concentrations by this method, the log I_0/I value at one spectral position is applied to the analytical curve of the material which has its major absorption at that wave-length, and the first approximation of percent concentration for that component is read from the curve. The log I_0/I value at a second spectral position is corrected by subtracting the contribution of the first component at this wave-length. The corrected log I_0/I value is applied to the analytical curve of the material which has its major absorption at this position to obtain the first approximation for this component. The log I_0/I value at a third spectral position is corrected for the contribution of the first and second components and the corrected log I_0/I value is applied to the appropriate curve to obtain the first approximation for this third component. This procedure is continued until the first approximation is obtained for all components of the mixture. Successive approximations are obtained by repeating this process for each component, always using the latest approximate concentration of the other components. This is continued until two consecutive sets of approximations are the same. The last set of values is the analysis of the mixture.

The analytical curves can be used graphically, as just described, or they can be used to obtain mathematical expressions to make the same approximations. In this paper the latter will be called a method of applied corrections. The analytical curves, in general, are not straight lines (see Fig. 7). However, a straight line drawn between the points on the curve corresponding to concentration = 0 and concentration = 50 percent does not deviate far from the analytical curve at any point. Each of these straight lines is represented by an equation such as (1). The slopes of the straight lines are the approximate absorption coefficients, so that the optical density (log I_0/I) of a mixture at a given spectral point can be written from Eq. (2) as:

$$(\log I_0/I)_{\lambda_j} = b_{1_j}c_1 + b_{2_j}c_2 + b_{3_j}c + \cdots b_{n_j}c_n, \quad (4)$$

where b_{i_j}, $b_{2_j}\cdots n_{n_j}$ are the slopes of the straight lines referred to above for components 1, $2\cdots n$ at wave-length λ_j, and c_1, $c_2\cdots c_n$ are the concentrations. There is one of these equations for each of the 1, 2, $3\cdots n$ wave-lengths.

For the four-component mixtures the equations are:

$$\begin{aligned}
\left(\log \frac{I_0}{I}\right)_{\lambda_1} &= 0.01442c_1 + 0.00270c_2 \\
&\quad + 0.00840c_3 + 0.00499c_4, \\
\left(\log \frac{I_0}{I}\right)_{\lambda_2} &= 0.00193c_1 + 0.00391c_2 \\
&\quad + 0.00136c_3 + 0.00601c_4, \\
\left(\log \frac{I_0}{I}\right)_{\lambda_3} &= 0.00155c_1 + 0.00082c_2 \\
&\quad + 0.00622c_3 + 0.00757c_4, \\
\left(\log \frac{I_0}{I}\right)_{\lambda_4} &= 0.00080c_1 + 0.00125c_2 \\
&\quad + 0.00092c_3 + 0.02792c_4,
\end{aligned} \quad (5)$$

where the λ's and c's are as follows:

$\lambda_1 = 9.12\mu$ c_1 is the concentration of 2,3 dimethylbutene−1,

$\lambda_2 = 10.31\mu$ c_2 is the concentration of 2,3 dimethylbutene−2,

$\lambda_3 = 11.89\mu$ c_3 is the concentration of 2,2,3 trimethylbutene,

$\lambda_4 = 12.30\mu$ c_4 is the concentration of methylpentenes.

With considerable effort the above four equations can be solved for the concentrations, giving Eqs. (6).

$$
\begin{aligned}
c_1 &= 76.28\left(\log\frac{I_0}{I_1}\right) - 52.72\left(\log\frac{I_0}{I_2}\right) \\
&\quad + 1.335\left(\log\frac{I_0}{I_3}\right) - 0.7350\left(\log\frac{I_0}{I_4}\right), \\
c_2 &= -32.10\left(\log\frac{I_0}{I_1}\right) + 304.0\left(\log\frac{I_0}{I_2}\right) \\
&\quad - 55.45\left(\log\frac{I_0}{I_3}\right) - 45.47\left(\log\frac{I_0}{I_4}\right), \\
c_3 &= -14.48\left(\log\frac{I_0}{I_1}\right) - 12.52\left(\log\frac{I_0}{I_2}\right) \\
&\quad + 171.7\left(\log\frac{I_0}{I_3}\right) - 41.67\left(\log\frac{I_0}{I_4}\right), \\
c_4 &= -0.2710\left(\log\frac{I_0}{I_1}\right) - 11.69\left(\log\frac{I_0}{I_2}\right) \\
&\quad - 3.214\left(\log\frac{I_0}{I_3}\right) + 39.19\left(\log\frac{I_0}{I_4}\right).
\end{aligned}
\tag{6}
$$

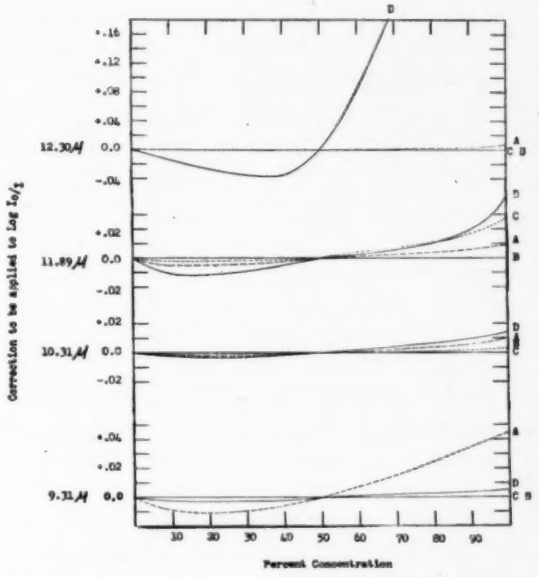

FIG. 8. Correction curves for four-component mixture used with method of applied corrections. (See Fig. 7 for explanation of *A*, *B*, *C*, and *D*.)

Equations (6) are used in connection with a series of correction curves which are obtained in the following manner: the differences between the $\log(I_0/I)$ values as obtained from the analytical curves and the straight lines mentioned above are plotted against the concentrations of each component at each wave-length. For the four-component mixture, these are shown in Fig. 8.

TABLE VI. Results of analyses of synthetic mixtures of four components.

Sample no.	2,3 dimethylbutene −1 Actual	2,3 dimethylbutene −1 Spec.	2,3 dimethylbutene −2 Actual	2,3 dimethylbutene −2 Spec.	2,2,3 trimethylbutene Actual	2,2,3 trimethylbutene Spec.	Methylpentenes Actual	Methylpentenes Spec.
U–1	25.0%	25.2%	25.0%	23.2%	25.0%	25.7%	25.0%	24.9%
U–2	30.0	30.4	20.0	18.5	30.0	31.4	20.0	19.9
U–3	20.0	20.1	30.0	29.3	35.0	36.9	15.0	15.1
U–5	33.3	33.2	33.3	33.9	33.3	33.6	0.0	0.0
U–6	33.3	34.0	33.3	33.5	0.0	0.0	33.3	33.3
U–7	0.0	0.0	33.3	34.0	33.3	34.3	33.3	33.6
U–8	33.3	33.5	0.0	0.0	33.3	34.3	33.3	33.7
O–1	25.0	24.6	25.0	23.9	25.0	24.4	25.0	25.2
O–2	12.5	11.5	62.5	63.5	12.5	11.2	12.5	12.3
O–3	42.0	42.8	18.0	17.3	20.0	19.0	20.0	19.4
O–4	36.0	35.6	18.0	16.9	26.0	25.1	20.0	20.5
O–5	33.3	33.6	33.3	31.9	33.3	32.6	0.0	0.0
O–6	33.3	33.6	0.0	0.0	33.3	33.5	33.3	33.0
O–8	33.3	33.1	33.3	33.0	0.0	0.3	33.3	33.0
O–9	50.0	50.7	0.0	0.0	50.0	50.1	0.0	0.0
O–10	0.0	0.0	0.0	1.1	50.0	49.7	50.0	49.9
O–11	2.5	1.9	3.0	3.0	90.0	88.8	4.5	4.9
Av. dev.	0.36%		0.72%		0.77%		0.25%	
Max. dev.	1.0		1.8		1.9		0.6	

TABLE VII. Results of analyses of synthetic mixtures of five components.

Sample no.	2,2 dimethylbutane Actual	Spec.	2,3 dimethylbutane Actual	Spec.	2 methylpentane Actual	Spec.	3 methylpentane Actual	Spec.	n hexane Actual	Spec.
H–1	20.0%	20.4%	20.0%	19.8%	20.0%	19.2%	20.0%	19.6%	20.0%	19.8%
H–2	10.0	10.4	10.0	10.1	10.0	9.7	10.0	9.6	60.0	59.2
H–3	5.0	5.4	5.0	5.3	5.0	5.0	55.0	54.0	30.0	28.4
H–4	2.5	2.8	52.5	51.8	2.5	2.2	27.5	27.1	15.0	15.1
H–5	1.2	1.6	26.3	25.9	51.2	50.3	13.8	13.1	7.5	7.8
H–6	50.6	50.7	13.1	13.3	25.6	24.7	6.9	6.8	3.8	4.4
Av. dev.	0.33%		0.32%		0.54%		0.50%		0.60%	
Max. dev.	0.4		0.7		0.9		1.0		1.6	

To make an analysis the log (I_0/I) values of the mixture are determined at each of the selected spectral positions and are substituted in Eqs. (6). The first approximate concentrations are obtained from these equations. The correction to be applied to the experimentally determined log (I_0/I) at each wave-length position is determined by subtracting the sum of the values obtained from the correction. These new log (I_0/I) values are then used in Eq. (6) and second approximate concentrations are determined. This process is carried on until the concentrations are the same for two consecutive approximations. The last set of values is the analysis. In the present work, three approximations have been sufficient.

DISCUSSION OF DATA

In order to check the methods, synthetic mixtures have been made and analyzed. The results are shown in Table VI for the four-component mixture and in Table VII for the hexanes. It will be seen that in no case does the analysis obtained deviate from the actual composition

TABLE VIII. Comparison of results by two methods.

Sample no.	2,3 dimethylbutene −1 Graphical approximation	Applied correction	2,3 dimethylbutene −2 Graphical approximation	Applied correction	2,2,3 trimethylbutene Graphical approximation	Applied correction	Methylpentenes Graphical approximation	Applied correction
O–3	20.1%	19.8%	29.3%	29.1%	36.9%	37.0%	15.1%	15.1%
O–4	35.6	35.5	16.9	16.6	25.1	24.7	20.5	20.4
O–5	33.7	33.6	32.2	31.9	32.5	32.6	0.0	0.0
O–11	2.0	1.9	2.9	3.0	89.2	88.8	5.0	4.9

TABLE IX. Data showing the effects of extraneous elements.

Sample		2,3 dimethyl-butene −1	2,3 dimethyl butene −2	2,2,3 trimethyl-butene	Methyl-pentene	2 methyl butene −2	Octene cut
U–5	As made	33.3%	33.3%	33.3%	0.0%	0.0%	0.0%
	Analysis	33.2	33.9	33.6	0.0	Assumed Absent	
	As made	32.5	32.5	32.5	0.0	2.5	0.0
	Analysis	33.4	35.8	28.1	2.4	Assumed Absent	
U–7	As made	0.0	33.3	33.3	33.3	0.0	0.0
	Analysis	0.0	34.0	34.3	33.6	Assumed Absent	
	As made	0.0	32.5	32.5	32.5	0.0	2.5
	Analysis	0.0	33.5	33.5	32.6	Assumed Absent	
U–8	As made	33.3	0.0	33.3	33.3	0.0	0.0
	Analysis	33.5	0.0	34.3	33.7	Assumed Absent	
	As made	31.5	0.0	31.5	31.5	2.5	2.5
	Analysis	35.9	0.0	34.4	34.0	Assumed Absent	

by more than 2.0 percent of the total mixture. The average error for all components in all mixtures shown in the two tables is 0.5 percent.

All the synthetic mixtures have been analyzed by the graphical approximation method, and some have been analyzed by both methods. Results obtained by the two methods for four samples are compared in Table VIII.

The complete analysis of a four-component mixture can be made in 45 minutes with the method of graphical approximations, and in 30 minutes with the method of applied corrections.

It should be pointed out that the presence in the unknown mixture of compounds for which analyses are not made will cause large or small errors depending upon whether the extraneous materials absorb strongly or weakly at any of the spectral positions. It has been found in the case of the four-component mixture that many of the unknowns submitted for analysis have contained two extraneous compounds. Synthetic mixtures including 2.5 percent of each of these components were prepared and analyzed, assuming the extraneous components absent. The results of this study are shown in Table IX. It will be noticed that these concentrations of the extraneous components cause errors up to 4.0 percent in the analyses. If the approximate amount and effect of the extraneous components can be determined, and they frequently can, errors such as those shown in the example can be eliminated or at least minimized by making appropriate corrections.

SUMMARY

A method has been described for analyzing multicomponent mixtures of hydrocarbons in the liquid phase by means of their infra-red absorption spectra. A constant thickness absorption cell is used, and analytical curves are established on the basis of synthetic binary mixtures of the different components in the multicomponent mixtures to be analyzed. Two procedures for using the analytical curves to convert optical densities to concentrations by means of successive approximations have been described. Four- and five-component mixtures are completely analyzed in less than 45 minutes per sample and the average error is 0.5 percent of the total sample.

Wide Range Static Strength Testing Apparatus for Glass Rods*

T. C. Baker† and F. W. Preston
Preston Laboratories, Butler, Pennsylvania
(Received November 1, 1945)

By adapting an electro-dynamic loudspeaker, an apparatus was assembled to test the strength of glass rods in flexure. This apparatus will apply the stress in 2 to 3 milliseconds and permit static loading for times as short as 0.01 second. Using an additional long time loading apparatus, which simultaneously tested eighteen rods, it was possible to run static fatigue tests on glass rods from 1000 seconds to 86,400 seconds. The method of testing and errors due to the apparatus are discussed.

INTRODUCTION

WHENEVER an attempt has been made to measure the strength of glass, it has been found that the rate of application of the stress greatly affects the results. If the load applied to the specimens is increased continuously, it is found that the specimens that are loaded slowly break at much lower stresses than those which are loaded rapidly. If the load is applied by increments, with definite time intervals between each addition, the specimens which are loaded with long waits between steps break at much lower stresses than those loaded with short waits between the steps. Moreover, a specimen under constant load may survive several hours before it breaks. This apparent weakening of glass with increased time of loading has herein been denominated "fatigue." Since engineers commonly use the term "fatigue" to mean failure under oscillatory or repeated loads, we may denote the fatigue dealt with here as "static" fatigue, and the other kind as "dynamic" fatigue.

Naturally it is important to know, for both theoretical and commercial reasons, what the real nature of fatigue is. The theoretical questions are: what is the strength of glass for very long loading periods, and does its instantaneous strength approach the value suggested by molecular theory? The commercial questions are: what safety factors should be allowed for bottles containing pressure, and what impact stresses will a glass object stand? Although there had been considerable speculation on these questions, the data were so limited as to make no generalization really sound. The object of this work was the extension of the data by several orders of magnitude to both shorter and longer times.

Probably the most relevant data would show how long a specimen survives at a given stress. Unfortunately, to answer this question directly with experimental methods would be too tedious, but the inverse question, whether or not the specimen survives a given length of time at a predetermined stress, lends itself readily to experimental technique. After sufficient data had been collected to answer this question, plotted curves would provide the answer to the original question. Accordingly, the method finally decided upon was to load the test specimen for a definite interval of time at a predetermined stress. If the specimen survived the test, it would be loaded at an appreciably higher stress and the test repeated.

Round glass rods were chosen as the only satisfactory test specimens because of their availability in several compositions, and because they have no cut or ground surfaces to confuse the issue.

When a constant load is to endure for only 0.01 second, the problem of applying the load and removing it is far more difficult than when the load is to be held constant for hours, because for the brief application the load must be built up with great speed and without producing oscillation. Therefore, two types of apparatus were designed: a short time loading apparatus that would apply the load for periods ranging from 0.01 second to 100 seconds, and a long time loading apparatus that would apply the load for periods ranging from 1000 seconds to 24 hours (86,400 seconds).

DESCRIPTION OF APPARATUS

The Short Time Loading Apparatus

The short time loading apparatus is essentially a dynamic motor consisting of a modified radio

* This apparatus was developed at the Preston Laboratories in 1938 and 1939 for a project sponsored by the Hartford-Empire Company.

† Present address: Libbey-Owens-Ford Glass Company, Plaskon Division, Toledo, Ohio.

loudspeaker. Instead of the usual voice coil, an armature or moving coil assembly was developed which would withstand the loads that had to be applied.

A schematic diagram of the apparatus is shown in Fig. 1. A glass rod (1) is supported by two knife edges (2). A wire bail (3) is looped over the middle of the glass rod and is connected to two lugs (4) on the armature (5). An oversize field coil (6) which is actuated by a 12-volt storage battery (7) produces the magneto-motive force of a central field magnet (8). The magnetic circuit is carried from the central magnet through a shell (9) to the air gap (10), in which the armature (5) is freely suspended from the rod. When the key (11) is closed, the armature is actuated by the current flowing from the battery (12) of about 120 volts. The current is regulated by a resistance (13) and is measured by an

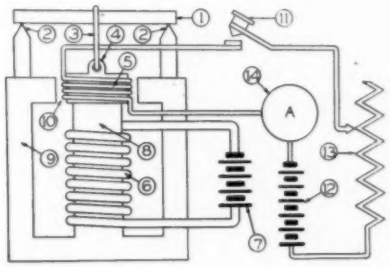

FIG. 1. Schematic diagram of the quick-loading apparatus.

ammeter (14). Forces up to 30 lb. can be produced momentarily by the armature.

Details of the Dynamic Motor

An eighteen-inch dynamic loudspeaker was used as the basis of the dynamic motor. The size of the field coil was practically doubled to provide a much stronger magneto-motive force. The magnetic air gap was operated at approximately 10,000 gauss for the smaller armatures, and as low as 7,000 gauss for the larger ones. In Fig. 2 the rod is shown in position to be tested. Several armatures were designed for different purposes. For the 0.01-, 0.1-, and 1-sec. loading durations the requirements were light weight and large damping coefficient to permit quick action without overtravel. The time interval was so short that the motor coil could carry large currents

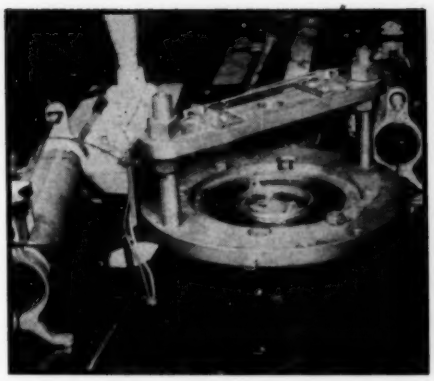

FIG. 2. A rod in position to be tested.

without overheating. However, for the 10-second and 100-second periods the chief requirement was that the coil should not overheat, necessitating a larger motor coil and greater weight, yet the time of application of the load could be much longer so that smaller damping coefficients and greater weight could be tolerated. The load could be satisfactorily applied by reducing the circuit resistance by hand, thus bringing the current to its correct value in approximately $\frac{1}{4}$ second.

Figure 3 shows a cross-sectional diagram of one side of the armature. An aluminum form serves as a frame and a spool. The wire bail to the rod is fastened at the hole (1) in the lug (2). A stiffening ring (3) prevents the form from collapsing due to the pull of the wire bail. A motor winding (4), which carries the current from the 120-volt battery, consists of a double layer of No. 28 wire. The damping winding (5) is made of several turns of fine, uninsulated, aluminum wire. However, the damping winding is insulated from the aluminum spool and from the motor winding by

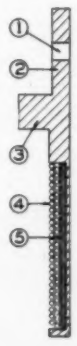

FIG. 3. Cross section of voice coil.

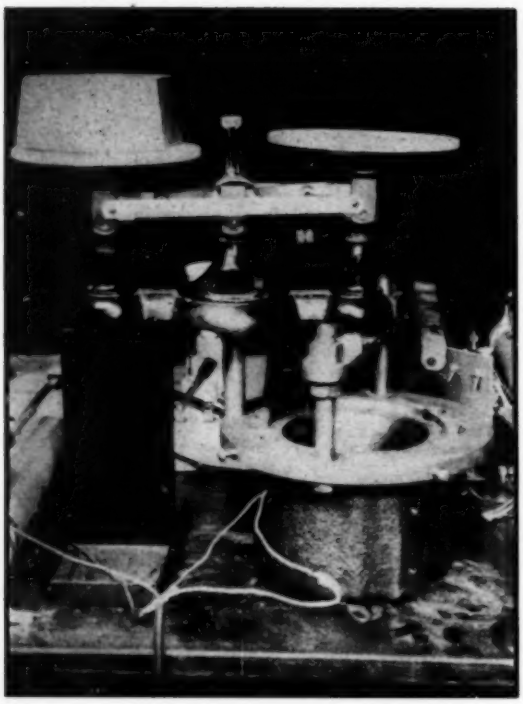

FIG. 4. Trip scale for calibrating the dynamic motor.

a layer of insulating enamel. It was possible to thicken the spool and omit the damping winding in the design of some of the armatures.

The operation of the dynamic motor depends upon the fact that a force is exerted on a wire carrying current in a magnetic field. This force is given by $F=BlI$, where F is the force, B is the flux density in gauss, l is the length of conductor in the field, and I is the current flowing through the wire, in c.g.s. electromagnetic units. Thus the force is directly proportional to the current in the motor winding. As long as there are approximately the same number of turns of wire in the magnetic field, the force will be substantially constant for small displacements of the armature. In practice, the armature can be displaced over a range of $\frac{3}{32}$ inch while the force remains constant to $\pm\frac{1}{2}$ percent. The quick-loading armature designed for 0.01-second loading produces a force of 3 pounds per ampere.

When the motor winding moves across the magnetic field, a back e.m.f. is developed. This back e.m.f. is given by $E=Blv$, where E is the electromotive force in c.g.s. electromagnetic units, l is the length of conductor in the magnetic field, B is the flux density, and v is the velocity. Thus, when the coil moves, it is possible to determine its velocity by means of an oscillograph and so tell whether it is behaving as it should.

The damping of the armature is due to the counter currents induced in the ring and damping winding by the motion of these conductors in the magnetic field. By definition, the coefficient of damping is $k=F/v$ where k is the damping constant, v is the velocity, and F is the force produced in opposition to the velocity. By combining this with the formulas $F=BlI$, and $E=Blv$, it turns out that $k=B^2l^2I/E=B^2l^2/R$. Here R is the electrical resistance of the conductor in the circuit. In the present case the damping constant k depends on three factors: the damping due to the aluminum spool, that due to the motor winding, and that due to the damping winding. Each of these factors can be computed from the formula $k=B^2l^2/R$. The coefficient of damping in the spool is the most difficult to determine because the path of the current extends beyond the boundaries of the uniform magnetic field. The currents in the damping winding and in the motor winding, on the other hand, are confined within the part of the field where the geometry is relatively simple. The three separate coefficients have to be added together to obtain the total damping. When an armature is made, a good estimate of the actual value of the coefficient can be obtained by studying the voltages across the motor coil with the aid of an oscillograph, as will be explained later. Corrections can be made by adding to or subtracting from the damping winding enough wire to give the desired coefficient.

The contribution of the motor winding to the damping constant is rather small if the circuit resistance stays fairly large. With a field strength of 10,000 gauss, and with 50 ohms in the circuit, the contribution is 4 lb./sec., and with 20 ohms in the circuit the contribution is 10 lb./sec. The circuit resistance was usually at least 20 ohms. This variation of 6 lb./sec. will change the total damping coefficient by only 3 or 4 percent.

A preload is applied to the armature by passing a small current through the motor coil in order to take the slack out of the wire bail. This preload puts a maximum stress upon the specimen of around 1000 to 2000 lb./sq. in. This is sufficiently below the breaking stress at any of the durations, and under any of the conditions where it is used,

that it causes no appreciable fatigue. This matter will be discussed more fully later.

Several armatures were designed for quick loading, because none is effective for more than a small range of rod sizes. For example, to test the rods that vary in diameter from 0.210 inch to 0.230 inch, a coil assembly was designed which has a damping coefficient of 168 lb./sec. and which weighs 23 grams.

For the 10- and 100-second loads a six-layer coil was designed which provides adequate loads at current values low enough to prevent overheating. The additional weight and reduced damping of this coil offer no problem at the relatively slow loading rates appropriate for these long loading periods.

Calibrating the Dynamic Motor

In order to measure the force exerted by the armature, a trip scale is mounted with the center of one pan over the motor coil. Figure 4 shows the trip scale in position. The wire bail of the armature is attached below the empty pan, and the opposite pan is loaded with a ten-pound weight. The empty pan is held down by hand, keeping the armature in its working range, while the current is increased until the coil just supports the ten-pound weight. Such determinations can be made to about $\frac{1}{2}$ percent accuracy with an ammeter readable to about $\frac{1}{4}$ percent of full scale. A better ammeter would be of no value as there is sufficient damping and friction in the dynamic motor to make finer readings uncertain. With a satisfactory ammeter only one calibration point is necessary, since the relation between the current through the motor coil and the force exerted by it is as linear as can be measured, if the field magnet is properly saturated. Of course, the current through the field coil must be kept constant or the calibration will change.

The Timing Device

The timing device which was designed to time the 0.01-second, 0.1-second, and 1.0-second intervals appears in Fig. 5. It consists of a 100-lb. pendulum mounted on a heavy frame and has a period of 2 seconds. The pendulum is released by a magnet and is caught at the end of its swing by a latch. At the start of the swing a limit switch is closed to energize the field magnet; at the end

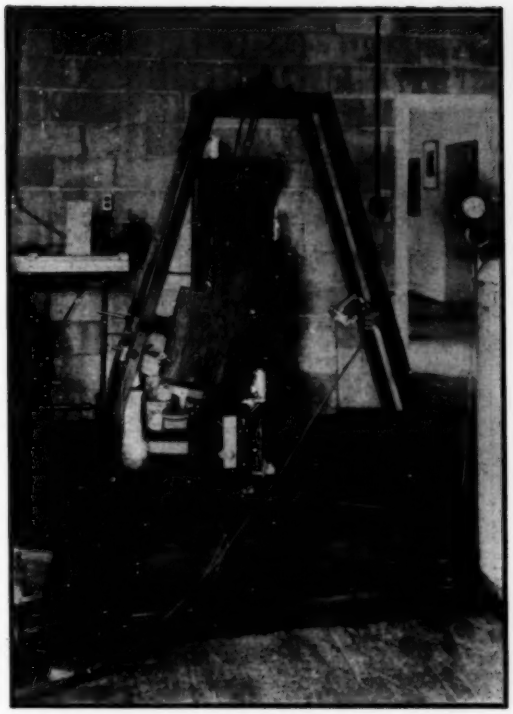

FIG. 5. The timing device.

of the swing another limit switch breaks the field coil circuit when the test cycle is complete.

The 0.01-second and 0.1-second intervals are controlled by means of a cam on the pendulum bob, which closes a pair of contacts in the middle of the swing. At the end of the interval another cam opens the contacts, and the resulting arc is blown out with a powerful jet of CO_2. The arc is greatly diminished in about 0.0001 second, but it takes about 0.001 second to blow it out. Without the blast of CO_2 it is nearly impossible to put out the arc at all because the contacts open only $\frac{1}{4}$ inch and currents up to 6 amperes at 120 volts d.c. have to be interrupted. The timing cams are calibrated by observing the oscillograph pattern and making the indicated adjustments.

The 1.0-second interval is timed by having the pendulum close a switch in the middle of its forward swing, and open it on the return swing. Since the pendulum has a 2-second period, this interval is one second.

The 10- and 100-second intervals are timed by a stopwatch. A slidewire rheostat shown in Fig. 2 and indicated by (*13*) in Fig. 1 is operated by hand to apply and release the load.

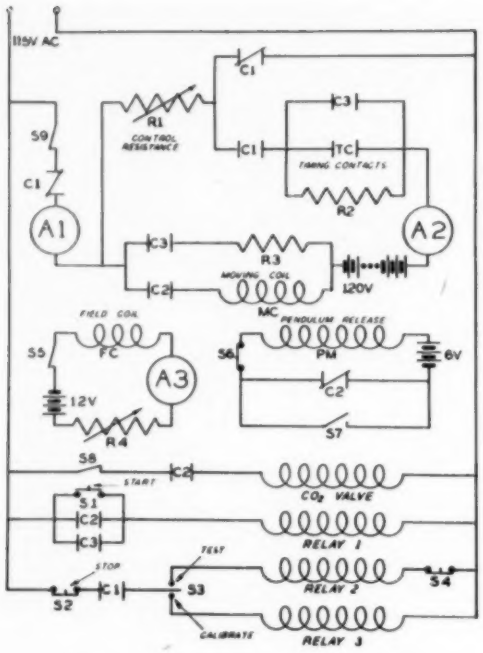

FIG. 6. The electrical control circuit.

Accessories to the Apparatus

Before many tests had been made, it became evident that a great deal of accessory apparatus was necessary. While the current in the loading circuit is being adjusted preparatory to a test, a dummy resistance is substituted for the motor coil in order to protect the latter from overheating. This resistance has to be switched in when the current is adjusted and out when a rod is tested. The control resistance becomes heated during the loading current adjustment, so that an a.c. current must be supplied to it between times to keep it warm and maintain its resistance constant. The CO_2 used to blow out the arcs of the timing contacts is turned on and off with an electric valve, because otherwise the flow would quickly dissipate the supply.

It was soon found that the manual switching arrangement was too complicated. Turning the wrong switch could easily cause an accident or spoil the test. For example, the pendulum bob had to be released when testing but not when calibrating. An interlocking circuit was finally evolved which was relatively foolproof and which reduced the switching procedure to a minimum. This circuit is shown in Fig. 6, and is described below.

It has been found that a cathode-ray oscillograph is indispensable. The timing cams are adjusted with the oscillograph, and the trace of every test is watched on the oscillograph screen to be sure that everything goes correctly. By watching the voltage developed across the motor winding as indicated by the oscillograph it is possible to tell whether the load goes on smoothly, whether the armature sticks, whether the rod breaks, or whether the contacts arc excessively.

Operation of the Apparatus

Because of the fact that the rods to be tested vary in diameter, the experimental procedure is somewhat complicated. First it is necessary to construct a chart giving the relationship between the maximum fiber stress of the rod and the current through the motor winding for every rod diameter. Each rod is carefully measured for maximum and minimum diameter and then is oriented in the apparatus so that the maximum fiber stress will come at one end of the minimum diameter.

Referring to Fig. 6 the sequence of operations is as follows: the knife switch (*S*5) is closed to energize the field magnet, and the manual switch (*S*3) is set on "calibrate"; the start button (*S*1) is pressed, and the current indicated by the ammeter (*A*2) is set to the proper value (as given by the stress *vs.* current table) by adjusting the control resistance (*R*1). Finally, to test the specimen, the switch (*S*3) is set on "test," and the start button (*S*1) is pushed again. At this

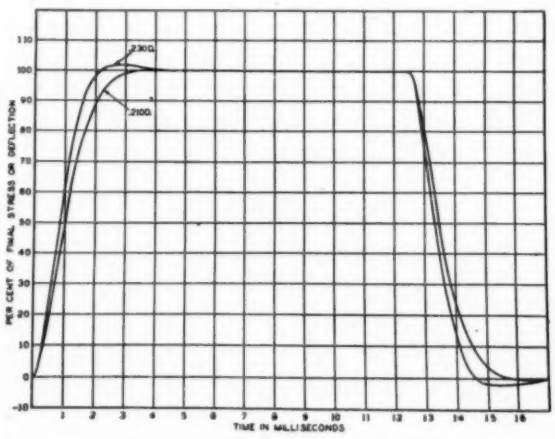

FIG. 7. Theoretical curve of load of 0.01-second duration for rods 0.230 and 0.210 inch in diameter.

point it may be helpful to trace on Fig. 6 the sequence of part of the resulting operations.

Closing ($S1$) energizes the coil of relay (1) which causes an open contact ($C1$) of this relay to close and energize the coil of relay (2). Other contacts ($C1$) open to turn off the a.c. supply maintaining the temperature of the control resistance ($R1$) and close to make the moving coil circuit ready for closure of the timing contacts (TC). The coil of relay (2) being energized by closure of contacts ($C1$), the contact points ($C2$) open in the pendulum release circuit, allowing the pendulum to fall. Thus the pendulum bob is released, and by closure of the open contacts ($C1$) of relay (1) the preload controlled by ($R2$) is turned on, the CO_2 valve is opened, and the timing contacts (TC) become operative. The pendulum bob swings down and operates the timing contacts (TC). This energizes the moving coil (MC) of the armature from the 120-volt battery, and loads the specimen. At the end of its swing, the pendulum bob operates a limit switch ($S4$) which shuts off the apparatus while the pendulum is caught by a mechanical latch. In the meantime the operator watches the oscillograph to see that everything has functioned properly. If the rod has not broken, the pendulum is reset, the current adjusted for a higher stress, and the whole procedure repeated.

Dynamics of Quick Loading

In order to get some idea of the accuracy of the measurements it is necessary to study the loading mechanism as a vibrating system. Since most of the mass is in the armature and most of the compliance is in the rod, the problem may be treated as a vibrating system with a single degree of freedom. The differential equation becomes:

$$m\frac{d^2y}{dt^2}+k\frac{dy}{dt}+sy=F,$$

where y is the displacement of the center of the rod, m is the effective mass of the whole system, k is the damping constant, s is the stiffness of the rod at its center, and F is the suddenly applied force. The load F is applied at $t=0$, so the equation is subject to the boundary conditions:

$$y=0 \quad \text{and} \quad dy/dt=0 \quad \text{when} \quad t=0.$$

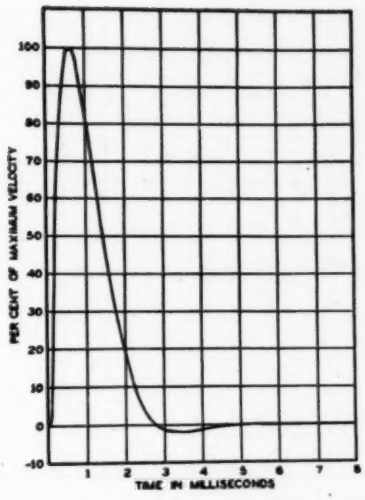

FIG. 8. Theoretical armature velocity curve during application of the load.

The solution of the equation becomes:

$$y=\frac{F}{s}-\frac{F}{s\cos\phi}e^{-kt/2m}\cos(\omega t-\phi),$$

which is plotted for two rod diameters in Fig. 7. Then

$$\frac{dy}{dt}=\frac{F}{s}\frac{\omega}{\cos^2\phi}e^{-kt/2m}\sin\omega t,$$

which is plotted in Fig. 8. In these equations:

$$\cos\phi=\frac{\left(\frac{s}{m}-\frac{k^2}{4m^2}\right)^{\frac{1}{2}}}{(s/m)^{\frac{1}{2}}} \quad \text{and} \quad \omega=\left(\frac{s}{m}-\frac{k^2}{4m^2}\right)^{\frac{1}{2}}.$$

As shown in Fig. 7, the displacement is minimum at $t=0$ and passes through a maximum at 2.8 milliseconds or, in general, at $t=\pi/\omega$.

Likewise, as seen in Fig. 8, the velocity passes through a maximum followed by a minimum, and these occur at $t=(\pi/2-\phi)/\omega$ for the maximum and $t=(3\pi/2-\phi)/\omega$ for the minimum.

These correspond to the maximum and minimum e.m.f.'s across the motor coil as indicated at D and G in Fig. 9, which is described later.

The ratio between the overtravel, i.e., the excess displacement over that for the steady load, and the steady load displacement is $e^{-\pi\tan\phi}$. The ratio of the minimum velocity to the maximum velocity is also $e^{-\pi\tan\phi}$. Therefore, because the voltage induced in the moving coil is proportional

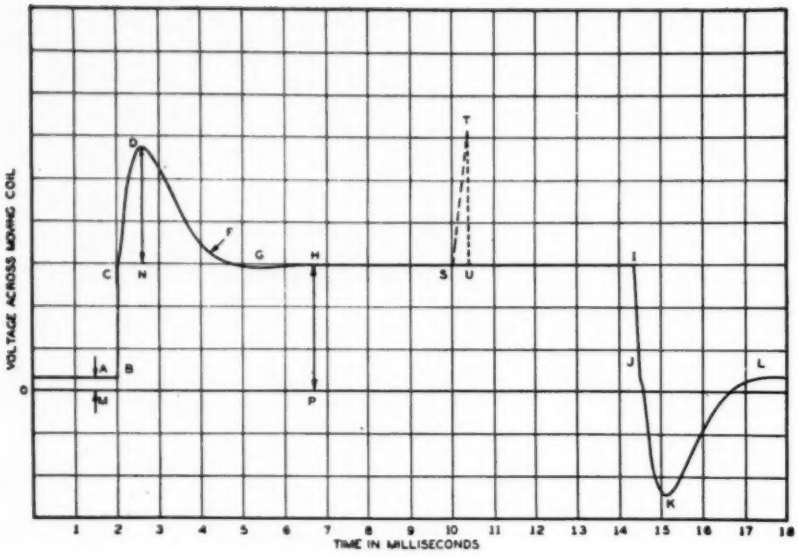

FIG. 9. Oscillograph trace produced during a 0.01-second test.

to its velocity, $e^{-\pi \tan \phi}$ must equal the ratio of the departures from the steady load voltage at D and G in Fig. 9. By measuring this ratio in the actual tests, the amount of overtravel and the damping coefficient can be readily computed. It turns out that for 2 percent overtravel, $k = 1.20(ms)^{\frac{1}{2}}$. For a range of rod sizes to be tested with an armature of given mass and damping coefficient, the largest diameter is determined by the condition that there should be no more than 2 percent overtravel. The smallest diameter is determined by not allowing the duration of the load to be decreased by more than 10 percent for the 0.01-second test.

Originally it was intended to load the rods in one millisecond, which would require the use of rods greater than $\frac{1}{4}$ inch in diameter, with a 4-inch span between supports. Unfortunately, the rather surprising increase of strength of glass in the shorter time ranges completely overtaxed the equipment with the larger rods. It would have required a larger field magnet, much higher d.c. voltages, and a general redesign of the apparatus. So we have had to use rods 0.220 ± 0.010 inch in diameter with a 5-inch span, and to be content with loading the rods in 2 to 3 milliseconds instead of the one millisecond originally planned. However, as one can see from Fig. 7, the time the rods are under stresses between 80 percent and 98 percent of the full loads is not too great.

A typical armature designed for measuring rods of approximately 0.220-inch diameter has the following constants:

$$m = 0.051 \text{ lb.}, \quad k = 168 \text{ lb./sec.}$$

It turns out that this coil causes a momentary 2 percent overtravel on rods of 0.230-inch diameter, and it can be used with rods of 0.210-inch diameter without decreasing the time of full loading by more than 10 percent. Figure 7 shows a theoretical loading curve for rods 0.230 inch and 0.210 inch in diameter. The constants of the system with the 0.230-inch diameter rod are:

$$m = .060 \text{ lb.}, \quad k = 168 \text{ lb./sec.},$$

and

$$s = 194{,}000 \text{ lb./sec.}^2.$$

The mass constant is increased over the mass of the armature by the effective mass of the rod.

The constants for the rod 0.210 inch in diameter become:

$$m = .059 \text{ lb.}; \quad k = 168 \text{ lb./sec.},$$

and

$$s = 135{,}000 \text{ lb./sec.}^2.$$

In Fig. 8 is a theoretical curve of the velocity of the armature for a rod 0.230 inch in diameter. It turns out that this pattern is closely followed when the velocity is studied in the cathode-ray oscillograph.

Oscillograph Patterns

Since the velocity of the armature produces an

e.m.f. given by

$$E = Blv, \text{ and since } v = dy/dt,$$

then

$$E = Bl\frac{F\omega}{s\cos^2\phi}e^{-kt/2m}\sin\omega t,$$

and we should expect the voltage developed across the armature to have this e.m.f. as one component. The other component is, of course, the *IR* drop across the coil. Accordingly, when the oscillograph is connected to read the voltage across the armature, a pattern is given as shown in Fig. 9. The line *ABCDIJKL* is a trace of the oscillograph in a 0.01-second test. *AM* is the *IR* drop due to the preload current; *HP* is the *IR* drop due to the full load current. The voltage *DN* is the maximum e.m.f. due to the velocity. The load comes on at about *F*, and the overtravel occurs in the region between *F* and *G*. The time the load is on is between *F* and *I*. If a rod breaks, a pattern results as shown by the dotted line *STU*.

It is thus quite easy to determine from the oscillograph pattern whether the load has been properly applied, how long the load was on, whether the rod broke, and whether or not any deleterious accident, such as the armature sticking, took place during the test. It is somewhat difficult to estimate the amount of overtravel by increasing the scale, because the *IR* drop is considerably larger than the e.m.f. due to velocity in the 2 percent overtravel region. It is found easier to use an auxiliary winding of a few turns of No. 40 wire around the outside of the armature when damping coefficients are being estimated by the overtravel.

Accuracy of Tests

The quick-loading device is able to apply a load in 2 to 3 milliseconds, maintain it for 10 milliseconds, and then remove it in ½ millisecond. Even when a range of rod sizes is tested, the error in timing the load is less than ±5 percent, and the overtravel is less than 2 percent. Since the overload is on for only about 10 percent of the time it is doubtful that a 2 percent overload would cause as much as 1 percent difference in the results, because of the rapid increase of strength of glass with shortening of duration of loading. An added factor in favor of accuracy is

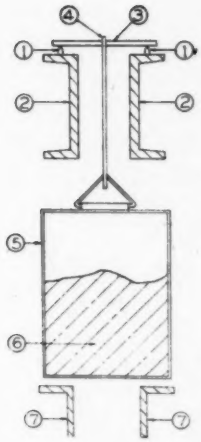

FIG. 10. Cross section of the long time loading device.

that, when a large number of rods are tested, several will not be overloaded, because they are on the low side of the diameter range. Therefore, for the 0.01-second test, the average result can be relied upon to at least 1 percent as far as the overloading is concerned.

The overload will not be serious in the 0.1-second and 1-second tests, because it will occur for only about 1 percent and 0.1 percent of the total time under load. The manner of application of the 10- and 100-second loads makes overloading in these tests impossible. Thus it is safe to say that 1 percent accuracy for the load and ±5 percent accuracy for the timing of the load are available for all the short-time loading points.

The Long Time Loading Device

The problem in the long time loading device was to test several rods simultaneously so that the length of time and expense of the tests would be kept to a minimum. Figure 10 shows a cross-sectional diagram of the apparatus. Two knife edges (1) are fastened to stiff channels (2), and support a rod (3). A central knife edge (4) is attached to a container (5) holding sand. When the rod breaks, the container falls on the angles (7) which are supported on a different frame from the channels. In this way, when a rod breaks, the fall of the container does not create a shock that would seriously affect the other rods still on test. The apparatus is in three tiers, each simultaneously testing six rods. It is thus possible to conduct tests on 18 rods at a time. The apparatus

is located in the basement where the vibration conditions are quite satisfactory, as no heavy machinery or railroads are in the vicinity. Tests with dial indicators have shown no serious vibration present.

A table was constructed giving the load *versus* the extreme fiber stress for every rod diameter. In making a test, the diameter of the rod is measured, and the load is determined from the table. The container is then filled with sand to make up the proper load and a special levering device is used to apply the load gently. In general, an accuracy of 1 percent could be attained in measuring the load and its duration. The 1,000-, 10,000-, and 86,400-second tests were made with the long-time loading device.

ACKNOWLEDGMENT

We are greatly indebted to Major J. M. McCormick, formerly of the Preston Laboratories, for his work and helpful suggestions in constructing the switching system whereby the labor in making tests on the short time loading apparatus was greatly reduced.

Fatigue of Glass under Static Loads

T. C. Baker† and F. W. Preston

Preston Laboratories, Butler, Pennsylvania

(Received November 1, 1945)

Static loading tests were run on glass and porcelain rods $\frac{1}{32}$ inch in diameter for times ranging in duration from 0.01 second to 24 hours, by using specially designed apparatus. It was found that glass can support for 0.01 second about 3 times the stress that would break it in 24 hours. The effects are generally the same for all glassy materials. Porcelain showed the effect somewhat less than glass. It appeared that adsorbed moisture and gases reduced the strength.

INTRODUCTION

IT has been recognized for many years that glass fatigues* under a perfectly steady load, breaking unexpectedly and without apparent cause under a stress it has long endured. Therefore, in measuring the mechanical strength of glass, the duration of the test must be specified as well as various other circumstances, some of which are discussed in this paper.

Whereas most glassware gets broken by impact, that is, by loads whose duration is measured in microseconds and which vary widely even in so short a time, yet some glassware is subjected to constant loads of long duration—for instance, soda, champagne, and beer bottles, aquarium windows, gauge glasses, and so on. An understanding of the relation between short time strength and long time strength is therefore important.

This relationship has already been worked out roughly over a substantial range of loading intervals by several experimenters, so that from a strictly practical point of view there is reason to believe we know enough to risk no hazards to the public. The interest, accordingly, shifts to the nature of "static" fatigue, and to such questions as whether the glass has any strength at all under an exceedingly long loading. If the strength after a great period is not zero, what is the value of it, and what is the meaning of it? On the other hand, we have reason to suspect that at loads of very short duration the strength may be very great. Is it theoretically infinite, or is it finite? If the latter, how great is it, and can any clear meaning be ascribed to it? Or is the question somewhat meaningless, in view of the inertia effects which make "steady" loads of very short duration inconceivable?

At first we had hoped our investigations would shed some light on these theoretical questions, but as more evidence accumulated all our beliefs as to the nature of fatigue in glass tended to change, and we felt much less inclined to specu-

* This use of the term "fatigue" appears to us perfectly legitimate, though it is not the same as the usual engineering usage. If necessary, our fatigue may be distinguished as "static" fatigue, and the engineering usage as "dynamic" or "vibration" fatigue.

† Present address: Libbey-Owens-Ford Glass Company, Plaskon Division, Toledo, Ohio.

late on the strength of glass and the ultimate effects of fatigue until the concept of strength was more precisely defined and the nature of fatigue was more thoroughly understood. Our initial feeling was that fatigue was due to the thermal effects at the tip of a flaw. The highly stressed bonds at that point were supposed to break when their momentary energies grew greater, due to the random shuffling of the thermal energies between the atoms. If this were the case, the cause of fatigue would be the same for long and short durations of load, and so we could expect a correlation between time and breaking strength. One might then assume that, if we had data encompassing a few orders of magnitude, we could extrapolate to both longer and shorter times with reasonable safety. However, as our work progressed it soon became apparent that atmospheric conditions were a factor in the fatigue of glass and that the phenomenon was so complicated that we could have little justification for extrapolation to either shorter or longer times, except as mere speculation.

The data presented are therefore disappointingly restricted, from the viewpoint of determining ultimate "strength" of glass. On the other hand, certain practical questions are answered as to the reliability of testing procedures, and at the same time a sounder understanding of the nature of the phenomenon has emerged, which may lead to a valuable line of research.

These tests were designed to investigate the phenomenon of strength decay, or fatigue, of glass in its normal condition, that is, with the amount of surface damage ordinarily present in commercial glasses, rather than the fatigue in glass having specially prepared, pristine surfaces. Glass samples were used, therefore, which had light surface damage easily visible under a microscope, which made their strengths comparable to that of commercial glassware. It is quite possible that all the breaks started at these flaws, and so the flaws in glass may be an essential part of the phenomena that we have studied. Other effects noticed in glass fibers, or other glass objects having pristine surfaces, may bear no simple relationship to the results obtained in the presence of large flaws.

Since it is not possible to experiment for an indefinitely long time and report the results to the present generation, and since there are, on the other hand, practical difficulties in experiments for an infinitesimal time, we are limited to a range of duration which is not extremely extensive in "powers of ten" (orders of magnitude). From this relatively restricted range, we may perhaps hazard good guesses as to what might happen at somewhat shorter and somewhat longer periods of loading. The validity of our guesses depends on how accurately we can plot a curve of strength *versus* duration of load over the accessible range.

In the work herein reported, this range has been considerably extended beyond that of previous investigators. The extension is largely at the short duration end. This direction was chosen by one of us (T.C.B.) as offering more immediate promise than the other, because experimental conditions can be more readily kept constant for a brief time than for a long time. For instance, conditions such as temperature and humidity are important. Further, a lot of experimenting can be done in a matter of weeks or months at the short time end, while only a little can be done in many years at the other.

The essence of the short time loading experiments is the use of "electromagnetic loads," which can be very powerful while substantially free of inertia, so that the loads can be applied in 0.003 second without significant overtravel or oscillation. The quick-loading apparatus was described in a previous paper[1] in which its details and accuracy were discussed. This apparatus was not used for experiments lasting minutes or hours, since gravity provides a more convenient steady force. For these longer periods of testing, the essence of the set-up is the simultaneous testing of many specimens under conditions as constant as possible in respect to temperature and humidity.

The tests were made in flexure on $\frac{7}{32}$-inch glass rods, the simplest method experimentally. The shortest practical duration was about 0.01 second with our apparatus. Theoretically, somewhat shorter times are practical in making tests in direct tension on fibers, but the experimental

[1] T. C. Baker and F. W. Preston, "Wide range static strength testing apparatus for glass rods," J. App. Phys. **17**, 162 (1946).

difficulties were believed to be greater and apt to introduce more error. The longest tests lasted 24 hours. It is clear from the shape of the curves that little more would have been learned by extending the time to ten days, or even to one hundred or one thousand days. Furthermore, since each specimen must be tested at several successively greater loads, such tests would have taken many years to complete, even if experimental conditions could have been maintained constant.

It is not unthinkable that the curve may yet be extended, experimentally, farther than we have gone, but it seems at present unlikely that much practical, or even theoretical, information could be acquired thereby. Therefore, in the belief that the subject has reached a measure of completeness, we present an account of some of our experiments.

EXPERIMENTAL PROCEDURE

Because the strength of glass seems to be a function of its previous history of exposure both to the atmosphere and to mechanical contact, special precautions had to be taken in order to keep constant the effects of handling, adsorbed moisture, etc., in measuring the variation of breaking stress with changing duration of the load. Ideally, the controlled experimental procedure should start during the manufacture of the glass canes from which the rods were cut. Unfortunately, that was impossible. Our experimental procedure was constrained to begin after the glass reached the laboratory, which naturally left uncertain the previous history of the canes.

The initial step was to select canes that met certain specifications as to diameter and taper, and cut them into rods six inches long. These rods were then distributed among six or eight samples, of 25 rods each, and their diameters were measured and recorded. The rods were next set aside for a week or two so that any recent mechanical damage would tend to reach equilibrium, and the rods would have a chance also to come to equilibrium with the laboratory atmosphere. Finally, the rods were broken in the strength-testing apparatus.

Selection of Canes

In order to get comparable test samples, glass canes were used, whenever possible, which had been made at the same time. After being cut into four-foot lengths the canes were sent to the Hartford-Empire Company to be annealed, where special precautions were taken to prevent extra damage during the annealing process. The annealed canes were then individually wrapped in tissue paper and sent to the Preston Laboratories. There each cane for a test lot was examined, and only those which met the following specifications were used.

Specifications for Cane

Taper per foot:	less than 0.005 inch
Out of roundness:	less than 0.005 inch
Diameter:	0.220 ± 0.010 inch
Radius of curvature of axis:	greater than 5 ft.

Canes showing unusual abrasion were rejected.

Each cane was cut into six-inch lengths, or rods, and these were distributed among either six or eight samples, depending on whether the cane was three feet or four feet long. The method of distribution was as follows: the first rod from the first cane was put into the first sample, the second rod was put into the second sample, and so on. The second cane was distributed by putting the first rod into the second sample, the second rod into the third sample, and so on, until the last rod was put into the first sample. The subsequent canes followed out the progression. This method of distribution meant that each sample contained a rod from each cane, and each contained approximately the same number of rods cut from the ends and the middle of the canes. Thus 25 four-foot canes would make eight samples of 25 rods each, 25 three-foot canes would make six similar samples.

Care of Test Samples

As the canes were cut, the six-inch rods were put into wooden blocks having twenty-six numbered holes bored 1 inch deep. Only twenty of these specimens were used for the tests, the other rods being saved for spares. For example, if an accident occurred in the test on one rod, the rods taken from the same cane were discarded from all the other samples, and a complete set of spares was substituted. Great care was used in handling the rods during and after cutting, because new damage inflicted during subsequent handling could destroy the homogeneity of the specimens.

The ends of the rods were measured for maximum and minimum diameter, and a scratch was made at one end to indicate the direction of the minimum diameter of the rod. The central minimum diameter of the rod was estimated to be the average of the minimum diameters at both ends, and was recorded on the data sheet, next to the specimen number. In testing each individual rod the apparatus was adjusted to produce the appropriate stresses in accordance with special tables showing, for each value of load, the apparatus adjustment in terms of rod diameter.

The Apparatus

The rods were tested in cross bending, with a five-inch span. The load was applied by a single central knife edge. The two types of apparatus for testing the rods have been described in the previous paper. Briefly, one consisted of a modified dynamic loudspeaker to apply the loads of short duration (0.01 sec. to 100 sec.), and the other was a multiple loading device designed to accommodate numerous rods for the 1,000-sec. to 24-hour tests.

The load was applied to the rods as quickly as possible, left on for a predetermined time, and then removed as quickly as possible. The load was applied in two or three milliseconds and removed in $\frac{1}{2}$ millisecond in the 0.01-, 0.10-, and 1.0-second tests. In the 10- and 100-second tests about $\frac{1}{4}$ second was required to apply and to remove the load, and in the tests of 1000 seconds and over about four or five seconds were required. For the short time loading tests, tables were constructed giving the maximum stress in a rod as a function of the current through the armature of the dynamic loudspeaker, for all values of rod diameter. In making the tests, each rod was removed from the sample holder and placed in the testing apparatus with the minimum diameter in the direction of the load. This assured that the maximum fiber stress would be applied at the end of the minimum diameter. The rod was then tested at the minimum breaking load or at one loading interval below that. If the rod did not break, it was tested at an appreciably higher stress, the increment depending on the average strength.

In the case of the long time loading apparatus the procedure was very similar, except that instead of the moving coil used in the electromagnetic loading a two-gallon can filled with sand was used to supply the load.

The Loading Increment

Glass "fatigues" under constant load, and unless it recovers promptly upon the removal of that load (a matter that is not certain), the breaking of the glass at a given load might be affected adversely by any previous loadings, even though these might be of less intensity. Experimental evidence had been accumulated in the past, however, that when step-wise loading is used, previous, lower loads had very little or no influence if they were 10 percent or so below the breaking load. Thus if our increments of loading are 10 percent or more above previous loadings, we can ignore the effects of the latter. For good measure, it might be well to make the increments of the order of 20 percent.

On the other hand, if we use large increments the statistical data will fall into very few class intervals and the average will be uncertain. However, it was determined that, when we had five class intervals, the error would probably be quite a bit less than that from other sources. Accordingly, the loading increment chosen was 500 lb./sq. in. for samples whose averages were between 3000 and 6000 lb./sq. in.; 1000 lb./sq. in. for samples whose averages were between 6000 and 12,000 lb./sq. in.; and 2,000 lb./sq. in. for samples whose averages were over 12,000 lb./sq. in. The strength was generally found to vary over a 2 to 1 range for any sample. Thus in a sample with 12,000 lb./sq. in. average strength some specimens would break at about 8000 lb./sq. in. and some at about 16,000 lb./sq. in. This resulted in five class intervals for the data, using steps of 2000 lb./sq. in.

If a rod survived a test at 14,000 lb./sq. in. and broke at 16,000 lb./sq. in. it would be recorded as having broken at 16,000 lb./sq. in. Obviously, it could have broken at a load anywhere between 14,000 and 16,000 lb./sq. in., and on the average would break at 15,000 lb./sq. in. Therefore, it was necessary to apply the usual statistical correction for the magnitude of the class interval. When the loading increment was 2000 lb./sq. in.

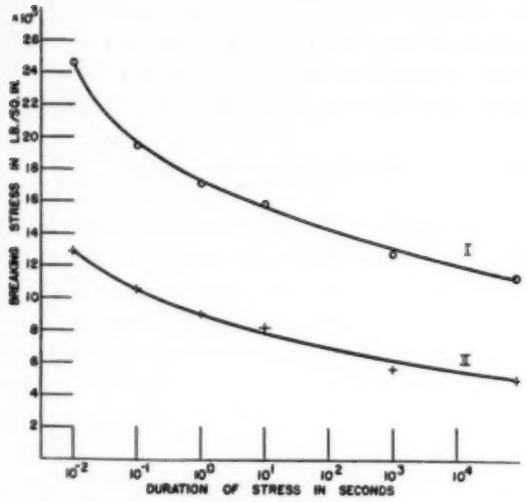

FIG. 1. I. Disannealed Pyrex, dry; II. Disannealed Pyrex, scratched, wet.

the correction would be −1000 lb./sq. in. When the loading increment was 1,000 lb./sq. in., then the correction would be −500 lb./sq. in.

Special Precautions

Special precautions were necessary to keep the temperature and atmospheric conditions as constant as possible during the tests. The room temperature was kept as near 75°F as possible. The rods were placed near the apparatus previous to the test so that thermal strains would not be introduced when the rods were inserted in the apparatus. A few minutes before the test the rod was wet with water at room temperature, and water was applied to the rod whenever it became dry during the successive loadings.

RESULTS OF VARIOUS STATIC LOADING TESTS

The results herein reported were obtained from tests run on five glasses and three porcelains. These are presented in Table I, which gives, for each loading period, the average breaking strength of 20 to 25 specimens. The results for the various glasses are plotted in Figs. 1 and 2, and the results for the porcelains are plotted in Figs. 3 and 4. All results are corrected for the loading increments, as described in the preceding section.

Lot I consisted of Pyrex rods which had already been cut to length, since there were no long canes available at the time of the tests. In that respect, this constituted an exception to our usual procedure. The rods were rather strongly disannealed, with a surface compression of 2000 to 4000 lb./sq. in., the average of several rods being about 3000 lb./sq. in. Moreover, as these were our first tests and the effect of moisture was not appreciated at that time, the Pyrex rods were tested dry. Various difficulties, including the fact that no really reliable average for the surface compression could be taken, greatly reduced the accuracy of these results.

Lot II was made up of the same type of disannealed Pyrex rods as used in lot I except that they were scratched circumferentially with a medium grade of emery. By this time the effects of humidity had been detected and the rods were tested wet.

Lot III consisted of samples made from four-foot, annealed, machine-drawn, soda-lime canes which were unusually straight and round and made an excellent stock for selection of samples.

TABLE I. Average breaking stress in pounds per square inch for various durations of load.

Lot	Material	Test Wet or Dry	0.01 sec.	0.1 sec.	1.0 sec.	10 sec.	100 sec.	1000 sec.	86,400 sec.	Ratio of 0.1-sec. to 24-hour test	Ratio of 0.01-sec. to 24-hour test
I	Disannealed Pyrex	Dry	24,600	19,600	17,100	15,900		12,800	11,300	1.7	2.2
II	Disannealed scratched Pyrex	Wet	12,900	10,600	9000	8250		5750	5050	2.1	2.5
III	Annealed soda-lime glass	Wet	19,900	15,900		10,500		7950	6450	2.4	3.1
IV	Annealed lead glass	Wet		19,000	14,900	11,200		9400	7950	2.4	
V	Fused silica	Wet		23,880		19,800	15,660	14,280	11,740	2.0	
VI	Porcelain Type *A*	Dry	15,800	13,900	12,300		9700		9100	1.53	1.74
VII	Porcelain Type *B*	Dry	15,400	13,500	11,900	9900	9400	9100	8900	1.52	1.73
VIII	Porcelain Type *C*	Dry	10,900	9400	8400	6900		6000	5900	1.59	1.85

Their composition was very close to that of bottle glass. Considerable care was taken in annealing and preparing comparable samples, and when certain check tests were run, the average strengths agreed to better than one percent, indicating excellent uniformity of the samples. These rods were tested wet.

Lot IV was composed of glass rods containing approximately 50 percent lead by weight. The glass was unusually soft and easy to scratch, and the resulting damage on some rods made the tests somewhat erratic. These rods were annealed, and the tests were conducted with the rods wet.

Lot V consisted of rods made from silica-glass canes three feet long. As the rods were apparently free of stress, no special annealing treatment was given them. All rods were tested wet.

Lot VI was composed of porcelain rods* of the following composition, fired at cone No. 9.

22 percent Kentucky Ball Clay
25 percent Florida Kaolin
37 percent Canadian Feldspar
10 percent Pennsylvania Flint
6 percent Water

The rods were tested dry because the effect of

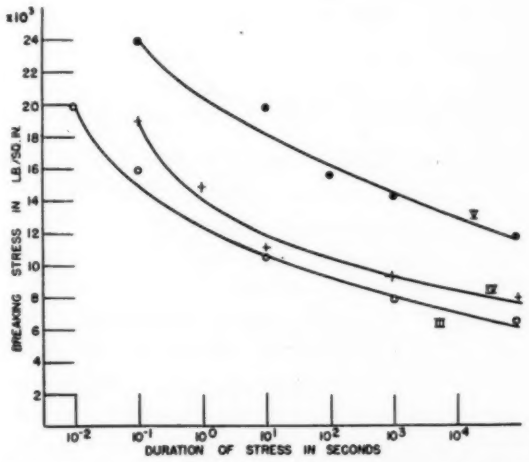

FIG. 2. III. Annealed soda-lime glass, wet; IV. Annealed lead glass, wet; V. Fused silica, wet.

moisture on the strength of porcelain is considerably less than on the strength of glass. The possible errors caused by not testing wet are probably less than two or three percent.

* Porcelain rods used in these experiments were supplied by George Aderhold of the Saxonburg Potteries, Saxonburg, Pennsylvania.

Lot VII had the same composition as lot VI but the porcelain was fired at cone No. 10 instead of cone No. 9. These rods were also tested dry.

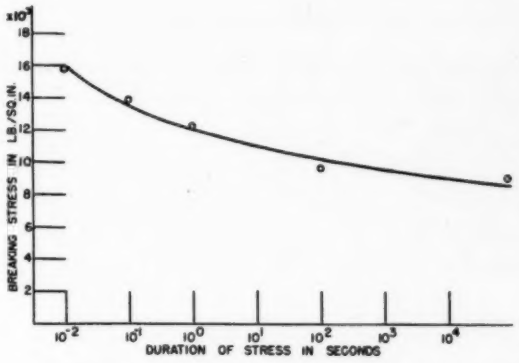

FIG. 3. VI. Porcelain, type A, dry.

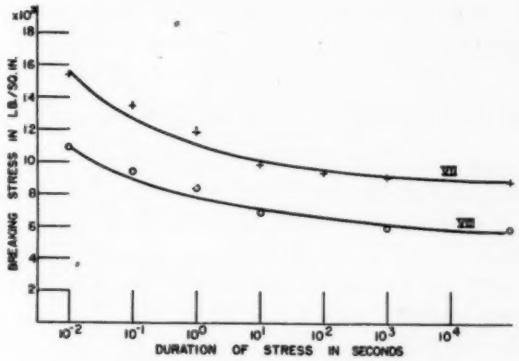

FIG. 4. VII. Porcelain, type B, dry; VIII. Porcelain, type C, dry.

Lot VIII consisted of porcelain rods of the following composition, fired at cone No. 12:

50 percent Canadian Feldspar
10 percent Florida Kaolin
30 percent Kentucky Ball Clay
10 percent Water

The rods were tested dry.

Of the results shown in Table I, those for soda-lime glass, lead glass, and fused silica may be considered most reliable. In the case of the Pyrex glass the records are ambiguous regarding the amount of the correction that was applied for the disannealing present in the rods. The amount of surface stress in the porcelain rods due to disannealing could not be determined, so some error from this cause may be present in these

data also. The rods of lots III–V, however, were known to be free of any disannealing stress and these data, therefore, do not include the possibility of such an error.

DISCUSSION OF ERRORS

At the present time, an exhaustive treatment of the errors in the fatigue testing of glass is quite impossible, because of the entanglement of the variables, which cannot as yet be independently investigated. However, a partial list of the factors will be given so that the reader may be assisted in evaluating the results.

1. Errors in Apparatus

In a previous paper the errors involved in applying the load and the errors of timing the duration of load were discussed. In general it was felt that these errors were not greater than ± 5 percent.

2. Errors in Measuring the Rod Diameters

This error was not large because the diameters could be measured to 0.0005 inch, or $\frac{1}{4}$ percent. Such an error would lead to only $\frac{3}{4}$ percent error in the applied stress, and since it was a statistical error it would practically disappear in the average for twenty rods.

3. Errors Due to Single Knife Edge

Since the rods were measured in cross bending, with a 5-inch span and single knife edge loading, a certain amount of error existed when the rod did not break exactly underneath the knife edge. At a quarter-inch away from the central loading point the stress would be 10 percent less than at the center. This changing stress caused a peculiar type of error to enter the results, because the long time loads nearly always broke the rod exactly under the knife edge, whereas under the short time loads the rod often broke as much as $\frac{1}{4}$ inch away from the central point. This would lead to a correction upwards in the short time strength, because the portion under highest stress was not broken, and therefore would have broken only at a still higher stress. Scratched rods nearly always broke under the knife edge, even in short time tests. The effect seems also to be a function of the number and kind of flaws, It is estimated that this error could reduce the average by as much as 5 percent in the short time loads.

4. Error Due to Scattering of the Data

The strength of the strongest rod in a sample might be twice as great as the weakest one. This scattering of the data resulted in a standard deviation for the individual rods that was about 10 percent of the average of the sample. The standard deviation of the average of 20 to 25 rods would be about 2 to 2.5 percent of the average. It would appear from the foregoing that the average strengths of different samples could be expected to agree to only 5 percent, and differences of as much as 8 percent would not be infrequent. On the other hand, actual check tests indicated that the procedure of preparing the samples had led to a strong correlation between them and that generally the average strength from sample to sample agreed to one percent or better. Unfortunately, insufficiency of data prevents an accurate computation of the correlation coefficient; and there is no assurance that the averages of 20 to 25 rods might not differ by as much as 5 percent due to purely statistical fluctuations.

5. Errors Due to the Loading Increments

The choice of the loading increments involved a compromise between two errors. One error would be that caused by the weakening of the rod from previous loading, and would become greater as the increment was made smaller. The other error would be due to an insufficient number of statistical class intervals, and would increase as the increments were made larger. This latter error is fully described in books on statistics[2] so that it need not be discussed here, except to state that it would probably be less than one percent in the average, when a loading increment of between 10 and 20 percent of the average is used.

The weakening effect of the previous loading has not been fully investigated. Some tests were made which indicated that a loading increment

[2] See, for example: G. U. Yule and M. G. Kendall, *An Introduction to the Theory of Statistics* (Charles Griffin and Company, Ltd., London, 1940) Chap. 6.

of 10 percent of the average or more, would cause less than a one percent decrease in the average strength.

6. Errors Due to the Atmospheric Conditions

Considerable data were obtained indicating that moisture and possibly gases affect the strength of glass. The specimens were tested wet after the phenomenon was discovered, but even then the presence of gases such as CO_2 possibly affected the results from one to five percent, the greater effect being for the longer load durations.

7. Errors Due to Temperature

Evidence has been obtained showing that temperature has a profound effect on both the strength and the fatigue of glass. It turns out that even small changes such as occur indoors will cause a change in the strength of glass amounting to one or two percent.

8. Errors Due to Storage of Rods

Since it was impossible to make all the tests at the same time, some of the rods were stored longer than others while the atmospheric conditions changed. There was some evidence that when rods were stored in a dry atmosphere for some time they did not have the same strength as rods stored in a damp atmosphere, even though they were tested wet in both cases. This resulted in another possible error of one or two percent in the final averages.

9. Combination of Errors

Considering these errors as a whole, it is estimated that the results cannot be considered accurate and controlled to more than ± 6 percent. Moreover, it must be appreciated that certain types of error will tend to distort or bias the data, making the short time strengths appear less than they should be in comparison with the long time strengths, or *vice versa*. Therefore, any generalizations that depend upon an accuracy of better than 10 percent in the results, or series of results, should be treated with extreme caution.

DISCUSSION OF RESULTS

Since a primary objective of this work was to investigate the fatigue in commercial glassware under normal conditions of temperature and humidity, the data are limited to normally scratched glass tested either wet or in an atmosphere of high humidity. As the difference in the strength of glass between 30 percent humidity and completely wet is only about 5 percent, the results are quite comparable. The surface condition of the rods was similar to the normally scratched and abraded condition found on bottles and window glass. Scratches, chatter marks, and percussion cones could be easily seen under a 50-power microscope.

Amount of Fatigue in Glassy Materials

The fact most apparent from the data is that all of the glassy materials tested exhibit the phenomenon of static fatigue to a marked degree. In the case of the soda-lime rods the 0.01-second strength is 3.1 times the 24-hour strength. The ratio of the 0.1-second strength to the 24-hour strength is between 1.7 and 2.4 for all the glasses tested. The corresponding ratios for porcelain ranged from 1.52 to 1.59.

Nature of Fatigue Curves

The plotted curves giving the relationship between the breaking strength and the logarithm of the duration of test show that there is a rapid decrease in strength up to a minute or so, and a very slow decrease from then on. The relationship between the strength and the logarithm of the duration of load is not linear, as has been previously supposed.[3] At present there is some question as to whether or not the curve is truly a monotonic decay, with steadily decreasing slope and steadily increasing radius of curvature, as we go to longer times. There remains a possibility, within the limit of accuracy of the tests, that there may be several points of inflection, implying deviations from our drawn curves.

Effect of the Condition of the Surface upon Fatigue

The condition of the surface has a profound effect on fatigue as well as upon the strength of the glass. Scratched glass loses much less strength in a given time interval than does unscratched glass. However, the percent loss of strength is roughly the same. This may be seen by comparing

[3] A. Smekal, Ergebr. d. exakt. Naturwiss. **15**, 106–188 (1936).

the tests on the scratched and unscratched Pyrex rods. The decrease for the scratched rods was 7850 lb./sq. in. and the decrease for the unscratched rods was 13,300. Yet the ratios of the 0.01-second strength to the 24-hour strength were 2.5 and 2.2, respectively. Unfortunately, this is all the data that are available for the comparison of scratched with unscratched rods, and the variable annealing stresses that existed in these rods as well as the different moisture conditions, tended to obscure the results.

That badly damaged glass fatigued in the same ratio as less damaged glass was borne out by the fact that the percent standard deviation of a sample of each kind tested at 0.01 second was approximately the same as that of a sample tested for 24 hours, although the strengths had changed by a factor of 3.1 to 1. Thus in the case of the soda-lime glass the standard deviation for the 0.01-second test, in which the average was 8500 lb./sq. in., was 800 lb./sq. in. In both cases the Pearson coefficient of variation was approximately 10 percent. Thus the stronger rods lost more strength than the weaker ones, yet they lost it in the same ratio. On the other hand, the fact that the rods broke under the central knife edge in long duration tests, but tended to break at some distance from it during the short duration tests, indicates that strong glass (i.e., glass with little surface damage) has a greater percentage loss of strength than weak glass. For it may be argued that in the short time tests some flaws made the rods weaker than other flaws did and the rods would break at 10 percent less stress. If these flaws were only $\frac{1}{4}$ inch away from the central knife edge, the rod would break there. Then if the minor and major flaws reduced the strength in the same ratio, we should get the breaks in about the same way on the long time tests. The fact that this does not happen indicates that the minor flaws must cause a greater fatigue rate in order to originate the breakage on the long time tests.

Effect of Chemical Composition

Because the loss of strength of glass is connected with surface damage, which cannot be accurately standardized between different glasses, it is difficult to make accurate judgments concerning the effect of chemical composition upon fatigue. Apparently the short time to long time strength ratios are about the same for all glasses studied. The results on the disannealed Pyrex rods have to be discounted because of the impossibility of applying a good correction for annealing stresses. We are left, therefore, with the results for silica glass, lead glass, and soda-lime glass as being perhaps accurate enough to judge this point. The ratio between the 0.10-second test and the 24-hour test is 2.4 in the last two cases, so no distinguishable difference is evident. The ratio however is only 2.0 in the case of the silica glass, so there is some evidence that silica glass fatigues slightly less than soda-lime or lead glasses.

In the case of the porcelains there is no question that they fatigue much less than the glass, as the ratio of the 0.10-second test to the 24-hour test ranges from 1.52 to 1.59. However, so little is known about the nature of fracture in porcelains, or aggregates in general, that it would be futile at this time to try to explain the fatigue in porcelain in terms of the fatigue phenomenon in glass, although they are probably closely related.

SUMMARY OF RESULTS

The results have corroborated previous investigations showing that the strength of glass depends on its surface damage, on the time it is under load, and upon atmospheric conditions. As the work progressed it became evident that these factors were interdependent in a complicated way. Nevertheless, to an accuracy of about 10 percent we can be assured that glass has about three times the strength under our briefest loads that it has under long time loads; that the relative loss of strength with time is about the same for lightly damaged and badly damaged glass surfaces, although the absolute strength varies radically with the damage; and finally, that chemical composition has only a small effect, if any, on fatigue.

The Effect of Water on the Strength of Glass

T. C. Baker† and F. W. Preston
Preston Laboratories, Butler, Pennsylvania
(Received November 1, 1945)

The strength of glass was measured in various surrounding media. It was found that glass is 20 percent stronger when dry than when wet, and two to two and a half times as strong when baked in vacuum than when tested wet (on tests of ten seconds duration). Apparently, the chief cause of the loss of strength, as compared with that in vacuum, is moisture, but gases, especially CO_2, seem to have some effect. It was found that fatigue of glass disappears when the glass is tested in a vacuum.

Autoclaving tests showed that glass is rapidly etched by water at higher temperatures, and that even silica glass is considerably attacked. It appears that the attack of water on glassy surfaces produces gels, and this attack goes on inside the flaws, thus considerably complicating the problem of the strength of glass.

INTRODUCTION

THE previous two papers[1,2] have shown that, under the conditions of the experiments therein described, there is a precipitate fall in the breaking strength of glass, including fused silica, and of porcelains in the first few milliseconds of loading, and a slower but steady fall with the lapse of further time. They have also shown that moisture seems to have something to do with this, so that the breakage of glass can perhaps not be understood simply in terms of stress, strain, and elastic constants; rather does "strength," as we usually measure it, involve the properties of the surrounding medium, perhaps a reaction with the surrounding medium, and so pass out of the field of engineering and even of physics into the domain of physical chemistry.

There have, indeed, both prior to the experiment detailed below and also between the time of the experiments (c1937–39) and the present (1945), appeared several papers by other investigators on the effect of the surrounding medium. Milligan,[3] for instance, found that exposing freshly cracked glass to water vapor or alcohol vapor considerably reduced its strength. He found that moistening a freshly scratched piece of glass reduced its strength 20 percent or more, and immersing the freshly scratched glass in dry paraffin oil increased the strength about 20 percent. Initial experiments of the authors indicated that changes of the relative humidity of the atmosphere would affect the results of strength measurements by 5 percent or more. It was thus evident that the surrounding medium played a very important part in tests for the strength of glass.

So it appeared desirable to investigate the effects of the surrounding medium on the strength of glass in greater detail than had been done heretofore. It was hoped that the studies would shed light on the causes of fatigue and possibly lead to a more complete understanding of the phenomenon of breakage.

Accordingly, the glass specimens were tested after they had been put into various solutions, and after they had been dried in desiccators; they were even tested in vacuum. Unfortunately, the results of the tests were generally not clear cut, and often it was not possible to duplicate them, so the general picture became more complicated with every new experiment. At the time the work was stopped a great many loose ends remained, and our understanding of the strength of glass had not become sufficiently fixed so that we could feel sure of our ground. Nevertheless, from a study of our data, in combination with that available in the literature, a general picture of the strength of glass began to emerge, indicating a much greater complexity than is usually supposed.

† Present address: Libbey-Owens-Ford Glass Company, Plaskon Division, Toledo, Ohio.

[1] T. C. Baker and F. W. Preston, "Wide range static strength testing apparatus for glass rods," J. App. Phys. **17**, 162 (1946).

[2] T. C. Baker and F. W. Preston, "Fatigue of glass under static loads," J. App. Phys. **17**, 170 (1946).

[3] L. H. Milligan, "Strength of glass containing cracks," J. Soc. Glass Tech. **13**, 351 (1929).

First of all, commercial glass has tiny flaws in its surface which can easily be seen with a microscope. After the flaw is made, water and gases enter it and radically change the nature of the surfaces and alter the physical and chemical conditions at the tip of the crack. If the glass at the flaw is under tensile stress, the water vapor affects the bonds at the tip of the flaw, causing great weakening. If the flaw is allowed to stand, the water vapor forms thin gels on the surfaces and rounds out the tip of the flaw, causing an increase in strength. There is reason to believe that complete equilibrium was not established in any of our experiments.

The "strength" of glass began to appear to have little meaning as a physical constant of the material. It might be more correct to say that the phenomenon of rupture is due to several causes, including tensile stresses at the surface of the glass, the time during which the tension is applied, the nature and depth of the flaws, and the penetration of atmospheric or other reagents into the inside of the flaws. It is obvious that a great stress in itself would be a sufficient condition to break the glass, yet there exists evidence that atmospheric and weather conditions also would cause some flaws to extend to the point of rupture.[4] So it is doubtful that any one single cause is an essential element in the breakage.

With such a complicated picture to investigate it becomes apparent that controlled tests are particularly difficult. Many of the factors cannot be truly controlled, such as the size and orientation of a flaw, so it is not surprising that effects should occur that could not be duplicated. For this reason much of the data in this paper has been included not to prove points finally but merely to indicate the nature of effects, so that future research on this problem will be on a sounder basis.

The strength of ordinary commercial glass depends primarily on the size, depth, and orientation of the tiny cracks and flaws on its surface. These flaws cause the strength to be reduced from a theoretical strength of several million pounds per square inch to one that varies between 2000 lb./sq. in. and 20,000 lb./sq. in. in glassware whose surface has been damaged by abrasion and impact. The effects of the surrounding medium upon the strength, therefore, can only be comparative. So, in our experiments, two or more samples of about 25 glass rods each were tested under different conditions and the ratio of their strengths determined.

Any surrounding medium seems to lower the strength by a certain ratio below the vacuum strength, rather than to subtract a fixed amount from the vacuum strength. For example, if the strengths of two comparable samples were obtained, one in vacuum and the other in air, and the strength in vacuum was 20,000 lb./sq. in. and in dry air 10,000 lb./sq. in., the ratio would be 2.0. Two other somewhat stronger samples tested in vacuum and dry air might have strengths of 30,000 and 15,000 lb./sq. in., and in this case also the ratio would be 2.0. This rule, that the surrounding medium affects the strength by a ratio, seems to be approximately true of all our studies on fatigue of glass as affected by the surrounding medium.

APPARATUS

The apparatus used to measure strengths of glass rods in the following experiments was the quick-loading apparatus described in a previous paper.[1] When it became necessary to measure the strength of glass in vacuum, the quick-loading apparatus was put into a vacuum chamber. Otherwise the rods were tested out in the open air after they had been treated according to the various procedures described.

The vacuum strength-testing apparatus included a vacuum chamber, consisting of a bell jar resting on a cylindrical steel shell, in which the entire quick-loading apparatus was placed. A glass rod is supported by two knife edges five inches apart. A wire bale is looped over the glass rod and connects to the armature which hangs freely in a magnetic air gap. A field coil produces the magnetic field in the air gap. This field coil was covered with cement to prevent outgassing when the vacuum was drawn. On either side of the glass rod were added two heater coils consisting of chromel wire wrapped around porcelain rods. An easily removable furnace shield prevented radiation from the heater coils from

[4] See A. Silverman and L. G. Ghering, "Deterioration of old whiskey bottles," Glass Ind. [9] **15**, 339 (1942).

warming the bell jar too much while the rod was being baked out. A glass window at the end of the furnace shield permitted observation of the rod during the test. The shield had several openings to the main chamber so that there was no doubt of its having the same vacuum as that in the main chamber. The vacuum chamber is enclosed by a large bell jar resting on a steel cylinder which has a flat bottom welded to it. The vacuum chamber is evacuated through an outlet leading to a McLeod gage and a diffusion pump.

PROCEDURE

The procedure for testing the strength of glass rods was described in a previous paper.[2]

Briefly, a table was constructed which gave the stress in terms of the current through the armature coil for every rod diameter. The diameter of each rod was measured before inserting it into the quick-loading apparatus. A minimum stress was put on the rod for a given length of time; if the rod did not break, it was then stressed at a higher level for the same length of time, and so on until it broke. The stress was increased in steps of 2000 lb./sq. in. if the average strength was greater than 12,000 lb./sq. in., and in steps of 1000 lb./sq. in. if the average strength was less than 12,000 lb./sq. in. Preliminary experiments enabled the operator to tell which increment to use. The average breaking stress of each sample of rods was corrected, as explained previously,[2] by subtracting one-half the increment from the average.

The procedure in testing glass rods for strength under vacuum was to insert the rod in the quick-loading apparatus, put the furnace shield into position and, after placing the bell jar on top of the iron cylinder, start the mechanical vacuum pump. Because of the large volume of the test chamber, the mechanical pump was operated for a half-hour or so before it became feasible to start the diffusion pump. After an hour and a half the vacuum would be down to 1 micron or less, at which time the rod would be baked out at about 350°C for 10 minutes. After baking out, the rod was allowed to cool for one hour because it lost heat very slowly. Even at the end of an hour, when the rod was tested for strength, the temperature of the rod was about 80°C.

TABLE I.

Test No.	Pressure	Temp. of bake out	Time of bake out	Duration of test	Average strength
1	0.05 micron Hg	350°C	10 min.	10 sec.	24,700 lb./sq. in.
2	0.2 micron Hg	350°C	10 min.	10 sec.	23,800 lb./sq. in.
3	0.1 mm Hg	350°C	10 min.	10 sec.	18,900 lb./sq. in.
4	760 mm (wet)			10 sec.	12,100 lb./sq. in.

RESULTS

Results of the Vacuum, Drying, and Autoclaving Tests

The strength of glass rods was measured under various degrees of vacuum with different heating treatments. These tests were aimed at discovering the effect of vacuums, and the effect of heating plus vacuums, upon the strength and fatigue of glass of various chemical compositions. In general, comparisons were made between the average strengths of twenty rods. In this way a series of twelve experiments was carried out on comparable samples to determine the effect of various treatments on "strength."

Experiment I—Variation of Vacuum, Soda-Lime Glass

Soda-lime rods approximately two years old were made into four comparable samples of approximately twenty rods each. The rods had been stored part of the time in an unheated warehouse and had been alternately moist and dry, causing a slight amount of weathering or bloom to form on their surfaces. Three of the samples were tested under vacuum as described above. The fourth sample was tested wet under atmospheric pressure with no heating. The results are shown in Table I.

From these results it can be seen that the strength is greatest in the highest vacuum. The strength of the glass when tested in the 0.05-micron vacuum is greater than the strength when the glass is tested wet at atmospheric pressure by a factor of 2.04. The tests are limited to ten-second duration. It is probably significant that the strength at 0.05 micron is slightly greater than at 0.2 micron, but since the probable error of the results is around 250 lb./sq. in. from statistical fluctuations alone, this conclusion will have to be treated with reserve.

TABLE II.

Test No.	Pressure	Temp. of bake out	Time of bake out	Duration of test	Average strength
1	0.1 micron Hg	350°C	10 min.	10 sec.	44,300 lb./sq. in.
2	0.1 mm Hg	350°C	10 min.	10 sec.	32,200 lb./sq. in.
3	10 mm Hg	350°C	10 min.	10 sec.	29,200 lb./sq. in.
4	760 mm Hg (wet)			10 sec.	17,700 lb./sq. in.

Experiment II—Variation of Vacuum, Pyrex Glass

Four comparable samples of carefully handled Pyrex rods were tested by the same procedure as used for the soda-lime rods in experiment I. The results are shown in Table II.

The strength is greatest in the highest vacuum and is less as the vacuum is reduced. In this experiment on Pyrex glass the strength in the 0.1-micron vacuum is 2.50 times the strength wet in the atmosphere.

Experiment III—Silica Glass

This experiment was made on two comparable samples of silica glass rods. The procedure was the same as above. The results are shown in Table III.

These tests show that for silica glass the ratio between the strength of rods baked out in vacuum and the strength of those tested wet is only 1.67 on the ten-second test.

TABLE III.

Test No.	Pressure	Temp. of bake out	Time of bake out	Duration of test	Average strength
1	0.05 micron Hg	350°C	10 min.	10 sec.	27,900 lb./sq. in.
2	760 mm Hg (wet)	350°C	10 min.	10 sec.	16,700 lb./sq. in.

Experiment IV—Porcelain

In order to see whether or not a similar effect is obtained with porcelain, strength tests were made on three comparable porcelain samples. For the first sample the procedure was to bake out the test specimens in a vacuum for 10 minutes and allow them to cool for an hour to about 80°C before testing. On the second sample the rods were dried for one week in a desiccator in the presence of phosphorous pentoxide, then taken out of the desiccator and quickly tested in the test chamber at atmospheric pressure in the presence of fresh phosphorous pentoxide. The third sample was tested wet, at atmospheric pressure. The results are shown in Table IV.

From these tests it can be seen that the ratio between the strength in vacuum and the strength wet is only about 1.5. The effect is apparently markedly less than on glass rods.

Experiment V—Effect of Heat, Soda-Lime Glass

There was some question as to whether or not heating had much effect upon the strength of glass rods under vacuum. This test was made to compare the strength of glass rods under vacuum with and without baking out. Since from the time the vacuum pumps were started to the time of test on the baked-out rods was about four hours, the sample that was not baked out was kept under vacuum for that time also. The results (Table V) were obtained on three comparable samples of 20 soda-lime rods.

TABLE IV.

Test No.	Atmosphere	Temp. of bake out	Time of bake out	Duration of test	Average strength
1	0.01 micron vacuum	350°C	10 min.	10 sec.	10,400 lb./sq. in.
2	Dried in desiccator			10 sec.	7400 lb./sq. in.
3	Wet			10 sec.	6950 lb./sq. in.

These tests clearly showed that the strength was greatest on the 10-second tests when the rods were baked out in vacuum.

Experiment VI—Effect of Vacuum on Fatigue, Soda-Lime Glass

In order to study the effect on fatigue of different levels of vacuum, four comparable samples of soda-lime glass rods similar to those in experiment I were used. These rods had been stored in an unheated warehouse and had visible

TABLE V.

Test No.	Pressure	Temp. of bake out	Time of bake out	Duration of test	Average strength
1	0.1 micron Hg	350°C	10 min.	10 sec.	25,950 lb./sq. in.
2	0.1 micron Hg	None		10 sec.	21,900 lb./sq. in.
3	760 mm Hg (wet)			10 sec.	12,900 lb./sq. in.

evidence of weathering on their surfaces. The results are shown in Table VI.

These results indicate that there is no fatigue when the rods are baked out at 0.1 micron of Hg vacuum, but there is considerable fatigue at 0.1 mm of Hg vacuum. The fact that the strength of the rods on the 0.1-second tests was greater for the lower vacuum than for the higher vacuum seems hard to explain, especially since the results could not be duplicated in experiment VII which was performed on another batch of soda-lime rods of the same chemical composition. However, when Test No. 3 was being conducted, it became evident as soon as a few rods had been tested that the data were going to be very different from that of Test No. 1, and the apparatus was carefully checked without discovering anything unusual. There was no doubt of the increased stress the rods were bearing; this was shown by the amount of bending they underwent before breaking. Moreover, check

TABLE VI.

Test No.	Pressure	Temp. of bake out	Time of bake out	Duration of test	Average strength
1	0.1 micron Hg	300°C	10 min.	0.1 sec.	25,900 lb./sq. in.
2	0.1 micron Hg	300°C	10 min.	10 sec.	25,900 lb./sq. in.
3	0.1 mm Hg	300°C	10 min.	0.1 sec.	32,200 lb./sq. in.
4	0.1 mm Hg	300°C	10 min.	10 sec.	21,600 lb./sq. in.

tests with a few remaining canes were run at conditions of Test 3, which confirmed the above results on this batch of rods.

Experiment VII—Effects of Vacuum and Heating on Fatigue

In order to investigate the peculiarities noticed in experiment VI, Tests 1 and 3, a series of tests was made on a new batch of soda-lime rods of the same chemical composition as those used in experiment VI. These rods were only a few months old and showed no signs of weathering at the time the tests were made. Various heat treatments were used to see if there was any indication of the effects found in experiment VI. The results are shown in Table VII.

These tests confirm the results of experiment VI in that there is practically no fatigue when the glass is baked out at high vacuum: The tests do show however that the increased strength

TABLE VII.

Test No.	Nature of treatment	Pressure	Duration of test	Average strength
1	Heated 15 minutes at 0.01 micron using P_2O_5	0.01 micron	10 sec.	25,520 lb./sq. in.
2	Heated 15 minutes at 0.01 micron, no desiccator	0.01 micron	10 sec.	25,330 lb./sq. in.
3	Heated 15 minutes at 0.1 mm; then again at 0.01 micron	0.01 micron	0.1 sec.	25,809 lb./sq. in.
4	Heated 15 minutes at 0.1 mm, tested cool	0.1 mm	0.1 sec.	25,619 lb./sq. in.
5	Heated 5 minutes at 0.1 mm	0.1 mm	0.1 sec.	25,050 lb./sq. in.
6	Heated 10 minutes at 0.1 mm; held 1 hr.; heated 19 minutes	0.1 mm	0.1 sec.	23,050 lb./sq. in.
7	No heating	0.1 mm	0.1 sec.	25,250 lb./sq. in.

on Test 3 of experiment VI was not a repeatable phenomenon on the newer rods, and that the 0.1-second strength at lower vacuum was practically the same as that at higher vacuum. It is our opinion that weathering had formed gels in the cracks that had very much influenced the strength tests in experiment VI.

Experiment VIII—Effect of Dried Air

In order to get some idea as to whether or not gases other than water vapor affect the strength of glass, four comparable samples of soda-lime rods were prepared. In the first test the rods of sample 1 were baked out and tested in vacuum as before. In the second test the rods of sample 2 were baked out at 0.01 micron and allowed to cool for 1 hour, then the air was allowed to enter after it had been dried by bubbling through two stages of concentrated sulphuric acid. After a period of half an hour, the rods were tested for strength. The third test, with sample 3, was the

TABLE VIII.

Test No.	Pressure	Temp. of bake out	Pressure of test	Duration of test	Average strength
1	0.01 micron Hg	300°C	.01 micron	10 sec.	25,500 lb./sq. in
2	0.01 micron Hg	300°C	760 mm after ½ hour	10 sec.	22,600 lb./sq. in.
3	0.01 micron Hg	300°C	760 mm after 24 hours	10 sec.	22,000 lb./sq. in.
4			760 mm wet	10 sec.	12,500 lb./sq. in

TABLE IX.

Test No.	Relative humidity	Duration of test	Average strength
1	0	100 sec.	11,300 lb./sq. in.
2	30%	100 sec.	10,200 lb./sq. in.
3	100%	100 sec.	9,800 lb./sq. in.

same as the second except that the rods remained in the dry air atmosphere for 24 hours before testing. The rods of sample 4 received no heat treatment and were tested wet at atmospheric pressure. The results are shown in Table VIII.

Apparently even dry air causes some reduction in the strength of glass, as can be seen from a comparison of Test 1 with Tests 2 and 3. However, it is possible that slight amounts of moisture were able to come through the drying apparatus and of course there must have been some SO_3 and H_2SO_4 gases present.

Experiment IX—Effects of Dry Storage

It was thought advisable to obtain comparative figures on the strength of "dry" glass rods as compared with glass under average atmospheric conditions and as compared also with thoroughly wet glass. The "dry" rods were dried in a desiccator for a week in the presence of P_2O_5 before testing. The results are shown in Table IX.

An increase of strength of about 15 percent above the strength when wet is indicated when rods are dried in a desiccator, and an increase of about 5 percent when the relative humidity is around 30 percent. However, this work was not too carefully controlled and is included merely to show approximately what can be expected.

Experiment X—Effect of CO_2, Soda-Lime Glass

A few tests had indicated that some factor other than water was a weakening agent. We suspected CO_2 because it is known that CO_2 in weak solution will dissolve silica more than will plain water. Four comparable samples were used. Each sample was put into a different liquid for two hours previous to testing and kept wet with the liquid during test. The liquids used were distilled water, distilled water carbonated at room temperature, distilled water with saturated $Ca(OH)_2$, and distilled water with normal NaOH. It was felt at this time that the differences of strength observed were due more to differences of fatigue rates rather than to a fundamental lowering of the "strength." Therefore the rods were tested for 100 seconds duration in hopes that differences would be more apparent. The results are shown in Table X.

There is some indication that the CO_2 is an additional weakening agent besides the water. If so, the rest of the data might be explained on the basis that the CO_2 that is normally in the air was kept away from the flaws. However, until more carefully controlled tests are available it will not be possible to be absolutely sure about the effect of CO_2.

Experiment XI—Effect of Etching by Water Vapor

Since the attack of water on glass appeared to be the chief cause of fatigue and the chief weakener of glass, some studies of the effect of water upon glass at an elevated temperature were tried. A high pressure autoclave allowing use of steam up to 1000 lb./sq. in. was used to make the tests. It was found that under prolonged treatment at pressures as high as 800 lb./sq. in. all glasses, including silica glass, were attacked severely by water. The soda-lime glasses were attacked the most, Pyrex glasses next, and silica glass least of all. The attack was similar to etching with hydrofluoric acid. In the case of the soda-lime glasses a very thick jelly-like layer formed on the surface. Since the etching was similar to that of hydrofluoric acid, one would expect the rods to get stronger when autoclaved. Unscratched silica rods and rods scratched with coarse emery were autoclaved at 700 to 800 lb./sq. in. for twenty-four hours and then removed and tested for strength (Table XI).

TABLE X.

Test No.	Liquid surrounding rod	Duration of test	Average strength
1	Distilled water	100 sec.	13,400 lb./sq. in.
2	Distilled water saturated with CO_2	100 sec.	13,150 lb./sq. in.
3	Saturated solution of $Ca(OH)_2$	100 sec.	13,950 lb./sq. in.
4	Normal solution of NaOH	100 sec.	13,750 lb./sq. in.

From these tests it is immediately evident that autoclaving can increase the strength of silica glass, probably by etching out the flaws.

Tests similar to those on the silica rods were made on soda-lime glass rods. In this case the rods were autoclaved for four hours at 600 lb./sq. in. then removed and tested wet in the quick-loading apparatus. The results are shown in Table XII.

These tests on soda-lime rods showed that their strength also could be increased by etching in an autoclave.

Experiment XII

Some further tests were made on the breaking strength of rods in an autoclave. A glass rod was supported by knife edges and loaded centrally with a heavy metal weight. The whole apparatus was put into the autoclave and the steam pressure was applied for about one hour. Then it was observed whether or not the rod had broken. When the rod did not break in the autoclave, it was next tested in the open and found to be very much stronger than comparable rods that had not been autoclaved. But such rods as did break in the autoclave broke at unusually low stresses of 2000 lb./sq. in., and even less, compared with about 5000 lb./sq. in. for the lowest breaking strength of comparable rods when tested for 24 hours in the open. It would appear therefore that glass can fatigue very much more in an autoclave than in ordinary atmospheric conditions.

Discussion of Results of Vacuum Tests

These experiments on the strength of glass in a moderately high vacuum show clearly that the strength of glass is much greater in vacuum than when the glass is wet and in the open, and that fatigue is greatly reduced or entirely eliminated by vacuum treatment.

The increase in strength due to baking in a vacuum is shown by experiments I–IV. The ratio of the vacuum strength to the wet strength is 2.5 for Pyrex, 2.0 for soda-lime glass, 1.7 for silica glass, and 1.5 for porcelain. Thus it would appear that this effect is dependent somewhat on chemical composition. The fact that it is relatively low for porcelain and silica glass (which are chemically resistant) would suggest that the effect is correlated with the chemical attack of moisture or gases at the tip of the crack.

It is quite evident that glass fatigues very little, if at all, in a high vacuum. Tests 2 and 3 of experiment VII show that the strength is 25,800 lb./sq. in. on the 0.1-second test and 25,300 lb./sq. in. on the 10-second test. Also, Tests 1 and 2 of experiment VI give the strength as 25,900 on both the 0.1-second and 10-second tests in high vacuums. The fact that there was very little fatigue at high vacuums was evident from observations with a cathode-ray oscillograph of the times required to break the rods. The rods generally broke as soon as the load came on or not at all; only occasionally was there definite evidence of delayed breakage. However, unless the rods were baked out at 350°C or more, at high vacuum, there was considerable evidence of fatigue. It would therefore appear that fatigue is caused primarily by the action of water vapor and adsorbed gases acting in the flaws. It is very doubtful that even heating the glass up to 350°C or more removed all the water vapor from the flaws, since they were in the neighborhood of 0.005-inch deep in the glass used and probably only a few Angstrom units wide at the tips. Too little theoretical knowledge is available to estimate the length of time required to evacuate the water vapor under those circumstances. It is possible that the most sensitive test of the presence of water vapor in the tip of a flaw is the occurrence of fatigue in strength tests.

There is considerable evidence that the "strength" of glass is a much more complicated

TABLE XI.

Test No.	Time autoclaved	Steam pressure	Duration of test	Average strength
1-Scratched	24 hours	700–800	10 sec.	30,000 lb./sq. in.
2-Scratched	0		10 sec.	6000 lb./sq. in.
3-Unscratched	24 hours	700–800	10 sec.	54,000 lb./sq. in.
4-Unscratched	0		10 sec.	19,000 lb./sq. in.

TABLE XII.

Test No.	Duration of autoclaving	Pressure of autoclave	Duration of test	Average strength
5	4 hours	600 lb./sq. in.	10 sec.	27,400 lb./sq. in.
6	0		10 sec.	13,000 lb./sq. in.

matter than is generally realized. Such evidence is apparent in a comparison between the tests in experiments VI and VII. In both cases the rods were of the same composition. The rods in experiment VI had been stored for a few years, some of the time in an unheated warehouse, and showed slight weathering. These rods showed a strength of 32,200 lb./sq. in. on the 0.1-second test in a 0.1-mm vacuum, as compared with 25,900 lb./sq. in. for rods baked out in a vacuum of 0.1 micron. Careful checks were made so there was no doubt of the phenomenon, yet it was unrepeatable in experiment VII on glass that was not so old and had been stored in a heated room most of the time.

The only hypothesis to explain these rather erratic results seems to be that gels form in the flaws which strengthen the glass but have much greater fatigue rates than glass. When the glass is thoroughly baked out, the gels crack or lose their strength to an extent that makes them a negligible factor.

The chemical attack of water on glass at elevated temperatures and pressures was shown in experiments XI and XII. It was somewhat surprising to see the rapidity of attack of water on silica glass at steam pressures around 700 to 800 pounds per square inch. That the flaws were etched out and that the strength of the glass was increased was clearly demonstrated. It was surprising to find that the process of fatigue could be remarkably speeded up at these temperatures, so that glass fatigues to much less than its 24-hour strength in a matter of an hour or possibly only a few minutes. These results strengthen our feeling that the process of fatigue is essentially a chemical attack.

The chemical attack upon glass by moisture is extensively discussed in the literature and summarized by Morey.[5] That a chemical attack inside the flaws should decrease the strength of glass is not surprising, as one would expect the bonds under the greatest tension to be those most ready to rupture and combine to form new compounds. This chemical attack will of course depend on two factors, the first being the ability of the water to penetrate to the tip of the flaw and the second being the chemical durability of the glass. The fact that all cracks are pretty much alike dimensionally as well as the fact that all glasses, including silica, are attacked by water probably accounts for the similarity of strength between glasses at room temperature. That there are differences in the amount of fatigue in glasses of different compositions and that the ratio between the strength of glass in vacuum and the strength of glass wet is different for different glasses indicate that there is a partial correlation between chemical composition and fatigue of wet glass. It was found[2] that silica appears to fatigue less than soda-lime and Pyrex, and the Pyrex appears to fatigue even more than soda-lime if one takes into account the fact that the samples of Pyrex glass had an initial compression. Then of course in the vacuum work just cited the ratio of the vacuum strength to the wet strength was greatest for Pyrex, with soda-lime following and, finally, the ratio for silica glass was least of all. In general, Pyrex glass is considered to be more chemically durable than soda-lime, but this is not necessarily true when the attacking medium is basic in nature. In a flaw there is no reason for the alkali to be leached out. Since probably the attack in both Pyrex and soda-lime glass is basic in nature the correlation with chemical durability seems to hold.

These tests on the strength of glass under different conditions of the surrounding medium give considerable insight into the ultimate questions pertaining to the fatigue of glass under constant load. Specifically, it seems to be necessary to distinguish between glass in which the flaws are of recent origin and glass in which the flaws have existed for some time and have been exposed to the atmosphere.

In the first case the glass has a definite strength under high vacuum no matter what the duration of the load (at least to the extent covered in our tests). When even slight amounts of moisture are present the glass loses strength with duration of load, although this loss is slight in moderate vacuum. As the humidity is increased, the loss of strength with duration of load becomes greater, that is, as the absolute vapor pressure of the water is increased a condition arises where fatigue is very rapid. Thus it appears that when the duration of load is decreased the strength of

[5] G. W. Morey, *The Properties of Glass* (Reinhold Publishing Corporation, New York, 1938), Chap. V.

glass approaches its vacuum strength. This suggests that in extrapolating fatigue curves to shorter times it would be unjustified to go to durations which yield strengths greater than the vacuum strength. Moreover, we should expect the fatigue curves, now extended experimentally only to 0.01-second duration, to level off as the duration of load is decreased to around 0.0001 second. In all probability the extrapolation of the present fatigue curves to shorter times is not legitimate.

In the second case, where the flaws have had time to weather and gels have formed inside them, the picture of the short time strength is too complicated to permit any definite statement. The short time strength probably is determined more by the strength of the gels than by the strength of the glass. Some glass may act like freshly scratched glass and some may show behavior characteristics similar to the weathered glass of experiment VI. The very short time strength can be equal to or greater than the vacuum strength, depending on the gels.

In the middle range of durations of load (from 0.01 second to perhaps several years) the decay of strength with time of wet glass at room temperature and atmospheric pressure may be represented by the equation

$$S=[C_1/\log C_2 t]+C_3.$$

This equation may be regarded as empirical, and other empirical formulae fit the results equally well. One such equation is discussed by Preston and Glathart in the fourth paper of this series, entitled "The Fatigue Modulus of Glass."[6]

Under "atmospheric" conditions, it is likely that there is very little difference in fatigue between glass with weathered flaws and glass with fresh flaws. But this may depend on the way we define "fatigue"; see the paper of Preston and Glathart mentioned above.[6]

If however the conditions of the atmosphere are changed the picture is greatly altered. As the temperature and water vapor pressure are increased the fatigue is rapidly accelerated until at pressures of a few hundred pounds of steam a decline in strength takes place in a few minutes that might take hours or years at room temperature. However, if the glass is not broken the flaws will etch out in a few hours and the specimen will become very much stronger than before. Ultimately, the attack of the steam will destroy the glass rods completely and so we may consider the strength to be zero for glass subjected to 1000 lb./sq. in. steam pressure for a week or two.

If a glass rod were under constant load and surrounded by water at room temperature, it is exceedingly probable that its strength would behave in a manner similar to that of glass subjected to elevated temperatures in an autoclave. For fairly high stresses the tips of the flaws would tend to round out without much extension and the glass would eventually become stronger. Ultimately, the glass would dissolve and be destroyed by the water, but many thousands of years would be required in the case of chemically resistant glasses.

It is a moot question as to what will happen to glass under load at room temperature in a dry atmosphere (relative humidity between 1 percent and 50 percent). There is evidence of chemical attack on most glasses under these conditions. The glass will fatigue in about the same way as it does when it is wet. Therefore, it is likely that for many glasses the ultimate results will be the same. Under high stresses the flaws will extend until breakage occurs. Under low stresses of about 1000 to 2000 lb./sq. in. the attack of the water will tend to round out the flaws and the glass will slowly get stronger. On the other hand, crystalline material may form, in the case of some of the less durable glasses, tending to force open the flaws and progressively extend them. In such a case the strength of the glass is zero for durations of load as short as a few years.[4]

CONCLUSIONS

In high vacuum, thoroughly baked out glass can be said to have a tensile strength fairly independent of the time of loading, at least for the shorter durations of load. If glass is exposed to moisture it rapidly loses strength under stress. In ten seconds the strength can decay to $\frac{1}{2}$ or $\frac{2}{5}$ of the vacuum strength, and it may decay to $\frac{1}{3}$

[6] F. W. Preston and J. L. Glathart, J. App. Phys. **17**, 189 (1946).

the vacuum strength in 24 hours. This strength decay appears to be caused by a chemical attack in the flaws of the glass by water and possibly by some gases such as CO_2.

It therefore appears that for very short durations of load the strength of freshly scratched glass approaches the high vacuum strength. For moderate durations of load ranging from 0.01 second to probably several days or so the strength of wet glass or glass under humid conditions approximately obeys the relationship

$$S=[C_1/\log C_2 t]+C_3,$$

where S is breaking stress, t is time, and C_1, C_2, and C_3 are arbitrary constants. For longer durations of load, several years or more, the chemical composition is so important as to be the controlling factor in strength, but there is reason to believe that at low stresses the flaws can etch out and the glass actually become stronger, in the case of chemically resistant glasses, so that glasses that survive for years may survive for several millions of years. Inevitably of course the chemical attack of the atmosphere will disintegrate the glass to a point where the strength is zero, in the case of silica glass in probably billions of years.

ACKNOWLEDGMENTS

The authors wish to acknowledge the help of Dr. Justin Glathart, of the Preston Laboratories at present (though not at the time of the experiments) for valuable editorial help, both in the matter of checking the ancient records against these present summaries, and in arranging the matter and the diction for the benefit of readers who had no contact with the early work. The authors realize that, in attempting to write at the end of the European war reports that should have been written at its beginning, they are apt to use terminology which the passage of time should have outmoded. Thanks to Dr. Glathart, we believe, however, that serious ambiguity has been avoided, and major errors in transcribing the old results reduced to very few or eliminated altogether. It is hardly to be expected that in the second and third papers no errors, even minor ones, remain, but we believe that the general picture has been presented as accurately as the experiments disclosed it.

The Fatigue Modulus of Glass

J. L. GLATHART AND F. W. PRESTON
Preston Laboratories, Butler, Pennsylvania
(Received November 1, 1945)

The decline in the breaking strength of glass with an increase in the length of time it is under stress has been noted by various experimenters. Based on the experimental results of T. C. Baker, an empirical relationship is obtained which indicates that the reciprocal of the breaking stress is a linear function of the logarithm of the duration of the stress. Certain implications of this relationship are discussed.

I. INTRODUCTION

VARIOUS experimenters have shown that a glass specimen may sustain a certain static stress momentarily but will ultimately fail under the same stress, with the mere passage of time. No complete theoretical basis for this effect has as yet been established, although Murgatroyd[1] has recently proposed a "viscous pocket" theory for the constitution of glass which, he states, is capable of accounting qualitatively for the observed decrease in strength with time.

The object of the present paper is to present an empirical relation which fits the strength-time curves of all the glasses for which adequate experimental data are available. Some of the implications of this relation are discussed.

II. THE STRENGTH-TIME RELATION

In another paper[2] T. C. Baker has given his experimental results of the fatigue effect in fused silica, three kinds of commercial glasses, and three porcelains. His results are summarized in Table I.

The total range of durations of stress is seen to be from 0.01 second to 24 hours (86,400 seconds), a range of nearly ten million to one. This is a tremendous range, and it becomes virtually necessary to plot it on a logarithmic base. The various ranges of strengths, however, are relatively small, from 23,880 to 11,740 lb./sq. in. in the case of fused silica, for instance, and from 19,900 to 6,450 lb./sq. in. in the case of soda-lime glass. It is natural to plot this on a linear or arithmetical scale. This method of plotting, f against $\log t$, was the one adopted by Smekal[3] who, over a smaller range of durations, reported a linear relationship. This came about, as James Bailey pointed out later,[4] because Smekal inadvertently misplaced some of his points by a factor of ten. Had they been correctly plotted, his line would not have been straight.

Baker adopted the same rather natural method of plotting, and obtained very definitely curved lines for all of his materials, the curvature being the more obvious because of his longer range of time intervals. Baker, with commendable caution, refused to indulge in any speculation regarding the strengths of his materials beyond the experimental time range, but warned that any point on any of his curves might be in error by as much as ± 10 percent.

The Preston Laboratories have received various inquiries and suggestions regarding this matter of the fatigue of glass, especially since the

TABLE I. Average breaking stress in pounds per square inch (and its reciprocal)* for various durations of load.

Material	0.01 sec.	0.1 sec.	1.0 sec.	10 sec.	100 sec.	1000 sec.	86,400 sec.
Disannealed Pyrex (dry)	24,600 (4.06)	19,600 (5.10)	17,100 (5.85)	15,900 (6.30)	— —	12,800 (7.81)	11,300 (8.85)
Scratched Pyrex (wet)	12,900 (7.75)	10,600 (9.43)	9,000 (11.11)	8,250 (12.12)	— —	5,750 (17.4)	5,050 (19.8)
Annealed soda-lime glass (wet)	19,900 (5.03)	15,900 (6.29)	— —	10,500 (9.53)	— —	7,950 (12.58)	6,450 (15.50)
Annealed lead glass (wet)	— —	19,000 (5.26)	14,900 (6.71)	11,200 (8.93)	— —	9,400 (10.63)	7,950 (12.58)
Fused silica (wet)	— —	23,880 (4.19)	— —	19,800 (5.05)	15,660 (6.39)	14,280 (7.00)	11,740 (8.52)
Porcelain *A* (dry)	15,800 (6.34)	13,900 (7.20)	12,300 (8.13)	— —	9,700 (10.32)	— —	9,100 (11.00)
Porcelain *B* (dry)	15,400 (6.50)	13,500 (7.41)	11,900 (8.40)	9,900 (10.10)	9,400 (10.64)	9,100 (11.00)	8,900 (11.23)
Porcelain *C* (dry)	10,900 (9.17)	9,400 (10.64)	8,400 (11.91)	6,900 (14.50)	— —	6,000 (16.67)	5,900 (16.95)

* Reciprocals are given in parenthesis, and are to be multiplied by 10^{-5}.

[1] J. B. Murgatroyd, J. Soc. Glass Tech. **28**, 406 (1944).
[2] T. C. Baker and F. W. Preston, "Fatigue of glass under static loads," J. App. Phys. **17**, 170 (1946).
[3] A. Smekal, Ergeb. d. exakt. Naturwiss. **15**, 106 (1936).
[4] J. Bailey, private communication.

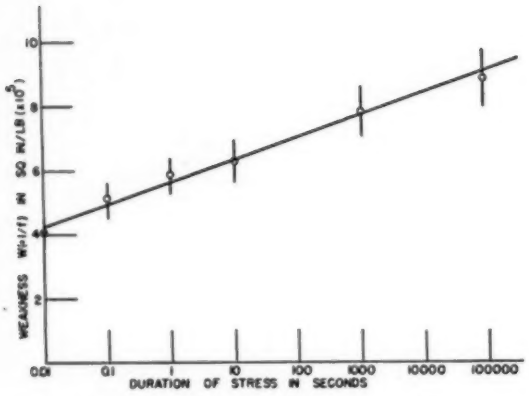

FIG. 1. Disannealed Pyrex glass, dry.

publication of the Philadelphia lecture,[5] and the matter has recently been considered by Murgatroyd and Haward.[6] In view of this interest, it seems desirable to discuss Baker's curves a little more fully with respect to whatever empirical information may be obtained from them.

We have known for some time that if $1/f$, the reciprocal of the breaking stress, is plotted against $\log t$ a straight line can be drawn which, for every one of Baker's materials, passes within the "possible error" he assigned to his values. A note to this effect appeared in *Nature*.[7] This relation has also been noted by Haward,[6] whose observations reached us after the note in *Nature* had been published.

Figures 1 to 8 show the straight lines that result when Baker's values are plotted in this way. Figure 9 is a similar plot of some previous data reported[8] from this laboratory, which were obtained on plate glass laths of dimensions $16'' \times 2'' \times \frac{1}{4}''$, considerably larger than Baker's round rod specimens. Although they cover a much shorter time range, these data are included because they were cited by Haward.[6]

In the case of two materials, fused silica and soda-lime glass, this reciprocal relationship is so exact that nearly every point lies on the straight line. In the case of the Pyrex glass and the lead glass the fit is also quite good, but the points for the porcelains deviate considerably, although even in these cases straight lines can be drawn within the errors assigned. The discussion presented in this paper will apply more particularly to the four glasses, Pyrex, soda-lime, lead, and silica.

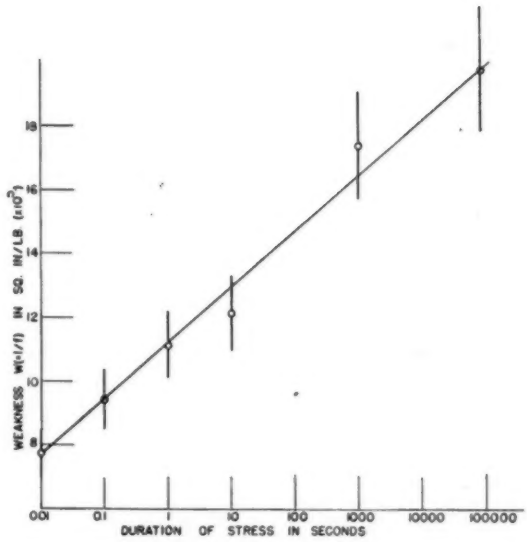

FIG. 2. Disannealed Pyrex glass, scratched, wet.

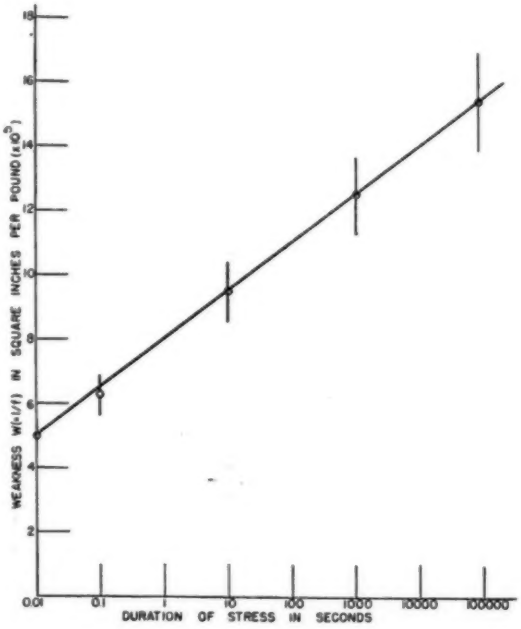

FIG. 3. Annealed soda-lime glass, wet.

Since the straight lines fit so well in these cases, it is natural to inquire as to their equations, and whether any theoretical basis can be found for them. We find that if there is any theoretical basis at all it is expressed in terms of concepts such as "weakness," rather than strength, and a "fatigue modulus."

[5] F. W. Preston, J. App. Phys. **13**, 623 (1942).
[6] R. N. Haward, Comment on Murgatroyd's paper. See reference 1, p. 427.
[7] F. W. Preston, Nature **156**, 55 (July 14, 1945).
[8] F. W. Preston, J. Am. Cer. Soc. **18**, 220 (1935).

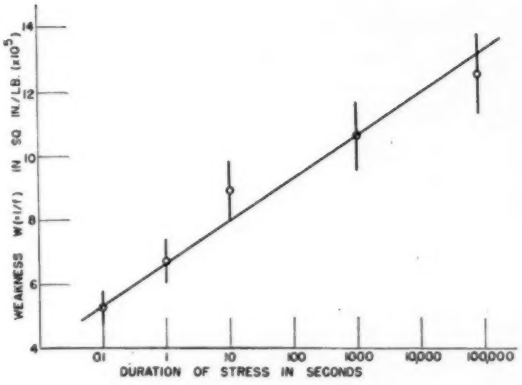

FIG. 4. Annealed lead glass, wet.

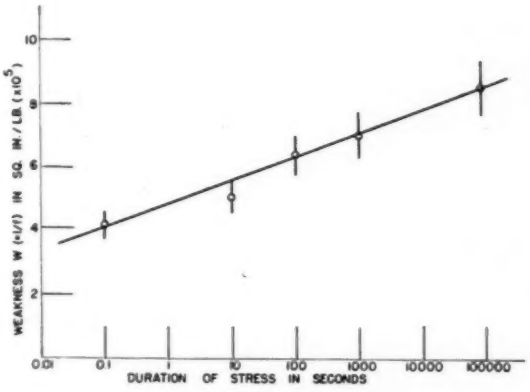

FIG. 5. Fused silica, wet.

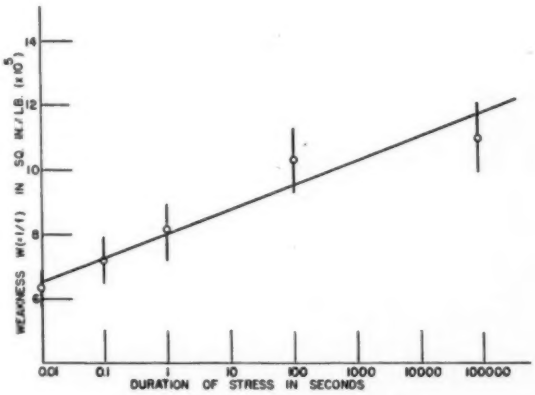

FIG. 6. Porcelain, type *A*, dry.

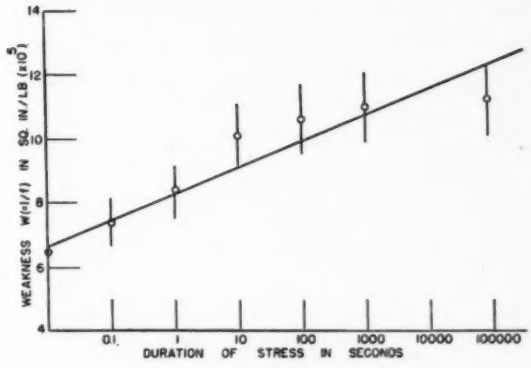

FIG. 7. Porcelain, type *B*, dry.

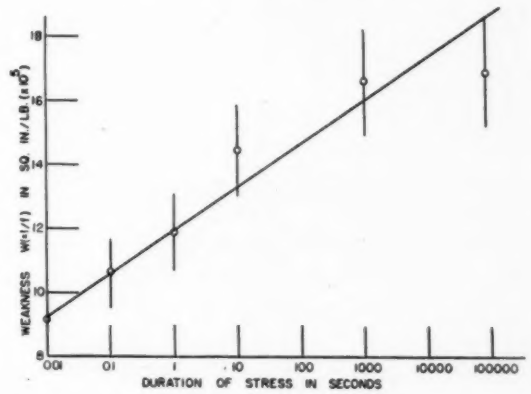

FIG. 8. Porcelain, type *C*, dry.

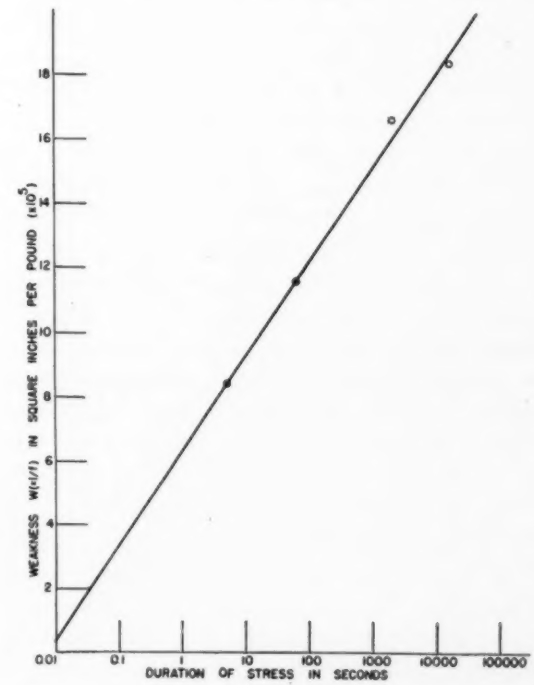

FIG. 9. Plate glass, dry.

It is more or less inevitable, also, that we should speculate on the extrapolation of the curves, to time intervals both longer and shorter than were attained in Baker's experiments. There is a practical necessity for speculating on the longer times, and fortunately there is no apparent reason why the curves should not continue as straight lines to times far beyond anything of

technological interest. At the short time end things are more complicated.

III. EXTRAPOLATIONS

The various curves (straight lines) which represent Baker's results are expressed by equations of the form

$$1/f = a + m \log t, \qquad (1)$$

where f is the breaking stress, t is the time, and a and m are constants. Each line is thus defined by its slope $d(1/f)/d(\log t)$ and by the point (t_0), where the line intersects the time axis.

With such materials, once the fact that they plot to straight lines is conceded, the question arising in the mind of the experimenter—or reader—is apt to be: "how far can the curves be extrapolated at each end with any confidence?"

(a) The Long Time End

The equation above would make the strength zero at infinite time. This is psychologically satisfying, and, furthermore, is required by some theories of strength which have been recently developed. Otherwise stated, it means that even a slight stress will break the glass if only it lasts for a sufficiently long time.

There seems to be nothing in the physics of long time loading that would cause us to deny the possibility that the straight-line law holds more or less indefinitely, provided temperature and humidity are constant and there is no physical change in the specimen other than changes which operate during our relatively brief loading intervals. The straight-line relation holds from 0.01 second to nearly 10^5 seconds, a range of time durations of 10^7 to 1. Our experiments end at a duration of one day, but there seems no reason why we should expect any departure from the linear relation if we extend the time range by a factor of 10^3, that is, from one day to three years, or even by a factor of 10^4, that is, up to thirty years. This is much longer than most bottles last, and for most of their lives they are not under stress. There are not many examples of plate glass, or other kinds of glass, that are expected to last, under stress, for so great a length of time.

If the curve were extended to the right, beyond one day, as far as we have determined it experimentally to the left, that is, in the ratio of 10^7 to 1, we arrive at a period of 30,000 years, or roughly the time that has elapsed since the maximum of the last ("Wisconsin") glaciation, and several times as long as all recorded history.

In Table II below we take the strength at the end of one day of stress as unity and calculate, for fused silica and soda-lime glass, the proportionate strengths at several other longer durations, on the assumption that this linear relationship holds indefinitely as we move to the right.

(b) The Short Time End

The strength-time equation would make the strength infinite for some very brief, but not infinitesimally short, duration (t_0). This point is obtained by extending the straight line of the graph to the left until it intersects the time axis. The values of t_0 for the various materials tested are shown in Table III.

This threshold time, t_0, is obtained from the equation of the curve and its value depends, therefore, on the way the straight line is drawn among the experimental points. It is interesting to note, however, that for all those glasses which were tested wet, the value of t_0 is in the neighborhood of 1 microsecond, whereas its value for those materials which were tested dry is very much less. However, other factors than moisture are involved, of course. For example, porcelains *A* and *B*, which had identical compositions but different firing temperatures, have nearly the same value of t_0, whereas porcelain *C*, of different composition, has a t_0 value 20 to 40 times as large.

TABLE II. Extrapolation at the long time end.

Material \ Duration	1 day	1 year	10^3 years	10^6 years	2×10^9 years	Infinite time
Fused silica	1.0	0.82	0.68	0.57	0.50	0
Soda-lime glass	1.0	0.80	0.65	0.55	0.46	0

TABLE III. The threshold time.

Material	t_0(sec.)	Material	t_0(sec.)
Soda-lime glass	5.0×10^{-6}	Pyrex (dry)	0.0085×10^{-6}
Lead glass	10.2×10^{-6}	Porcelain *A*	0.00004×10^{-6}
Fused silica	0.2×10^{-6}	Porcelain *B*	0.00008×10^{-6}
Pyrex (wet)	0.4×10^{-6}	Porcelain *C*	0.0016×10^{-6}

TABLE IV. Theoretical strengths at short durations.

Material \ Duration	10^{-2} sec.	10^{-3} sec.	10^{-4} sec.	10^{-5} sec.	10^{-6} sec.
Fused silica	28,200	37,000	50,700	80,700	196,000
Soda-lime glass	19,900	28,800	51,300	232,000	∞

At present, t_0 is merely a mathematical abstraction. It could not be even remotely approached experimentally with such a set-up as we were using. Yet on our logarithmic scale it is not very far beyond the short time end of the experimentally determined curve. In fact, for some of the materials it is much closer to the left-hand end of the experimental curve than this left-hand end is to the right-hand end, so the extrapolation, considered as a mathematical operation, is not too extravagant.

Physically, however, Baker probably carried the curve toward the short time end as far as it can be carried unless some totally different and much smaller set-up can be devised. Possibly some arrangement using a silver plated glass fiber supported on a short span in a magnetic field, and deflected by the discharge of a condenser through the silver plating, might serve to reach shorter time intervals.

Let us assume that by some means or other the curve could be extended, experimentally, to shorter times, and that it did, in fact, continue straight for some distance. The calculated strength values of fused silica and soda-lime glass at several shorter times are shown in Table IV.

The behavior of glass under very high stresses cannot be expected to parallel its behavior under moderate stresses, because we cannot expect Hooke's law to be obeyed at extreme strains. It seems not inconceivable that the straight-line law might apply fairly well until stresses of a million pounds per square inch are reached, with a resulting strain or extension of 10 percent in the length of the fiber. But it is scarcely likely that it could apply at stresses of ten million pounds per square inch, a figure equal to Young's modulus as calculated for small strains.

At the short time end the inertia of the material becomes an important factor and makes experimentation impractical, by any method as yet envisaged, much beyond the point to which Baker carried it.

Thus, for more reasons than one, the shape, or even the physical reality, of the curves beyond Baker's short time values must remain doubtful for the present, although the theoretical implications may make us wish to find means of extending them in that direction. This might be accomplished by totally different techniques, perhaps by impact testing, as hinted by Baker.

IV. THE CONCEPT OF "STRENGTH" OF GLASS

From the empirical equation

$$f_{et_0}/f = \log_e (t/t_0), \qquad (2)$$

which can be deduced from Baker's experimental results, it can be seen that the strength f is not a constant of the material but that it depends upon a variable (time, t) and on two constants of the material (or at least of the specimen). One of these is t_0, which is the maximum duration of stress for which the strength is theoretically infinite, and the other is f_{et_0}, which is the strength of the glass for a duration of stress et_0, where $e = 2.718$, the base of natural logarithms.

We may tentatively call t_0 the "threshold duration." It is the least interval of time in which a tensile stress, however large, can rupture the material (or the specimen). In our experiments on glass it is of the order of a microsecond, and in this time a crack can be propagated no more than $60{,}000 \times 10^{-6}$ inches $= \frac{1}{16}$ inch, and the stress pulse no more than $\frac{1}{8}$ inch. These dimensions seem to bear no relation to the ultimate structure of the material, but they are comparable with the shortest dimension of the specimen (0.22 inch), or with the shortest dimensions of an effective crack. They may even correspond somewhat closely with the radius of the smallest "mirror" (initiation crack) that can be produced under infinite stress. This in turn may be, and probably is, a function of the size of the specimen, and not a true constant of the material. Obviously, the mirror on a fine fiber has to be smaller than $\frac{1}{16}$ inch.

If t_0 is a property of the specimen rather than the material, then so is et_0, and likewise, presumably, is the strength at this time interval, or f_{et_0}.

Equation (2) above merely expresses an equality of ratios; it describes the "fatigue," but it says nothing about strength itself. The strength at one duration is expressed only in terms of the

strength at some other duration, not in terms of the physical constants of the material, or the dimensions of the specimen. Until t_0 and f_{et_0} can be so described, the equation is limited in exactly the same way as the experiments upon which it is based.

By differentiation of (2) we get

$$f_{et_0}\frac{d}{dt}\left(\frac{1}{f}\right)=\frac{1}{t}. \tag{3}$$

This eliminates t_0 from the picture but does not simplify things very much. The reciprocal of the breaking stress, that is, $1/f$, may be called the "weakness" of the specimen; it is the area that must be assigned to carry unit load, if the specimen is to last out the time interval t. If this is denoted by w, then

$$\frac{1}{f}\equiv w \quad \text{and} \quad \frac{1}{f_{et_0}}\equiv w_{et_0}. \tag{4}$$

So

$$dw/dt=w_{et_0}(1/t). \tag{5}$$

The rate of increase of weakness, dw/dt, we may call "fatigue." If so, Eq. (5) shows that fatigue is a property which varies inversely with the duration of stress.

Equation (2) may now be written

$$t/t_0=e^{w/w_{et_0}}, \tag{6}$$

and we then have, from Eq. (5),

$$\frac{dt}{dw}=\frac{t_0}{w_{et_0}}e^{w/w_{et_0}}. \tag{7}$$

t is the "lastingness," or endurance, of the specimen and is here expressed in terms of w, the area assigned to carry unit load.

We may write, finally

$$\frac{1}{t}\frac{dt}{dw}=\frac{1}{w_{et_0}}=f_{et_0}. \tag{8}$$

This says that the relative gain in endurance (as compared with the previous total endurance), due to unit increase in assigned area, is a constant of the material, or at least of the specimen.

In other words, if we want to increase the endurance by 1 percent we must add a constant number of square inches of cross-sectional area to carry unit load. The area, dw, to be added is inversely proportional to the "discriminant strength," f_{et_0}, since, from Eq. (8), $f_{et_0}\times dw$ is constant for a given value of dt/t.

TABLE V. Fatigue modulus.

Material	Modulus in.²/lb.	Material	Modulus in.²/lb.
Pyrex (dry)	3.0×10^{-6}	Fused silica	3.2×10^{-6}
Pyrex (wet)	1.6×10^{-6}	Porcelain *A*	3.3×10^{-6}
Soda-lime glass	6.5×10^{-6}	Porcelain *B*	2.4×10^{-6}
Lead glass	5.7×10^{-6}	Porcelain *C*	5.9×10^{-6}

If, instead of talking about a 1 percent increment in the life of the specimen, we define "fatigue" as that number of square inches that must be added to the cross-sectional area in order to double the life of the specimen, then $\delta t=t$ in Eq. (8) and

$$\delta w=w_{et_0}=1/f_{et_0}. \tag{9}$$

In this case, δw is the fatigue in square inches per pound of load.

For the various glasses tested the δw values in in.²/lb. are given in Table V.

It should be understood that δw is to be deduced from Eq. (8), not ascertained by determining experimentally what area must be added to a specimen to increase its life from, say, one minute to two minutes. δw is a kind of "modulus," in the sense that Young's modulus E is "that stress which would double the length of the specimen." In practice, we do not try to double the length of the specimen. Rather, we use a small increment of length, assume Hooke's law, and deduce E from the equation

$$(1/L)(dL/df)=1/E.$$

This compares with our Eq. (8)

$$(1/t)(dt/dw)=1/w_{et_0}.$$

Subject to this understanding, it seems we can say: Fatigue is that number of square inches that must be added to the cross-sectional area assigned to carry unit load (one pound) in order to double the life of the specimen.

V. PHYSICAL CONSIDERATIONS

The above discussion consists merely in the manipulation of the mathematical symbols in an attempt to interpret the straight-line relationship

derived from Baker's curves in terms of concepts which may find further application in this field.

There are other considerations however, some of which have been outlined. Another is the inherent unlikeliness that the lines representing the soda-lime glass and the silica glass actually cross one another to the left of the observed points, which would mean that the soda-lime glass becomes stronger than fused silica for stresses of sufficiently short duration. It seems more likely that, if the curves have any physical reality when extrapolated far to the left, they do not remain straight, but presumably flatten rapidly and become asymptotic to the time axis.

In all probability, this means in turn that our experimental straight-line relationship "in the visible" is itself only an approximation, even though it seems an extraordinarily good one in at least some of the instances.

Haward's theory[6] leads to an equation

$$S(e^{P_0/S}-e)=kt,$$

where S is the applied stress, t is the time required for the glass to break under this stress, and P_0 and k are constants. For $t=0$, this yields $S=P_0$, that is, the strength is not infinite, as would be required if our straight line held indefinitely.

On the other hand, Murgatroyd's viscous pocket theory[1] implies a relation identical with our Eq. (1). It is obvious that much more theoretical work needs to be done on the matter of the meaning of the "strength" of glass and on the relation of strength to time.

CONCLUSIONS

The ordinary concepts of "strength" do not apply to glass, at any rate not to glass as we know it, exposed to the earth's atmosphere and to atmospheric moisture. Under such normal conditions the "life" or "endurance" of a stressed glass specimen depends on the cross-sectional area which we assign to carry unit load. The greater the area we assign, the longer the life of the specimen, the life, or endurance, varying exponentially with the assigned area.

This permits the calculation of a certain constant, which we have called the "fatigue modulus," which describes the behavior of the specimen under the particular conditions of the experiment.

However, in all probability, this modulus is not so much a property of the substance of the specimen as it is a function of the surrounding atmosphere or, more accurately, of the conditions obtaining at the surface of the specimen.

Induction Heating of Hollow Metallic Cylinders

ANDREW GEMANT
The Detroit Edison Company, Detroit, Michigan
(Received December 14, 1945)

This paper deals with the heat input to hollow cylindrical metal cores subjected to induction heating. The rigorous expression for the heat input, valid for the whole frequency range, is developed and is presented by Eq. (27) of this paper. It is shown in an example how the equation is used for numerical computations. Existing approximate formulas for the low frequency and the high frequency range are checked by means of the rigorous equation; the maximum deviation between the rigorous and approximate equations is about 10 percent.

1. THE PROBLEM

As a result of the growing number of practical applications of induction heating of metals, many papers have been published that present the theory of induction heating and its usefulness in solving practical problems. One of the chief applications of the theory involves the calculation of the heat input to a metal core surrounded by a coil carrying alternating current. In the case of a solid core rigorous equations are usually given, from which are deduced the simplified equations that hold with good approximation, if the frequency is either higher or lower than certain critical limits.

When hollow cores are discussed, the rigorous equations referring to that case are not given. It is occasionally pointed out how these may be obtained, but the final equation is not presented.

Instead, only the approximate equations for frequencies above and below certain limits are given. This type of treatment can be found, for instance, in papers by Greig,[1] Wall,[2] and Baker,[3] as well as in a book by Warren.[4]

While the approximate equations just referred to seem to be sufficient for practical purposes, it appeared to the author that a presentation of the rigorous equations would be valuable for the following reasons:

(1) The practical importance of the problem certainly justifies knowledge of the rigorous solution.

(2) A reliable check on the validity of approximate solutions can best be made by means of the rigorous solution.

(3) It might well happen that certain variants of the hollow-core problem will be found for which the approximate solution is not applicable, in which case the knowledge of the rigorous solution would prove valuable.

The complete solution for the heat input to hollow cores in induction heating processes is presented in the following. First, a development of the equation is given, and next a numerical application is presented.

2. SOLUTION OF THE DIFFERENTIAL EQUATION

For the following analysis, the unit length of a hollow cylindrical metal core that is located coaxially within a coil is considered. An annulus of the metal of radius r and thickness dr is now considered. If the magnetic field parallel to the axis of the core is H (instantaneous value), then the total flux ϕ within the radius r is

$$\phi = 2\pi \int_0^r \mu H r dr, \tag{1}$$

where μ, the magnetic permeability, drops at the inner radius of the core from its value for the metal to unity. The electromotive force E along the circumference of the annulus is (with t = time)

$$E = -\partial\phi/\partial t. \tag{2}$$

The current density G along the circumference of the annulus is

$$G = E/2\pi\rho r, \tag{3}$$

where ρ = electrical resistivity. Finally, the gradient of the magnetic field intensity H is

$$\partial H/\partial r = -4\pi G. \tag{4}$$

These four equations contain four variables: H, ϕ, E, and G as functions of r and t. Elimination of three of the four permits the setting up of the differential equation for any one of the four. For H, one has:

$$\frac{\delta^2 H}{\delta r^2} + \frac{1}{r}\frac{\delta H}{\delta r} = \frac{4\pi\mu}{\rho}\frac{\delta H}{\delta t}. \tag{5}$$

Since the alternating current in the coil is sinusoidal, H can be replaced by $He^{2\pi i f t}$, where H now stands for the complex amplitude and f = frequency of the alternating current. Similarly, $\partial H/\partial t$ can be replaced by $2\pi i f H e^{2\pi i f t}$. Equation (5) then takes the form

$$\frac{d^2 H}{dr^2} + \frac{1}{r}\frac{dH}{dr} - ik^2 H = 0, \tag{6}$$

where

$$k^2 = 8\pi^2 \mu f/\rho. \tag{7}$$

In the following H stands for r.m.s.-value instead of amplitude; the form of Eq. (6) is obviously not affected by this change. The solution of Eq. (6) can be found from the solution[5] of the differential equation of the general form:

$$\frac{d^2 y}{dx^2} + \frac{1}{x}\frac{dy}{dx} + me^{in}y = 0$$

(m and n = constants), whose solution is:

$$y = Z_0(m^{\frac{1}{2}} e^{in/2} x),$$

where Z_0 is the sum of two Bessel functions of the first and third kind, both of zero order and each multiplied by an arbitrary complex constant. Substituting $-k^2$ for m and $\pi/2$ for n, the solution of Eq. (6) becomes

$$H = Z_0(i^{\frac{1}{2}} kir), \tag{8}$$

in which Z_0, as stated before, is the sum of J_0 and $H_0^{(1)}$, Bessel functions of the first and third kind, each multiplied by a constant. It is convenient to introduce the so-called modified Bessel

[1] James Greig, World Power **25**, 246 (1936).
[2] T. F. Wall, Engineer **173**, 209 (1942).
[3] R. M. Baker, Trans. A.I.E.E. **63**, 273 (1944).
[4] A. G. Warren, *Mathematics Applied to Electrical Engineering* (Chapman & Hall, London, 1941).
[5] E. Jahnke and F. Emde, *Tables of Functions* (Dover Publications, New York, 1943).

functions according to the definitions

$$I_0(x) = J_0(ix)$$

and

$$K_0(x) = \frac{\pi i}{2} H_0^{(1)}(ix),$$

so that Eq. (8) becomes

$$H = A I_0(i^{\frac{1}{2}}kr) + B K_0(i^{\frac{1}{2}}kr), \tag{9}$$

where A and B are the complex constants of integration.

By using Eq. (9), the other essential variables, namely the current density G and the electromotive force E can be computed. Since both are sinusoidal and have the same frequency f as H, the form of Eqs. (3) and (4) is not changed if G and E from now on stand for the complex r.m.s. values, instead of instantaneous ones. From Eq. (4):

$$G = -\frac{i^{\frac{1}{2}}kA}{4\pi} I_0'(i^{\frac{1}{2}}kr) - \frac{i^{\frac{1}{2}}kB}{4\pi} K_0'(i^{\frac{1}{2}}kr), \tag{10}$$

where the prime indicates differentiation after the argument. Further, from Eq. (3):

$$E = -\frac{i^{\frac{1}{2}}kr\rho A}{2} I_0'(i^{\frac{1}{2}}kr) - \frac{i^{\frac{1}{2}}kr\rho B}{2} K_0'(i^{\frac{1}{2}}kr). \tag{11}$$

Eqs. (9)–(11) give the essential variables as functions of the radius r within the metal part of the hollow core.

3. COMPUTATION OF THE CONSTANTS OF INTEGRATION

The next step is the evaluation of the constants of integration A and B from the boundary conditions. The two boundary conditions are:

(1) For $r = a$ (a = radius of the outer surface of the hollow cylinder), H assumes the value H_0 which is the field inside the coil that is unaffected by the metal core.

(2) For radii from zero to b (b = inner radius of the hollow cylinder) the field is constant and equal to H_b, the value that obtains from Eq. (9) for $r = b$. The first condition yields the equation:

$$H_0 = A I_0(i^{\frac{1}{2}}ka) + B K_0(i^{\frac{1}{2}}ka). \tag{12}$$

The second condition can be expressed in the following manner. First, H_b is written:

$$H_b = A I_0(i^{\frac{1}{2}}kb) + B K_0(i^{\frac{1}{2}}kb). \tag{13}$$

The total flux within the air space, ϕ_b, is then $b^2\pi H_b$. Further: $\partial\phi_b/\partial t = i2\pi^2 f b^2 H_b$. But this must be equal to $-E_b$, where E_b, the e.m.f. at $r = b$, is given by Eq. (11), if r is replaced by b. Hence, the second boundary condition yields the equation:

$$A\left[\frac{k\rho}{2} I_0'(i^{\frac{1}{2}}kb) - (\sqrt{i})2\pi^2 f b I_0(i^{\frac{1}{2}}kb)\right]$$

$$+ B\left[\frac{k\rho}{2} K_0'(i^{\frac{1}{2}}kb) - (\sqrt{i})2\pi^2 f b K_0(i^{\frac{1}{2}}kb)\right] = 0. \tag{14}$$

The constants A and B can be evaluated in terms of H_0, a, and b from Eqs. (12) and (14). At this stage of the calculation, it is convenient to replace the Bessel functions by their real and imaginary components. The following notations are customary:

$$I(i^{\frac{1}{2}}x) = ber\ x + i\ bei\ x$$

and

$$K_0(i^{\frac{1}{2}}x) = ker\ x + i\ kei\ x.$$

The corresponding differential forms are:

$$I_0'(i^{\frac{1}{2}}x) = i^{-\frac{1}{2}}\ ber'\ x + i^{\frac{1}{2}}\ bei'\ x$$

and

$$K_0'(i^{\frac{1}{2}}x) = i^{-\frac{1}{2}}\ ker'\ x + i^{\frac{1}{2}}\ kei'\ x.$$

In order to obtain A and B in convenient forms, the following notations are introduced:

$$\begin{aligned} u &= ber\ ka, \\ v &= bei\ ka, \\ w &= ker\ ka, \\ z &= kei\ ka, \\ p &= 2\ bei'\ kb - kb\ ber\ kb, \\ q &= -2\ ber'\ kb - kb\ bei\ kb, \\ s &= 2\ kei'\ kb - kb\ ker\ kb, \\ t &= -2\ ker'\ kb - kb\ kei\ kb. \end{aligned} \tag{15}$$

Evaluation of the constants A and B can now be carried out. The result is:

$$A = H_0 \frac{(s+it)}{(u+iv)(s+it) - (p+iq)(w+iz)} \tag{16}$$

and

$$B = H_0 \frac{-(p+iq)}{(u+iv)(s+it) - (p+iq)(w+iz)}. \tag{17}$$

Both complex constants can be written as:

$$A = A_r + iA_i \tag{18}$$

and

$$B = B_r + iB_i, \tag{19}$$

where the four real constants are given by Eqs. (16) and (17); numerical computation of these four constants is carried out according to standard methods.

It is easy to verify that for $b=0$, the solid core, B, becomes zero. The result for H in Eq. (9) is then given by the I_0 function alone.[1]

It may be added that the present treatment holds not only for the case of a hollow metallic cylinder, but also for the general case of a solid core surrounded by a solid cylinder of another material. ϕ_b is then not simply $b^2\pi H_b$, but a more involved function of b and the constants of the solid core, as known from the equations valid for the solid cylinder. Since ϕ_b is still linear in H_b, Eq. (14) will have the same general form, and only the second terms in the expressions (15) will be correspondingly more involved.

4. CALCULATION OF THE HEAT INPUT

The heat input into the hollow cylinder is calculated from the current density—Eq. (10)—in conjunction with Eqs. (18) and (19). The heat input per unit length W is given by its value $|G|^2\rho$ for unit volume, integrated over the cross-sectional area of the cylinder:

$$W=2\pi\rho\int_b^a |G|^2 r dr. \tag{20}$$

In order to solve this integral, it may be conveniently written in the form

$$W=2\pi\rho\int_b^a G\bar{G}r dr, \tag{21}$$

in which $\bar{G}$ is the conjugate complex value of G. This integral can be solved by making use of the following general integral relation in which Y_p and Z_p denote two different Bessel functions of pth order, both the sum of two functions of the first and third kind:

$$\int Y_p(\alpha x)Z_p(\beta x)x dx = \frac{\beta x Y_p(\alpha x)Z_{p-1}(\beta x)-\alpha x Y_{p-1}(\alpha x)Z_p(\beta x)}{\alpha^2-\beta^2}.$$

Here α and β are constants.

$Y_p(\alpha x)$ is now identified with G, $Z_p(\beta x)$ with $\bar{G}$, and x with r of Eq. (21). The four functions appearing on the right-hand side of the above equation, as well as α and β, can then be easily evaluated, as follows.

Concerning $Y_p(\alpha x)$, it is given by Eq. (10), or, recalling the general relation

$$Z_0'(x)=-Z_1(x)$$

by

$$Y_p(\alpha x)=\frac{i^{\frac{1}{2}}kA}{4\pi}I_1(i^{\frac{1}{2}}kr)+\frac{i^{\frac{1}{2}}kB}{4\pi}K_1(i^{\frac{1}{2}}kr). \tag{10a}$$

From this it follows that $p=1$ and $\alpha=i^{\frac{1}{2}}k$.

Expressing $Y_p(\alpha x)$ in the form of tabulated functions, Eq. (10) is converted, by using the form of I_0' as given in Section 3, into:

$$Y_p(\alpha x)=-\frac{kA}{4\pi}(ber'\,kr+i\,bei'\,kr) -\frac{kB}{4\pi}(ker'\,kr+i\,kei'\,kr). \tag{22}$$

Concerning $Z_p(\beta x)$, or $\bar{G}$, it should be recalled that the conjugate value of any function is given by replacing all i's occurring in it by $-i$. Hence, from (10a) it follows that $\beta=(-i)^{\frac{1}{2}}k$ and from (22):

$$Z_p(\beta x)=-\frac{k\bar{A}}{4\pi}(ber'\,kr-i\,bei'\,kr) -\frac{kB}{4\pi}(ker'\,kr-i\,kei'\,kr), \tag{23}$$

where $\bar{A}$ and $\bar{B}$ are given by Eqs. (18) and (19) with $-i$ instead of i.

As to $Y_{p-1}(\alpha x)$, Eq. (10a) is used in replacing I_1 by I_0 and K_1 by K_0. It then follows that

$$Y_{p-1}(\alpha x)=\frac{kA}{4\pi}(i^{\frac{1}{2}}\,ber\,kr-(-i)^{\frac{1}{2}}\,bei\,kr) +\frac{kB}{4\pi}(i^{\frac{1}{2}}\,ker\,kr-(-i)^{\frac{1}{2}}\,kei\,kr) \tag{24}$$

and

$$Z_{p-1}(\beta x)=\frac{k\bar{A}}{4\pi}[(-i)^{\frac{1}{2}}\,ber\,kr-i^{\frac{1}{2}}\,bei\,kr] +\frac{kB}{4\pi}[(-i)^{\frac{1}{2}}\,ker\,kr-i^{\frac{1}{2}}\,kei\,kr]. \tag{25}$$

Equations (22) to (25) represent the four functions to be substituted into the numerator of the right-hand side of the general integral given above. The denominator is given by

$$\alpha^2-\beta^2=2ik^2.$$

In carrying out the substitution indicated, the four constants A_r, A_i, B_r, and B_i are found to occur in four combinations as follows:

$$\begin{aligned} A_r^2+A_i^2&=\kappa,\\ B_r^2+B_i^2&=\lambda,\\ A_rB_r+A_iB_i&=\mu,\\ A_rB_i-A_iB_r&=\nu. \end{aligned} \tag{26}$$

With these quantities, the heat input W becomes:

$$W=\frac{\rho}{8\pi}\Big|_b^a kr\kappa(ber\ ber'+bei\ bei')+kr\lambda(ker\ ker'+kei\ kei')+kr\mu(ber\ ker'+bei\ kei'+ber'\ ker+bei'\ kei)+krv(bei\ ker'-ber\ kei'+bei'\ ker-ber'\ kei)\Big| \tag{27}$$

where, for sake of simplicity, the argument kr after each function is omitted.

It can be seen that, for the solid core for which $B=0$, only the first of the four terms within the bracket remains, giving the known solution for this case.

5. NUMERICAL CALCULATION OF A SPECIAL CASE OF HOLLOW CORE

In order to show the use of Eq. (27), a numerical example treated by R. M. Baker[3] will be discussed. That author calculated the heat input by means of two approximate equations and a check of these, as explained in Section 1 of the present paper, can now be carried out by using the rigorous solution as given. It will be shown in the course of this section that the approximate equations are in good agreement with the rigorous one.

For low frequencies, characterized by the condition that the depth of current penetration is larger than the wall thickness, Baker uses the formula

$$W=\frac{61.8\times10^{-16}f^2a^3t_w\rho H_0^2}{\rho^2+15.5\times10^{-16}f^2a^2t_w^2},$$

where W, the heat input per unit length, is given in watts/cm and t_w, the wall thickness, is measured in cm, ρ is measured in ohms cm, and $\mu=1$ (non-magnetic metal).

For high frequencies, characterized by the condition that the depth of current penetration is smaller than the wall thickness, the formula

$$W=7.92\times10^{-4}a(f\rho)^{\frac{1}{2}}H_0^2$$

is used. At the frequency where the two calculated curves cross they are smoothed into one.

In order to check the two approximate equations, one of the cases calculated by Baker was recalculated by means of the rigorous Eq. (27) developed in Section 4 and valid for the whole frequency range. This special case refers to a non-magnetic metal ($\mu=1$), an outer diameter of the cylinder of 10 cm ($a=5$), and a wall thickness of 1 millimeter ($b=4.9$). ρ is taken as 7×10^{-6} ohm cm ($=7\times10^3$ e.m.u.). Since the heat input is proportional to H_0^2 according to all the equations used, W/H_0^2 is calculated. A frequency range from 300 to 50,000 is covered.

Before giving the results of the complete calculation, the computation will be shown in detail for one particular frequency. A frequency very close to the crossing point of the two approximate curves is selected, i.e., 17,900. From Eq. (7) we then have $k=14.2$, which gives $ka=71.20$ and $kb=69.78$.

The first step is the evaluation of the sixteen Bessel functions involved for ka and kb as arguments. For arguments up to 10, the functions have been tabulated previously.[5] They are sometimes found under the real and imaginary parts (*Re* and *Im*) of the respective J and $H^{(1)}$ functions. It is useful to remember the following identities:

$$ber\ x=Re\ J_0(i^{\frac{1}{2}}x), \qquad ker\ x=\frac{2}{\pi}Im\ H_0^{(1)}(i^{\frac{1}{2}}x);$$

$$bei\ x=-Im\ J_0(i^{\frac{1}{2}}x), \qquad kei\ x=\frac{2}{\pi}Re\ H_0^{(1)}(i^{\frac{1}{2}}x);$$

$$ber'\ x=-Re\ i^{\frac{1}{2}}J_1(i^{\frac{1}{2}}x), \qquad ker'\ x=\frac{2}{\pi}Im\ i^{\frac{1}{2}}H_1^{(1)}(i^{\frac{1}{2}}x);$$

$$bei'\ x=Im\ i^{\frac{1}{2}}J_1(i^{\frac{1}{2}}x), \qquad kei'\ x=\frac{2}{\pi}Re\ i^{\frac{1}{2}}H_1^{(1)}(i^{\frac{1}{2}}x).$$

For arguments larger than 10, tables do not exist, but there are asymptotic formulas that permit the computation. The eight formulas are listed below. Let

$$F=e^{x/\sqrt{2}}/(2\pi x)^{\frac{1}{2}} \quad F'=(\pi/(2x))^{\frac{1}{2}}e^{-x/\sqrt{2}}$$

and

$$\varphi=x/(2)^{\frac{1}{2}}+\pi/8 \quad \psi=x/(2)^{\frac{1}{2}}-\pi/8.$$

Then:

$$ber\ x=F[(1+0.088/x)\cos\psi+(0.088/x+0.070/x^2)\sin\psi],$$

$$bei\ x=F[(1+0.088/x)\sin\psi-(0.088/x+0.070/x^2)\cos\psi],$$

$$ber'\ x=F[(1-0.265/x)\cos\varphi-(0.265/x+0.117/x^2)\sin\varphi],$$

$$bei'\ x=F[(1-0.265/x)\sin\varphi-(0.265/x+0.117/x^2)\cos\varphi],$$

$$ker\ x=F'[(1-0.088/x)\cos\varphi-(-0.088/x+0.070/x^2)\sin\varphi],$$

$$kei\ x=F'[-(1-0.088/x)\sin\varphi-(-0.088/x+0.070/x^2)\cos\varphi],$$

$$ker'\ x=F'[-(1+0.265/x)\cos\psi+(0.265/x-0.117/x^2)\sin\psi],$$

$$kei'\ x=F'[(1+0.265/x)\sin\psi+(0.265/x-0.117/x^2)\cos\psi].$$

Using these formulas, the following data are obtained for the particular frequency mentioned above:

$$ka=71.20$$

$$ber=0.3033\times10^{21} \quad ker=0.01800\times10^{-21}$$

$$bei=-0.1070\times10^{21} \quad kei=-0.00920\times10^{-21}$$

$$ber'=0.3068\times10^{21} \quad ker'=-0.01936\times10^{-21}$$

$$bei'=0.1587\times10^{21} \quad kei'=-0.006165\times10^{-21}$$

$$kb=69.78$$

$$ber=0.03220\times10^{21} \quad ker=0.04800\times10^{-21}$$

$$bei=-0.1246\times10^{21} \quad kei=0.02828\times10^{-21}$$

$$ber'=0.1106\times10^{21} \quad ker'=-0.01429\times10^{-21}$$

$$bei'=-0.06443\times10^{21} \quad kei'=-0.05414\times10^{-21}.$$

The next step is the evaluation of the eight quantities given by Eq. (15), by means of which A and B from Eqs. (16) and (17) are calculated. The four components shown in Eqs. (18) and (19) are then in the present case:

$$A_r=2.823\times10^{-21}H_0,$$

$$A_i=0.8252\times10^{-21}H_0,$$

$$B_r=-1.609\times10^{21}H_0,$$

$$B_i=0.8668\times10^{21}H_0.$$

These data permit evaluation of the four quantities shown in Eq. (26), and in this manner all magnitudes occurring in Eq. (27) are known. In the present case the result is

$$W=1.43\times10^{-3}H_0^2$$

in watts/cm, if H_0 is measured in e.m.u.

The calculation was carried out for five selected frequencies and the result of the complete calculation, representing the heat input as a function of frequency, is shown in Fig. 1. The solid line is calculated from Eq. (27), the dotted line is Baker's curve. As can be seen, the two methods are strictly identical below the frequency for which the depth of penetration is equal to the wall thickness; for higher frequencies the approximate formula gives values slightly higher than those from the rigorous equation. For still higher frequencies the two curves merge again; it can be shown that for depths of penetration markedly less than the wall thickness Eq. (27) degenerates to the second of the approximate formulas given. The highest frequency for which computation was made is 4000 kc (not shown in Fig. 1); W, according to both equations, is 20.9 watts/cm.

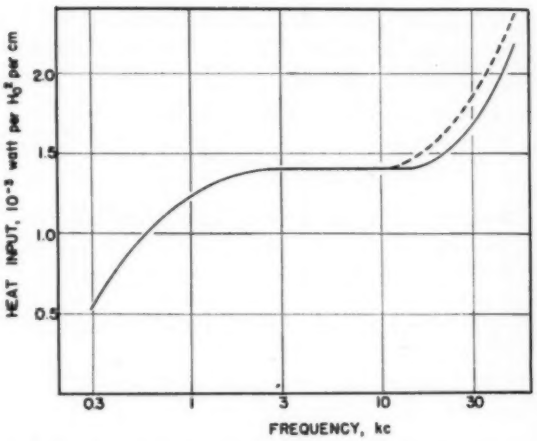

FIG. 1. Heat input as function of the frequency for a special case of a hollow cylinder. Solid line calculated from Eq. (27); dotted line calculated by R. M. Baker from approximate formulas.

The Tensile Properties of Several Special Steels and Certain Other Materials under Pressure

P. W. BRIDGMAN
The Physics Laboratories, Harvard University, Cambridge, Massachusetts
(Received November 16, 1945)

INTRODUCTION

IN a series of papers[1] the effect of hydrostatic pressure on the tensile properties of a large number of different steels has been investigated. The pressure effects on all these steels fell approximately into a one-dimensional pattern, the behavior being determined by a single parameter, the hardness or the absolute magnitude of the yield point at atmospheric pressure. In spite of the great ostensible variety of the steels, they were, nevertheless, restricted to a range of only a few percent in any of the conventional alloying elements, and to a hardness range below 50 Rockwell *C*. In the present investigation two different series of steels were used falling outside the previous limits. The first of these comprised four stainless steels running up to 18 percent Cr and 10 percent Ni; the second was a series of five different hardnesses of a carbon steel, running from 48 to 63 Rockwell *C*.

In anticipation of the results, it was found that two of the stainless steels fall markedly outside the previous pattern, but the others fell approximately within it.

In addition to the measurements on the steels, qualitative measurements were made on several other materials.

In the discussion, the new results of this paper and previous unclassified results are surveyed together.

APPARATUS AND METHODS

The apparatus and method for making the tensile tests have been fully described in the previous communications; only a brief characterization will be made here. The tensile specimens, of an over-all length of 1 inch and a diameter varying about a mean of 0.1 inch, depending on the absolute strength, are completely surrounded by a fluid in which pressures up to 30,000 kg/cm² may be produced and maintained during stretching. The specimen is stretched by a forked yoke driven by the piston with which pressure is produced. The tension on the specimen is measured within the pressure chamber by the change of resistance of a "grid," in this way avoiding errors from the friction of the piston. Simultaneous measurements were made of hydrostatic pressure, tension on the specimen, and elongation of the specimen, for progressively increasing elongations. The elongation can be determined with adequate accuracy only in the range of plastic flow, after reaching the maximum load. The parameters singled out for determination from the complete data and presented in the following are: maximum load, load at fracture, reduction of area at fracture, and character of the fracture—all as functions of the pressure. In many experiments stretching was not pushed to fracture; for these the final loads were determined instead of the load at fracture.

In calculating the stresses from the data the change of geometrical configuration due to necking is so large that it was necessary to make allowance for the distribution of stress across the neck. This was done by methods which have been outlined in several papers.[2] The stress system at the neck of a tension specimen can be analyzed into the sum of three stress systems. The first of these is the hydrostatic pressure in the ambient liquid; the second is a tension along the axis of the specimen, *constant* across the section, called the "flow" stress in the following; the third is a variable hydrostatic tension (three equal components of principal stress) varying from zero at the outer surface of the neck to a maximum on the axis according to a formula given in detail in

[1] Eight Reports to the Watertown Arsenal by P. W. Bridgman, from March, 1943 to December 21, 1944, numbered No. WAL 111/7, No. WAL 111/7-1, etc., through No. WAL 111/7-7. See also P. W. Bridgman, Rev. Mod. Phys. **17**, 3–14 (1945). There are also several reports by P. W. Bridgman to the N.D.R.C., on which the confidential classification had not yet been lifted at the time of writing.

[2] P. W. Bridgman, Trans. A.S.M.E. **32**, 553–574 (1944); Metals Technology, Technical Publication No. 1792 of Am. Inst. Min. Met. Eng. (Dec. 1944) with supplement in April, 1945; Wat. Ars. Report, No. WAL 111/7-4.

the references. It follows that the "flow" stress is not equal to the average tension across the section (total tensile load divided by the actual area of the neck), but is less than it. The factor by which it is less will be called the "correction factor." In the following work the correction factor varied through an extreme range from 1.0 to 0.7.

THE MEASUREMENTS

1. Stainless Steels

Measurements were made on four different varieties of stainless steel. For these I am indebted to Dr. A. L. Feild of the Rustless Iron and Steel Corporation. The designations, compositions, and heat treatments are given in Table I.

The material was supplied in $\frac{1}{4}$-inch rods. These had been drawn to approximately the final size, then annealed and pickled. After this they were given a final cold drawing pass with further reduction in cross-sectional area of 5 percent. The final hardnesses on the Rockwell *B* scale were 87, 93, 95, and 93, respectively, for H-26, H-50, H–29, and H-88.

Seven runs were made on each of these four steels at pressures ranging from atmospheric to 25,000 kg/cm². In four of these runs, including the run at atmospheric pressure, the test was carried to fracture, and in the three others it was stopped short of fracture. The purpose of the latter runs was to obtain points on the strain hardening curve comparatively free from the error introduced by the disturbing local flow which is very likely to occur in the moment of fracture.

These steels fall into two groups, of markedly different properties. At atmospheric pressure H-26 and H-50 break in the fashion normal for a steel of high ductility, with a reduction of area of about 78 percent. Necking starts, as is normal, at a strain of about 0.2. Under pressure these two steels show an increase of ductility so large that the maximum pressure was not pushed beyond 19,000 kg/cm², the reduction of area at this pressure being so extreme that error is introduced by deviations from geometrical regularity because of finite grain size. The two other steels, H-29 and H-88, break with the same reduction of area at atmospheric pressure, but the character of the stress-strain curve is quite different, since the elongation is much greater and necking does not start until a strain of 0.65 is reached. Under pressure the increase of ductility is not nearly as large as for the two other steels, and pressure could be raised to 25,000 without enough reduction of area to introduce error from geometrical irregularity.

TABLE I.

	C	Mn	P	S	Si	Cr	Ni	Mo	Cu
H-26	0.094	0.36	0.023	0.022	0.35	12.26	0.46	0.50	ND
H-50	0.067	0.50	0.020	0.030	0.51	17.49	0.41	*ND*	*ND*
H-29	0.058	0.70	0.030	0.013	0.85	18.51	8.95	*ND*	0.20
H-88	0.051	0.59	0.030	0.020	0.47	18.31	10.27	*ND*	0.20

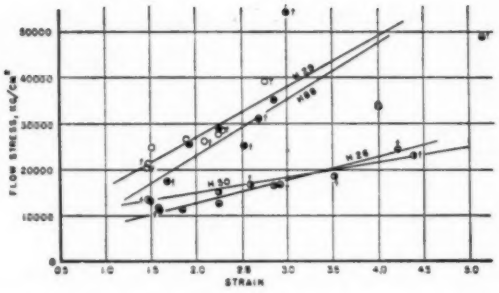

FIG. 1. The flow stress as a function of strain (natural) for four stainless steels. An *f* on a number of points indicates the occurrence of fracture.

Because of the much greater reduction of area before necking starts, the contour of a tension specimen of H-29 or H-88 has a different shape from the other two or from the other steels investigated previously. Since the shape of the contour determines the correction for stress distribution across the neck, the shape of the contour, that is, the radius of curvature of the contour at the neck, was measured for all specimens of all four steels. The curve of a/R (radius of curvature of the contour at the neck divided by the radius of the cross section at the neck) against strain was normal for H-26 and H-50, but for H-29 and H-88 it lies below the normal curve in the initial stages, cutting the axis at a strain of 0.65 instead of at 0.2, and approaches coincidence with the normal curve at a strain of 3.5. The corrections for the stress distribution in H-29 and H-88 were determined by utilizing these special measurements of a/R.

The results are reproduced graphically. In Fig. 1 is shown the flow stress in terms of the

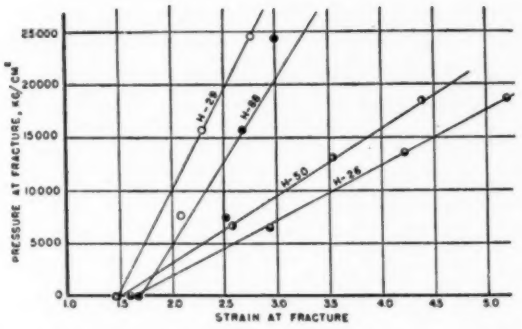

FIG. 2. The hydrostatic pressure at fracture as a function of the strain at fracture for four stainless steels.

strain; the concealed variable is the hydrostatic pressure, which in general is greater for the larger strains. An *f* written against some of the points indicates that the specimen was fractured during the test. In general the scattering of the points is somewhat greater for the fractures; this is due to distortion in the process of fracture, which may be considerable at the largest strains. Within experimental error the relation between flow stress and strain is linear in the present range. More accurate measurements under especially favorable conditions have shown that the curves are slightly concave toward the axis of strain.

In Fig. 2 is shown the pressure at fracture against the strain at fracture. In accordance with the great majority of previous results, the relation is assumed to be linear, and is so shown. The strain at fracture can be determined with some accuracy, however, and instances have already been found in which the relation is almost certainly not linear within experimental error. It is therefore not at all impossible that the relation for H-88 should be represented by a curve concave toward the pressure axis.

In Fig. 3 is shown the flow stress at the maximum load (that is, at the point where necking starts) as a function of the pressure of pulling. For all four steels this flow stress increases linearly with pressure, by some 3 percent per 10,000 kg/cm² for H-26 and H-50, and by some 13 percent for the same pressure increment for H-29 and H-88. The former rate, 3 percent, is somewhat less than for most steels previously investigated; the latter rate, 13 percent, is distinctly higher. Except for a factor constant with respect to pressure, the "flow stress at maximum load" is the same as the technical "tensile strength." The factor to reduce from flow stress to tensile strength is 0.83 for the first two steels and 0.52 for the second two; this factor is determined by the strain at which necking starts, the "tensile strength" being calculated on the original cross section.

The fracture of all four stainless steels roughly follows the same pattern previously found. At atmospheric pressure the fracture is of the conventional "cup-cone" type. With increasing pressure the tensile part of the fracture (bottom of the cup) becomes progressively less in extent relative to the total cross section, and eventually disappears, the fracture becoming all shear above a certain pressure. In the lower part of the domain of completely shearing fracture the surface of shear is conical; at higher pressures this multiplies into a double cone, and at still higher pressures the shearing fracture shifts to a single distorted plane. These features are all present in the stainless steels. In Fig. 4 is shown the ratio of the area of the tensile part of the fracture to the total area of the fracture as a function of the hydrostatic pressure prevailing at the moment of fracture. The fracture becomes all shear at a lower pressure for the two steels H-26 and H-50 than for the two others, H-29 and H-88. The intermediate episode of shearing fracture on single or multiple conical surfaces is confined to a comparatively narrow pressure range, and was definitely observed for only one specimen, most of the shearing fractures being on a single distorted plane. The general character of the fracture was always more irregular and coarsely granular than for ordinary carbon steels.

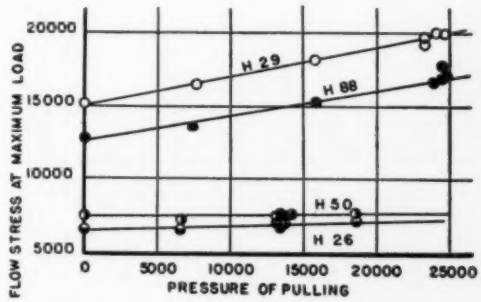

FIG. 3. The flow stress at the maximum load (i.e., at the beginning of necking) as a function of the prevailing hydrostatic pressure for four stainless steels.

2. Steels of Hardness Greater than Rockwell C 48

I am greatly indebted to Captain John H. Hollomon, who had the specimens prepared at the Watertown Arsenal under his direction. The specimens were all made from the same bar of high carbon steel. They were heat-treated by holding at 1525°F for 30 minutes and then quenching into oil at room temperature. They were then drawn in batches of ten to five different temperatures so chosen as to give median hardnesses of 48, 51, 56, 60, and 63.

These experiments followed a number of unsuccessful attempts to demonstrate an effect of hydrostatic pressure on the ductility of tool steels of hardnesses greater than 60. The preliminary attempts had encountered brittle failure at the shoulders of the test specimen because of stress concentration. After a number of trials the shape of the specimen shown in Fig. 5 was arrived at. The specimens were rough finished at the Arsenal to the shape shown and heat-treated. They were finished to final dimensions at Harvard by grinding; I am greatly indebted to the skill of Mr. Charles Chase for this operation. The minimum diameter of the finished specimen was varied somewhat with the absolute strength of the steel; it was so chosen as to demand approximately the same maximum load for all heat treatments. The hardness of each specimen was determined on the flats ground on the ends as indicated. From each batch of ten, the four or five were selected whose hardness was closest to the median. Since the primary object of these measurements was to determine how much ductility was imparted by pressure, these specimens were all pulled to fracture at pressures ranging from atmospheric to a maximum of 28,000 kg/cm². The strain at fracture at atmospheric pressure as a function of hardness is shown in Fig. 6.

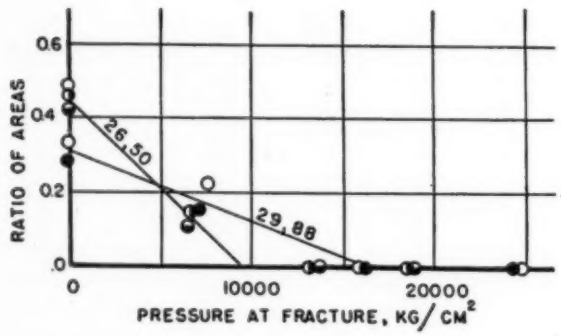

FIG. 4. The ratio of the area of the tensile part of the break (bottom of the cup) to the total area as a function of the pressure at which the break occurs for the four stainless steels. The two groups H-26, H-50 and H-29, H-88 are so nearly equal that a single line is drawn to represent the average behavior of the two.

The same sort of measurements were made on these as on the stainless steels.

In Fig. 7 is shown the flow stress at fracture as a function of the strain at fracture. The error from distortion in the act of fracture is much less for these hard steels than for the softer steels, and Fig. 7 therefore gives essentially the strain hardening curves. The points are somewhat more scattered than for the softer specimens. Again the relation is linear within the

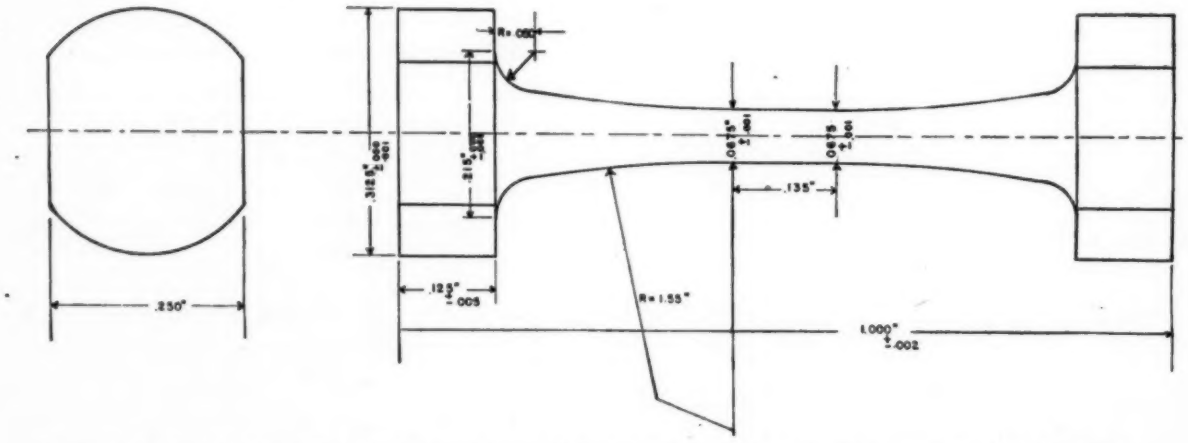

FIG. 5. The special shape of the tensile specimens of the hard steels. Diameters given provide for finish grinding.

FIG. 6. The strain at fracture at atmospheric pressure of the hard steels as a function of the Rockwell *C* hardness.

limits of error. Two atmospheric points for hardness 63 lay distinctly out of line with the others and are not plotted; it is probable that there was some surviving stress concentration effect here. Only a single experiment under pressure was made on the 63 group, at 24,000 kg/cm². A slight but measurable ductility was found, the strain at fracture being 0.06. In view of the very small ductility at this pressure it did not seem worth while to try for measurements on this hardness at lower pressures.

In Fig. 8 is shown the hydrostatic pressure at fracture as a function of the strain at fracture. Again the relation seems to be linear within experimental error. The lines drawn in Fig. 8 are the best lines through the points of each group. Doubtless if a larger number of measurements had been made, lines would have been found more uniformly spaced in terms of the hardness. A vertical line in Fig. 8 means zero effect of pressure on ductility. The rapid decrease of pressure effect on ductility with increasing hardness in this hardness range is noteworthy.

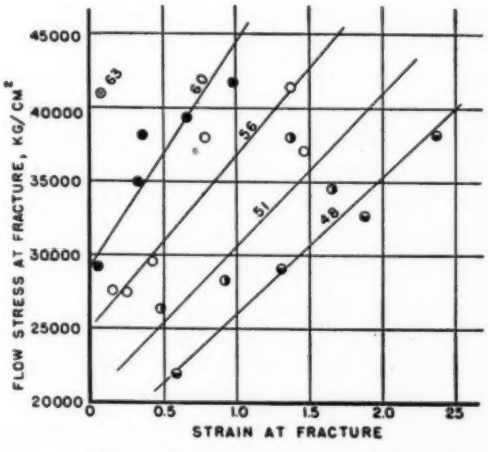

FIG. 7. The flow stress at fracture as a function of the strain at fracture for the hard steels. The figures on the lines indicate the average Rockwell *C* hardness of the group.

In Fig. 9 is shown the flow stress at maximum load as a function of the hydrostatic pressure at fracture. Since the hydrostatic pressure at fracture was only slightly higher than the hydrostatic pressure at the time of maximum load, this is practically a graph of flow stress at maximum load against the prevailing hydrostatic pressure. The factor for reducing from flow stress to tensile strength is 0.82 for all the specimens of Fig. 9. As in the case of Fig. 3, the

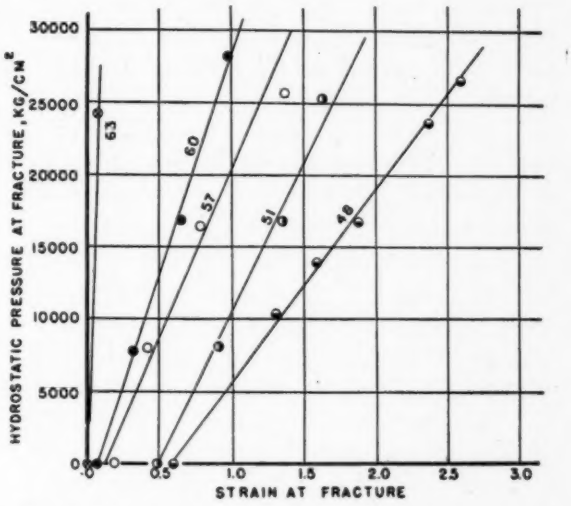

FIG. 8. The hydrostatic pressure at fracture as a function of the strain at fracture for the hard steels. The numbers on the lines indicate the average Rockwell *C* hardness of the group.

flow stress at maximum load increases somewhat with increasing pressure. The increase is greater on a percentage basis for the harder heat treatments.

In Fig. 10 is shown the ratio of the area of the tensile part of the fracture to the total fractured area as a function of the pressure. At atmospheric pressure the tensile part of the fracture occupies a progressively greater part of the total area as hardness increases, the fracture of the steel of hardness 63 being practically all on a single fine grained tensile plane except for a very narrow rim of shear around the edge. As usual, the tensile break disappears at high pressure. The pressure at which it disappears is practically the same for all the hardness groups except the hardest, which differs abruptly from the others. The multiple shearing fracture does not often appear in the harder steels, but at the lower end of the hardness

range is more common. The most common type of shearing break is on a single distorted plane; this is always highly burnished. In a couple of instances there were also fissures on longitudinal planes.

3. Tensile Properties under Pressure of Other Materials

In addition to the tests on the two series of steels just described, other sorts of material were examined, chiefly from a qualitative point of view and primarily to determine whether ductility is imparted to all sorts of material by pressure.

A number of experiments were made on gray cast iron. This was the ordinary gray cast iron of commerce, fine grained and without obvious imperfections. Several experiments were first made in which the specimen was given the conventional shape of most of the previous specimens. These tests all gave negative results, the specimen fracturing under pressure with a clean tensile break and no evidence of plastic flow. Two specimens were then tried with the special shape shown in Fig. 5 to avoid any effects of stress concentration. These were both pulled at 29,000 kg/cm². One was exposed directly to the action of the pressure transmitting liquid, *iso*-pentane, whereas the other was copper plated in order to prevent penetration by the liquid into any pores that there might be. Both experiments gave the same completely negative result, clean fracture perpendicular to the axis of the specimen, with no measurable reduction of diameter. It is perhaps natural to ascribe the negative results to the microscopic grains of pure graphite known to be present in this material.

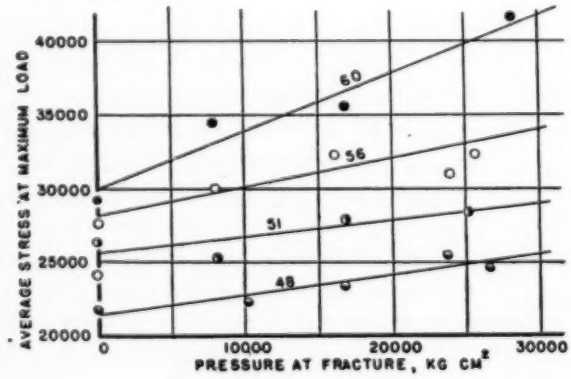

FIG. 9. The "average longitudinal stress," which in this case is the same as the flow stress, at the maximum load as a function of the hydrostatic pressure for the hard steels. The numbers on the lines indicate the average Rockwell *C* hardness of the group.

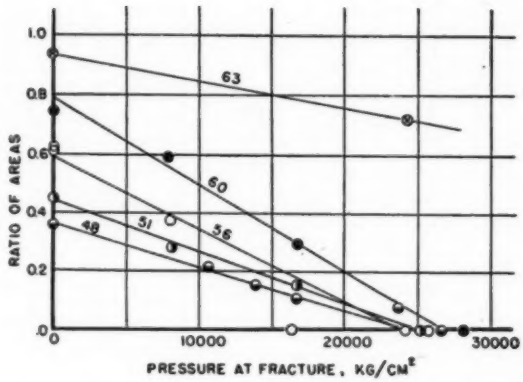

FIG. 10. The ratio of the area of the tensile part of the break (bottom of the cup) to the total area as a function of the pressure under which the break occurs for the hard steels. The numbers on the lines indicate the hardness group.

For unity of presentation, certain results with other materials which have already been described elsewhere will be referred to again here.[3] Tension tests under pressure on specimens of the conventional shape were made on aluminum, copper, bronze, and brass. The ductility of all these is markedly increased by pressure. In general it is not possible to push the strains to such extreme values without loss of geometrical regularity with these materials as with the steels. The cross section is likely to become dominated by a single crystal grain, so that the section becomes rectangular or square, with the result that the stress at the section becomes inhomogeneous and the determination of the stress-strain relation is thwarted. No serious attempt was made to find whether this effect was due to abnormally large grains in the virgin material or whether large grains were developed by the process of straining under pressure; my general impression in the case of aluminum and copper was that it was the latter.

Qualitative measurements were also made on a number of other materials that could not be readily fashioned into the conventional tensile specimens. These materials were made into slender rods, approximately 1 cm long and 0.8 mm in diameter, supported near the two ends

[3] P. W. Bridgman, Rev. Mod. Phys. **17**, 3–14 (1945).

and subjected to a push at the center by a blunt wedge. Stops so limited the travel of the wedge that ductile materials were bent to a maximum angle of 135°. The experiment consisted in exposing the rod to the bending action of the wedge under hydrostatic pressure and observing whether there was any measurable difference between the amount of bending in the neighborhood of the fracture (if there was a fracture) as compared with atmospheric pressure. The apparatus was first tried with rods of a 1.50 C tool steel, hardened glass hard and drawn to various temperatures. At 29,000 kg/cm² the undrawn specimen broke with no appreciable bending, but all the others received the whole 135° bend without fracture. Of these the specimen drawn at 200°C broke at atmospheric pressure with no appreciable bending and the one drawn at 275° broke after bending through a slight angle. Repetition of the same experiment at 25,000 kg/cm² showed a rather rapid falling off of the pressure effect, the specimen tempered at 200° now breaking after bending only 40°.

At 29,000 gray cast iron broke with no appreciable bending, thus checking the result by the other method.

Other materials tested by the same method were: antimony, tellurium, bismuth (all in the single crystal condition), borax glass, hard rubber, and limestone. A rod of bismuth was recovered after an exposure at 15,000 permanently bent without fracture to an angle of 80°; whether the difference between 80° and 135° was due to elastic recovery was not investigated. Antimony, arsenic, and tellurium might be expected to show some ductility in analogy with bismuth, but loading of these three materials at 29,000 resulted in clean transverse fractures with no trace of any bending before the occurrence of fracture. Hard rubber was recovered after exposure to similar conditions unfractured and with a set of 10°; this set entirely disappeared and the rod became straight again on standing 12 hours at room temperature at atmospheric pressure. The elastic limit of hard rubber is thus obviously markedly raised by pressure. The borax glass was from the same source as that which Birch and Dane[4] had used in measuring the effect of pressure on viscosity at elevated temperatures. This glass deforms at atmospheric pressure with measurable velocities at temperatures as low as 300°; it might therefore be expected to show some measureable deformability under pressure at room temperature. No evidence of any bending before fracture was found, however, at a pressure of 29,000. Doubtless time effects are of importance here; the load was applied at such a rate as to reach the maximum deformation in a time of the order of a minute.

Limestone was of special interest because it had already been extensively investigated in the experiments of Griggs and of Balsley.[5] They found marked plasticity under compressive stresses in combination with hydrostatic pressure and also in *simple* tension, but much less ductility in bending. The pressures that could be reached in the present experiments were higher than those attained by Griggs and by Balsley, and the external conditions were somewhat more uniform, so that a positive result might perhaps be expected. The fracture was, however, completely brittle at pressures up to 29,000 kg/cm² when the test was performed in the regular way. It is known from the experiments of Birch and Bancroft[6] and others that the behavior of rocks under pressure is in many cases qualitatively altered if the pressure transmitting fluid is prevented from having access to the interior of the specimen by jacketing it with a suitable covering. The experiments were therefore repeated, encasing the limestone in a heavy sheath of lead or copper or steel, and bending under 29,000. The lead and copper jackets were probably completely successful; the specimens were markedly bent, and there were no obvious flaws, but the tests were not entirely conclusive because the specimens were broken on attempting to remove the jackets at atmospheric pressure. In the case of the steel jacket, both the jacket and the specimen broke brittlely with no obvious permanent deformation. The conclusion would therefore seem to be that the limestone is capable of receiving permanent deformation in tension

[4] E. B. Dane and F. Birch, J. App. Phys. **9**, 669–674 (1938).

[5] D. T. Griggs, J. Geol. **44**, 544–571 (1936); Am. Mineral. **23**, 28–33 (1938); Bull. Geol. Soc. Am. **51**, 1002–1022 (1940). J. R. Balsley, Trans. Am. Geophys. Union, Part II, 519 (1941).

[6] F. Birch and D. Bancroft, J. Geol. **46**, 113–141 (1938).

without fracture at pressures as high as 29,000. The extension of this conclusion to ordinary limestone is complicated by the fact that there is a polymorphic transition in the neighborhood of 25,000 so that the plasticity demonstrated above is plasticity of another modification than that existing under normal conditions.

In the endeavor to acquire further understanding of the effect of pressure on the mechanical properties of glass hard steel, another type of purely qualitative experiment was performed which has been previously made for other materials. If a thin ring of hard rubber or glass is slipped over a tightly fitting solid steel core and then exposed to hydrostatic pressure in a medium in which ring and core are both totally immersed, the ring will be split, just as if it had been expanded by driving a tupp into it. The simplest explanation is that the steel core, because of its much lower cubic compressibility, forces the ring to be stretched beyond the dimensions that it would normally assume under the hydrostatic pressure. This suggests that, for brittle materials, the normal zero from which to figure the extension which will produce brittle tensile fracture is the configuration which the material would assume under the mean equivalent hydrostatic stress of the total stress system.

The corresponding experiment was made with a 1.50 C tool steel by fitting a thin ring of the steel in the glass hard condition over a Carboloy core. The two were ground together with a slight taper, and were pushed snugly together, so that the steel ring was under a slight initial tension. The ring with core was then exposed to a pressure of 29,000 kg/cm². On releasing pressure, not only was the steel ring unbroken, but it was still a tight fit on the core, showing that it had received no appreciable plastic set. If *all* the elastic constants of Carboloy, as well as the cubic compressibility, are assumed to be about one-third the corresponding constants of steel, which has never been proved by direct experiment but which is not unplausible, it may be calculated that at the maximum pressure the steel ring was strained by about 2.5×10^{-2} beyond the dimensions which it would normally have had under a pure hydrostatic pressure of 29,000. This stretch is far beyond the elastic limit or fracture point at atmospheric pressure, and

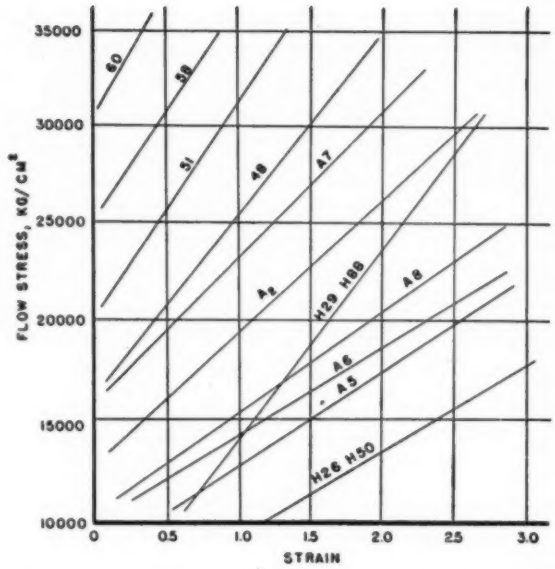

FIG. 11. The flow stress as a function of strain (strain-hardening curves) for all the steels of this paper and various 1045 steels previously described in Watertown Arsenal reports.

would demand a tension of approximately 750,000 p.s.i. So large an effect of hydrostatic pressure on the elastic limit has not been found previously for the softer steels. It may be, therefore, although this conclusion should be confirmed by other methods, that the comparatively small effect of pressure on the ductility of very hard steels is compensated by a large effect on the elastic limit.

Special attention was given to an investigation of the effect of pressure on the tensile properties of Carboloy. The interest in this lies in the fact that Carboloy containers, immersed in a medium carrying a high pressure, successfully withstand an internal pressure of more than 100,000 kg/cm².[7] The interiors of such containers are subject to large tensile strains and stresses, so that a large effect of pressure is indicated, Carboloy under normal conditions being brittle and with comparatively little strength in tension. The method used was the bending of slender rods, as before. No measurable plasticity in bending was imparted to a rod of grade 999 Carboloy by a pressure of 29,000 kg/cm². A special grid of greater sensitivity was then constructed and with this it was found that the bending force required to produce fracture at

[7] P. W. Bridgman, J. App. Phys. 12, 461–469 (1941).

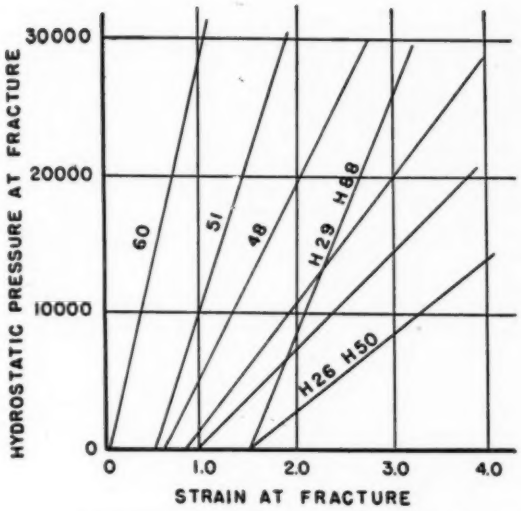

FIG. 12. Collected results for the steels of this paper and of a previous Arsenal report for the pressure at fracture as a function of the strain at fracture.

27,000 was at least threefold, and perhaps considerably more, greater than at atmospheric pressure. This very notable increase of strength must be an important factor in the functioning of the high pressure containers. The behavior is qualitatively the same as indicated in the last paragraph for hard steel.

DISCUSSION

In Fig. 11 are collected various results of the previous and the present investigations for flow stress *versus* strain for different grades of steel (that is, the strain hardening curves). The five lines designated by *A*2, *A*5, *A*6, *A*7, and *A*8 are

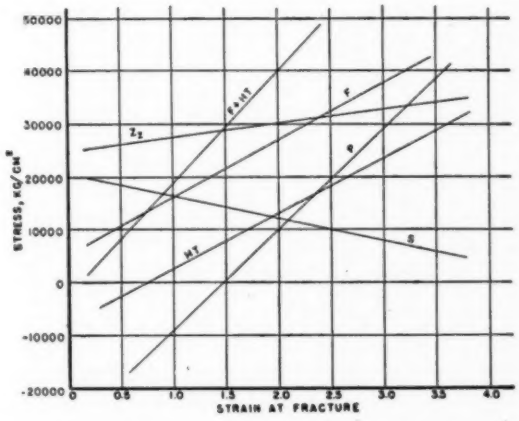

FIG. 13. Various significant stresses as a function of the strain at fracture for stainless steel H-29.

taken from the Watertown Arsenal reports, and refer to various heat treatments of a 1045 steel. The two groups of similar stainless steels are each averaged to give a single line. The lines of Fig. 11 form approximately a fan shaped family of non-intersecting lines, the slope of the line being higher the higher the absolute value of the stress, with the exception of the stainless steels H-29 and H-88. For these two steels the slope of the strain hardening line is higher than would be expected from the tensile strength at atmospheric pressure. That is, these two steels harden at an abnormally rapid rate.

Figure 12 shows a similar collection for different steels of the curves for pressure at fracture as a function of the strain at fracture, that is, the effect of pressure on ductility. The two undesignated lines are for the Watertown steels, which fall into two groups with respect to the property shown in Fig. 12. Again all the steels of this

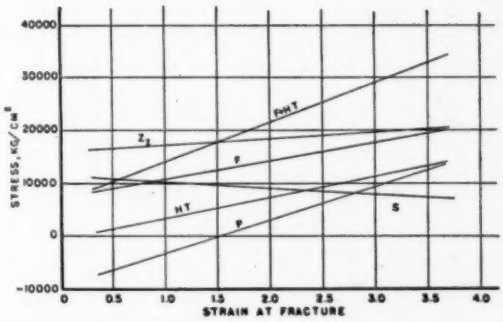

FIG. 14. Various significant stresses as a function of the strain at fracture for stainless steel H-50.

paper and two of the stainless steels fall into the same family of curves as the steels previously investigated, the increase of ductility under a given increment of hydrostatic pressure being greater the lower the absolute tensile strength. Again the two stainless steels H-29 and H-88 are exceptions. Their increase of ductility under hydrostatic pressure is abnormally low. Thus for these two steels a high rate of strain hardening with increase of strain goes with a low increase of ductility with increasing pressure.

The data of this paper bear on the question of the best criterion of rupture in the present range of conditions. In the fifth Arsenal report it was found that for the steels of those reports the mean hydrostatic tension (one-third the sum of

the three principal stresses, abbreviated in the following as S) was approximately constant at fracture. In Figs. 13–16 data are shown with respect to fracture for four representative steels of this paper, that is, stainless steels H-50 and H-29 and the groups of hardness 48 and 60. In these figures the lines of flow stress, F, and of hydrostatic pressure at the instant of fracture taken as positive, P, were first drawn as functions of strain. Next, from the line of flow stress was drawn the curve of "hydrostatic tension," HT, on the axis of the specimen. This hydrostatic tension is the second of the three components of the complete stress system described above. It was computed from the flow stress by multiplying by a somewhat complicated function of a/R which has been given in detail in the papers describing the corrections for stress distribution at the neck. This function of a/R may be expressed as one definite function of strain

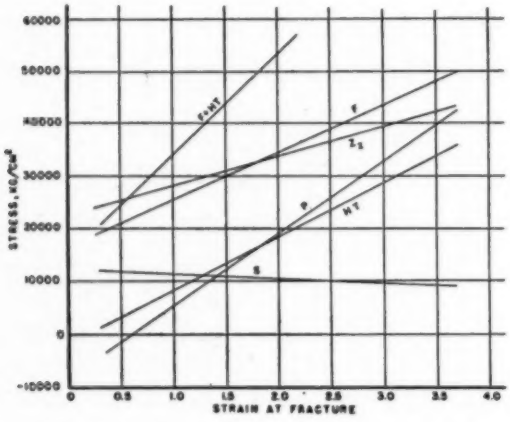

FIG. 15. Various significant stresses as a function of the strain at fracture for the specimens in the 48 hardness group.

for all normal steels, and as another function of strain for the two abnormal stainless steels. In both cases the conversion from a function of a/R to a function of strain was made with the use of empirical data. The function converting flow stress into "hydrostatic tension" is highly non-linear in the strain. It is a first empirical result that in the case of all steels, normal and abnormal alike, the curve for HT *versus* strain obtained with the use of this highly non-linear factor is linear within limits of error. It is a second empirical result that in all cases the line for HT

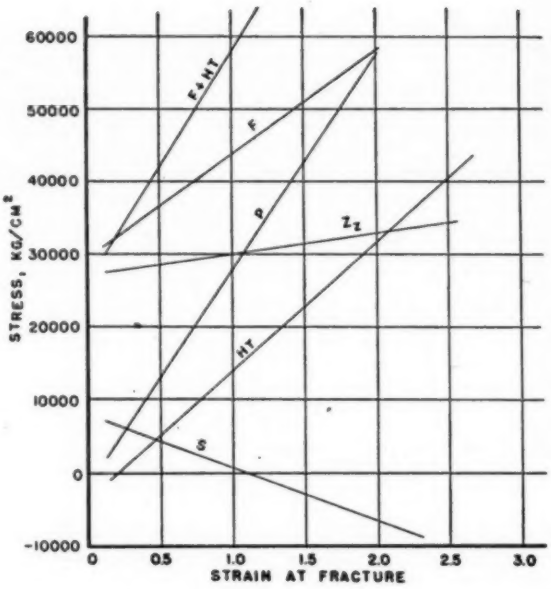

FIG. 16. Various significant stresses as a function of the strain at fracture for the specimens in the 60 hardness group.

rises approximately parallel to the line for F. Next, the two lines for F and HT were combined to give the line for $F+HT$. This is the axial stress at fracture that would be found on the axis of the specimen if there were no hydrostatic pressure. Inspection of the figures shows that in all cases it increases rapidly with strain. If the hydrostatic pressure is subtracted from $F+HT$ the actual stress Z_z on the axis at the instant of fracture will be obtained. This line is also shown in the figures. Finally, the line for the mean hydrostatic tension ($S=\frac{1}{3}F+HT-P$) was constructed.

This method of representing the results is somewhat different from any that I have em-

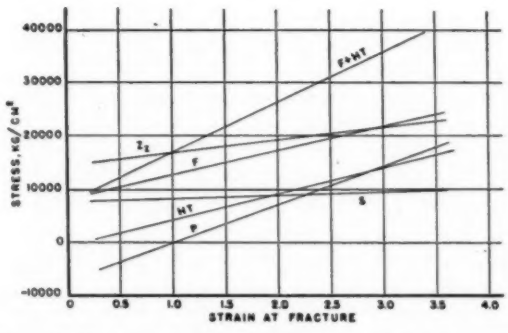

FIG. 17. Various significant stresses as a function of the strain at fracture for the steel A-5 of the fifth Arsenal report.

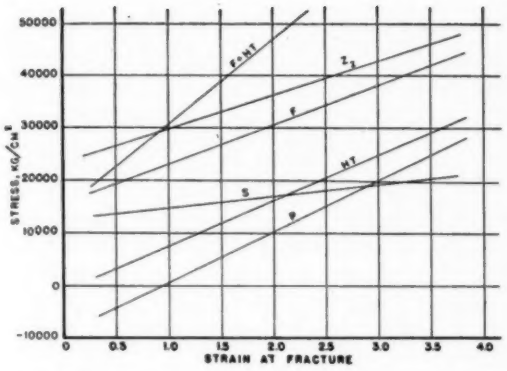

FIG. 18. Various significant stresses as a function of the strain at fracture for the steel A-7 of the fifth Arsenal report.

ployed before. Two of the steels previously examined in the Arsenal reports are therefore analyzed in the same way, and the results shown for $A5$ in Fig. 17 and for $A7$ in Fig. 18. These figures correspond exactly to the four figures just described for the steels of this paper.

In all six figures, 13 to 18, it is to be noted that the lines have physical significance for the conditions of the present experiments only for strains at which fracture occurs, that is, for strains to the right of the point where the line for P crosses the zero axis. To the left of this point fracture is formally indicated when the specimen is exposed to a hydrostatic tension instead of a pressure. What the actual physical behavior would be under such a tension is for the present conjectural.

A valid criterion for fracture will be represented by a horizontal line in the figures. Of the various lines in the figures it is obvious at a glance that the lines for Z_z and S come nearest to meeting this requirement. It also appears that S does not stand up as well as a criterion for the steels of this paper as it did previously for the two Arsenal steels $A5$ and $A7$. In this connection too much weight should not be given to the apparently large failure for the steel of hardness 60, since the entire experimental range of strain was only 0.0 to 1.0 and the experimental error is therefore higher than for the others. The criterion that Z_z is constant shows up as well on the average for the four steels of this paper as the criterion S. It is distinctly poorer for $A5$ and $A7$, however, so that on the whole it is not very good. The physical significance of the criterion of constant Z_z is that rupture occurs at a definite fiber stress, irrespective of the other stress components, and therefore irrespective of the component of elastic stretch in the same direction. This criterion has been used with some success by other investigators as a criterion of fracture in a limited range of conditions. However, in the wider range of conditions of this paper it would seem to have little physical significance, particularly when it is considered that under pressure the fracture loses its tensile character and becomes entirely shearing. The criterion definitely fails for such phenomena as the "pinching-off" effect.[8] The physical significance of the criterion that S be constant is that fracture occurs when the average volume distension reaches a critical value. There would seem to be some physical plausibility in such a criterion, but the data of this paper, as well as considerations which I have already advanced in other papers, show that it cannot be the sole determining factor in fracture. However, it seems to me that this must contain an important aspect of the mechanism responsible for fracture.

Of the various criteria which have been suggested for fracture, it is obvious that no criterion in terms of strain only can possibly be valid under present conditions in view of the enormous strains that can be reached under high pressures without fracture. Of the simpler criteria in terms of stress, it is obvious that the maximum shearing stress criterion cannot be valid. The maximum shearing stress is simply $\frac{1}{2}F$, and inspection of Figs. 13–18 shows that F and therefore $\frac{1}{2}F$ in all cases rises rapidly with strain, so that this criterion cannot be general. A physical argument could be made for the condition that $F+HT$ should be constant at fracture, since this has the physical significance of maximum tensile fiber stress calculated from a state of uniform hydrostatic pressure as the zero. This criterion however, evidently fails by a wider margin than any other indicated by the figures. Or, since the total component of hydrostatic stress on the axis, where fracture begins, is $HT-P$, a similar argument could be made for the reasonableness of the criterion that F should be constant at

[8] P. W. Bridgman, Phil. Mag. 63–80 (July, 1912).

fracture. This criterion is also evidently wide of the mark.

It is probably worth while calling attention to the fact that for all the steels the value of S at the lowest strain at which fracture occurs is approximately the same, namely 10,000 kg/cm².

SUMMARY

The tensile properties of the two stainless steels with low nickel content fall into the same pattern as the carbon or low alloy steels previously investigated. Two stainless steels with 9 and 10 percent nickel content fall outside the previous pattern in that necking starts at an abnormally high elongation, they strain harden as an abnormally rapid rate, and the increase of ductility under pressure is abnormally low. The carbon steels with Rockwell C hardness in the range 48 to 63 all fall in the previous pattern, the rate of strain hardening being greater and the effect of pressure on ductility being less the greater the hardness. Even the steel of hardness 63 shows a measurable ductility under a hydrostatic pressure of 24,000 kg/cm².

A search is made for a possible criterion of rupture by plotting various relevant stresses against the strain at fracture. No criterion emerges good under all conditions. The constancy of the mean hydrostatic tension (one-third the sum of the three principal stress components) remains the best criterion over the whole range of conditions, but in certain circumstances it may show considerable variation, and its margin of superiority over the criterion that the total fiber stress in the direction of fracture, Z_z, be constant at fracture, is not impressive. The maximum shearing stress criterion for fracture fails by a wide margin. No criterion of fracture in terms of strain components only can possibly be valid. Certain other plausible criteria on the stress components are also found not to hold.

In addition to the generalizations obtained from previous work, namely that the strain hardening curves are linear in the strain and that the ductility is a linear function of the hydrostatic pressure, two new empirical results emerge from the present method of plotting. These are: first, that the component of hydrostatic tension on the axis of the specimen arising from necking is a linear function of the strain at fracture and, second, that the line of hydrostatic tension *versus* strain is approximately parallel to the line of flow stress *versus* strain.

With regard to other metals than steel, aluminum, copper, bronze, and brass show an even greater effect of pressure on ductility than do the mild steels. These four metals were tested in the form of conventional tension specimens. The tensile properties of a number of other materials were tested by bending slender rods under pressure. Results were obtained in this way on hardened tool steels in various tempers in line with those obtained with the conventional tension specimens. Antimony, arsenic, tellurium, borax glass, cast iron, limestone (uncovered), and Carboloy showed no measurable plastic deformation before breaking by bending under hydrostatic pressure. Bismuth shows large plastic effects. Hard rubber acquires great plasticity and also shows prominent time effects. Limestone, when covered, will take permanent plastic deformation in bending under hydrostatic pressure, but the interpretation of the results is obscured by a polymorphic transition which takes place under pressure. Although Carboloy showed no plasticity in bending, it showed a bending strength under 29,000 kg/cm² more than three times greater than that at atmospheric. Another type of experiment pointed to a similar very large increase of the elastic distortion which glass hard steel will support without fracture in a medium under hydrostatic pressure. In general comment on the bending experiments, it would seem that because of the complicated nature of the conditions the results are not susceptible of as straightforward an interpretation as are the conventional tension tests. This is pointed by the fact that carboloy will show plasticity in simple compression under pressure although it shows no plasticity in bending. The same thing is indicated by the marked difference of plasticity of limestone in simple tension and in bending.

I am much indebted to Mr. L. H. Abbot for making the readings and manipulating the pressure apparatus.

Letter to the Editor

Letter to the Editor

GEORGE G. BRUCK
157 South Harrison Street, East Orange, New Jersey
December 22, 1945

IN 1937 Woodyard published in the *Proceedings of the I.R.E.* a paper in which he described the use of an oscillator as frequency discriminator. Recently the growing interest in circuit arrangements permitting frequency discrimination without amplitude sensitivity has brought about such developments as the "Ratio Detector."

The circuit described here is essentially an oscillator which falls in step with an incoming signal. The differential plate-current of the two halves of the tube is the discriminator output (Fig. 1).

This circuit lends itself to many other applications like f.i. frequency modulation, frequency stabilization, frequency modulation phonograph pick-up, etc.

A more complete paper on the theory and experimental results with this circuit will be published shortly.

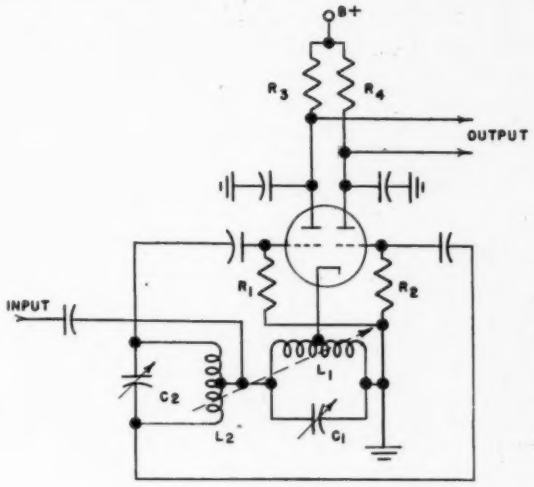

FIG. 1. F-m discriminator.

Here and There

New Appointments

Philip Nolan, who has spent the past three and a half years in fire control optics and infra-red research and development in the Navy's Bureau of Ordnance, recently joined the staff of the Farrand Optical Company, Inc., of New York as its chief physicist.

School and Society reports that G. W. Fox, professor of physics, Iowa State College of Agriculture and Mechanic Arts (Ames), has been appointed technical adviser to General Douglas MacArthur. Dr. Fox will spend about three months in Japan making recommendations as "to which scientific activities should be encouraged . . . and which, if any, discouraged."

After more than three years of war research with the Office of Scientific Research and Development and the U. S. Navy Bureau of Ordnance, George M. L. Sommerman has become associate professor of electrical engineering at The Technological Institute of Northwestern University.

Three new appointments were recently announced by the National Bureau of Standards. Hugh L. Dryden is now Assistant Director of the Bureau, Ferdinand G. Brickwedde is chief of the Heat and Power Division, and Robert Simha has become a member of the Division of Organic and Fibrous Materials with special responsibility for the coordination of fundamental research on the molecular properties of high polymers.

Necrology

Dr. Parke Benjamin Fraim, associate professor of physics at the Polytechnic Institute of Brooklyn, died January 13 at the age of 59.

Professor Harry Bateman, mathematician at California Institute of Technology, died in Utah on January 21 while on the way to New York, where he was to have been honored for outstanding work with Albert Einstein and other leading scientists. Professor Bateman was to be made a Fellow of the Institute of Aeronautical Sciences and receive a medal for his contributions to aeronautics. He had held full professorships in three fields—mathematics, physics, and acronautics—and was the author of many standard higher mathematics texts. At his death he was 63 years of age.

Physicist Honored in Chicago

Dr. Glenn T. Seaborg, co-discoverer of plutonium and elements 95 and 96, who is "on loan" to the Metallurgical Laboratory of the University of Chicago, has been named the outstanding young man of Chicago for 1945 by the Chicago Junior Association of Commerce. Dr. Seaborg has been on leave from the University of California for the past four years. He discovered plutonium in 1940. The announcement of his discovery, with three co-workers, of elements 95 and 96 was made last November. Dr. Seaborg, who is 33, has been in charge of the research at the University of Chicago for separating plutonium in amounts and purity required for war purposes. He has also been primarily responsible for the chemical separation procedures which were used in connection with the manufacture of plutonium at Clinton, Tennessee, and Hanford, Washington.

Technical Translations

The R. T. P.'s listed below are available from the Durand Reprinting Committee in care of California Institute of Technology, Pasadena 4, California.

These were selected for reprinting from the British Ministry of Aircraft Production R. T. P. List No. 122.

2478 Hohenemker	*Flow Tests on Steel Tubes under Combined Tension and Torsion.* (Z.A.M.M., Vol. II, No. 1, February, 1931, pp. 15–19.) (5 pages)
2480 Stablein, W.	*Measurement of the Characteristics of Frequency-Modulated Oscillations.* (Elektrische Nachrichten-Technik., Vol. 4, April, 1943, No. 20, pp. 102–111.) (12 pages)
2481 Heuvelink, H.	*The Testing of Graduations of Theodolites and Universal Instruments.* (Ztschr. f. Instrumentenkunde. Vol. 45, February, 1925, pp. 70–84.) (15 pages)
2492 Deuker, E. A.	*On the Stability of Elastic Shells Pt. I.* (Z.A.M.M., Vol. 23, April, 1943, No. 2, pp. 81–100.) (26 pages)
2493 Deuker, E. A.	*The Stability of Elastic Shells Pt. II.* (Z.A.M.M., Vol. 23, June, 1943, No. 3, pp. 169–179.) (13 pages)
2494 Pischinger, A.	*Oscillations in Gas Columns.* (Forschung, Vol. 6, No. 6, November–December, 1935, pp. 273–280.) (12 pages)
2495 Schmidt, F. R.	*The Induction and Discharge Process and Limitations of Poppet Valve Operation in a Four-Stroke Aero Engine.* (Luftfahrtforschung, Vol. 16, No. 5, 20.5.1939, pp. 251–275.) (45 pages)
2497 Volkersen, O.	*Rivet Load Distribution in Lap Joints of Constant Cross-Section under Tension.* (Heinkel Werke, Rostock L. F. F., Vol. 15, No. 1, 20.1.38, pp. 41–47.) (14 pages)
2498 Jegorow, G.	*Measurement of Direction Velocity and Pressure in a Three Dimensional Current.* (Luftfahrtforschung, Vol. 19, No. 9, 20.10.42, pp. 326–330.) (10 pages)
2499 Hiedemann, E.	*Physical-Chemical Effects of Supersonic Waves.* (Archiv f. d. Eisenhuttenwesen, Vol. 12, No. 4, October, 1938, pp. 185–193.) (17 pages)
2500 Lutz, O.	*Graphical Determination of Wall Temperature during Heat Transfer.* (Forschung, Vol. 6, No. 5, 1935, pp. 240–244.) (7 pages)
2501 Chwalla, E. Novak, A.	*The Theory of One-Sided Web Stiffeners.* (Der Stahlbau. Suppl. to Bautechnik, Vol. 10, No. 10, May 7, 1937, pp. 73–76.) (10 pages)

Bulletin of the Atomic Scientists of Chicago

The Atomic Scientists of Chicago have published several issues of the first volume of their Bulletin, an eight-page printed leaflet. Thus far articles have appeared under the following headings:

Technical Feasibility of Atomic Energy Controls
General Groves on the Future of the Atomic Bomb Projects
The Federation of Atomic Scientists
Denver Conference on Atomic Energy
UNO Faces the Problem of Atomic Energy Control
Structure of the UNO
British Public Opinion and the Atomic Bomb Menace
The Atomic Scientists Back the McMahon Bill
The Atomic Scientists and the Federation of American Scientists
The Distribution of Uranium in Nature
UNO Creates Atomic Energy Commission

In addition, the Bulletin always carries several columns under the heading "Congressional News."

The Bulletin has been featuring a series of articles on "Control Problems." Thus far it has included the following: general survey of the control problem, control of uranium mining, and control of a gaseous diffusion plant. The Bulletin is published at 1126 East 59th Street, Chicago 37, Illinois.

New Firm of Consulting Physicists

Paul Rosenberg Associates, consulting physicists, have announced the opening of offices in New York City. Work will be done in radar, ultrasonics, television, optics, nuclear physics, and general physics. The head of the firm, Paul Rosenberg, has recently completed four years' work at the Radiation Laboratory of the National Defense Research Committee at the Massachusetts Institute of Technology.

Dr. Meitner Arrives

Dr. Lisa Meitner, who is credited with establishing the mathematical data and equations in the breakdown of the uranium atom, arrived in New York from Stockholm on January 25. She came to the United States to join the faculty of the Catholic University of America in Washington.

New Booklets

Rheology Bulletin for December 1945, publication of The Society of Rheology, has the following table of contents:

Bibliography of Books on Viscosity, Viscometry and Rheology
Society of Rheology Annual Meeting Abstracts
Rheology Progress Abstracts (covering apparatus and methods, cellulose, clays, fibers, foams, general, ink, paints, petroleum products, plastics, polymers, proteins, theory)

General Radio Company, 275 Massachusetts Avenue, Boston 39, Massachusetts, has issued a 68-page *Postwar Supplement* to its *Catalog K*, now in the fourth edition. The Supplement brings all editions completely up to date.

Westinghouse Newsfront for January 1946, published by Westinghouse Electric Corporation, Pittsburgh 30, Pennsylvania, features articles on devices used in radar, research into the causes of rust and corrosion, industrial use of high frequency "cooking," and the value of electricity in increasing production, efficiency, and comfort on American farms.

Jarrell-Ash Company of 165 Newbury Street, Boston 16, Massachusetts, has issued a 16-page catalog of spectrographic equipment for research in spectroscopy and for spectrochemical analysis in metallurgy, mineralogy, agronomy, chemistry, medicine, and other fields.